

**STRUCTURAL CHARACTERIZATION OF POLYMER
BASED HONEYCOMB SANDWICH STRUCTURE
MANUFACTURED THROUGH ADDITIVE
MANUFACTURING**



Author

FAIZAN ALI AHMAD

Registration Number

328908

Supervisor

DR SHAHID IKRAM ULLAH BUTT

Co Supervisor

DR SALMAN KHAN

DEPARTMENT DESIGN AND MANUFACTURING ENGINEERING
SCHOOL OF MECHANICAL & MANUFACTURING ENGINEERING
NATIONAL UNIVERSITY OF SCIENCES AND TECHNOLOGY
ISLAMABAD, PAKISTAN

AUGUST 2024

STRUCTURAL CHARACTERIZATION OF POLYMER BASED
HONEYCOMB SANDWICH STRUCTURE MANUFACTURED
THROUGH ADDITIVE MANUFACTURING

Author

FAIZAN ALI AHMAD

Registration Number

328908

A thesis submitted in partial fulfillment of the requirements for the degree of
MS Design and Manufacturing Engineering

Thesis Supervisor:

DR SHAHID IKRAM ULLAH BUTT

Thesis Co-Supervisor:

DR SALMAN KHAN

DEPARTMENT DESIGN AND MANUFACTURING ENGINEERING
SCHOOL OF MECHANICAL & MANUFACTURING ENGINEERING
NATIONAL UNIVERSITY OF SCIENCES AND TECHNOLOGY,
ISLAMABAD, PAKISTAN

AUGUST 2024

THESIS ACCEPTANCE CERTIFICATE

Certified that final copy of MS/MPhil thesis written by **Regn No. 00000328908 Faizan ali Ahmad** of **School of Mechanical & Manufacturing Engineering (SMME)** has been vetted by undersigned, found complete in all respects as per NUST Statues/Regulations, is free of plagiarism, errors, and mistakes and is accepted as partial fulfillment for award of MS/MPhil degree. It is further certified that necessary amendments as pointed out by GEC members of the scholar have also been incorporated in the said thesis titled. **Structural Characterization of Polymer based Honeycomb sandwich structure manufactured through additive manufacturing**


Signature: 

Name (Supervisor): Shahid Ikram Ullah Butt

Date: 08 - Aug - 2024

Signature (HOD): 

Date: 08 - Aug - 2024

Signature (DEAN): 

Date: 08 - Aug - 2024



National University of Sciences & Technology (NUST)
MASTER'S THESIS WORK

We hereby recommend that the dissertation prepared under our supervision by: Faizan ali Ahmad (00000328908) Titled: Structural Characterization of Polymer based Honeycomb sandwich structure manufactured through additive manufacturing be accepted in partial fulfilment of the requirements for the award of MS in Design & Manufacturing Engineering degree.

Examination Committee Members

1. Name: Muhammad Salman Khan

Signature:

2. Name: Syed Hussain Imran Jaffery

Signature:

3. Name: Aamir Mubashar

Signature:

Supervisor: Shahid Ikram Ullah Butt

Date: 08 - Aug - 2024

Signature:

Head of Department

08 - Aug - 2024

Date

COUNTERSIGNED

08 - Aug - 2024

Date

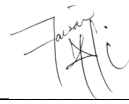
Dean/Principal

CERTIFICATE OF APPROVAL

This is to certify that the research work presented in this thesis, entitled “**Structural characterization of polymer based honeycomb sandwich structure manufactured through Additive Manufacturing**” was conducted by Mr. Faizan Ali Ahmad under the supervision of Dr Shahid Ikramullah.

No part of this thesis has been submitted anywhere else for any other degree. This thesis is submitted to the Department of Design and Manufacturing Engineering in partial fulfillment of the requirements for the degree of Master of Science in Field of Department of Design and Manufacturing Engineering by Department of Design and Manufacturing Engineering, National University of Sciences and Technology, Islamabad.

Student Name: Faizan Ali Ahmad

Signature:  _____

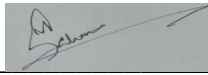
Examination Committee: -

a) External Examiner 1: Dr. Hussain Imran

Signature:  _____

(Asst Professor, DME SMME, NUST)

b) External Examiner 2: Dr. Muhammad Salman

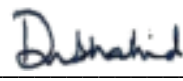
Signature:  _____

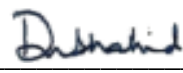
(Asst Professor, DME SMME, NUST)

c) External Examiner 3: Dr. Aamir Mubashir

Signature:  _____

(Professor, ME, SMME, NUST)

Supervisor Name: Prof. Dr. Shahid Ikramullah Signature:  _____

Name of Dean/HOD: Prof. Dr. Shahid Ikramullah Signature:  _____

AUTHORS DECLARATION

I Faizan Ali Ahmad hereby state that my MS thesis titled “**Structural characterization of polymer based honeycomb sandwich structure manufactured through Additive Manufacturing**” is my own work and has not been submitted previously by me for taking any degree from National University of Sciences and Technology, Islamabad or anywhere else in the country/ world.

At any time if my statement is found to be incorrect even after I graduate, the university has the right to withdraw my MS degree.

Name of Student: Faizan Ali Ahmad

Date: 8th August' 2024

CERTIFICATE FOR PLAGIARISM

It is certified that MS Thesis Titled “Mechanical Characterization of Polymer based Honeycomb Sandwich Structure Manufactured through Additive Manufacturing” by Faizan Ali Ahmad, Regn. No. 00000328908 has been examined by us. We undertake the follows:

- a. Thesis has significant new work/knowledge as compared to already published or is under consideration to be published elsewhere. No sentence, equation, diagram, table, paragraph or section has been copied verbatim from previous work unless it is placed under quotation marks and duly referenced.
- b. The work presented is original and own work of the author (i.e. there is no plagiarism). No ideas, processes, results or words of others have been presented as Author own work.
- c. There is no fabrication of data or results which have been compiled/analyzed.
- d. There is no falsification by manipulating research materials, equipment or processes, or changing or omitting data or results such that the research is not accurately represented in the research record.
- e. The thesis has been checked using TURNITIN (copy of originality report attached) and found within the limits as per HEC Plagiarism Policy and instructions issued from time to time.

Signature of Supervisor _____ 

Name: Dr. Shahid Ikramullah Butt

Declaration

I certify that this research work titled “*Structural characterization of polymer based honeycomb sandwich structure manufactured through additive manufacturing*” is my own work. The work has not been presented elsewhere for assessment. The material that has been used from other sources it has been properly acknowledged / referred.



Signature of Student

NUST-MS-DME-SMME-2024

Copyright Statement

- Copyright in text of this thesis rests with the student author. Copies (by any process) either in full, or of extracts, may be made only in accordance with instructions given by the author and lodged in the Library of NUST School of Mechanical & Manufacturing Engineering (SMME). Details may be obtained by the Librarian. This page must form part of any such copies made. Further copies (by any process) may not be made without the permission (in writing) of the author.
- The ownership of any intellectual property rights which may be described in this thesis is vested in NUST School of Mechanical & Manufacturing Engineering, subject to any prior agreement to the contrary, and may not be made available for use by third parties without the written permission of the SMME, which will prescribe the terms and conditions of any such agreement.
- Further information on the conditions under which disclosures and exploitation may take place is available from the Library of NUST School of Mechanical & Manufacturing Engineering, Islamabad.

Acknowledgements

I am thankful to my Creator Allah Subhana-Watala to have guided me throughout this work at every step and for every new thought which You setup in my mind to improve it. Indeed, I could have done nothing without Your priceless help and guidance. Whosoever helped me throughout the course of my thesis, whether my parents or any other individual was Your will, so indeed none be worthy of praise but You.

I am profusely thankful to my beloved parents who raised me when I was not capable of walking and continued to support me throughout in every department of my life. Without the prayers of my mother this would not have been possible

I am thankful to my wife for enabling me regain and recollect all my energies to complete my MS after significant pause.

I would also like to express special thanks to my Supervisor, Dr Shahid Ikram Ullah Butt for his help throughout my thesis and also for course, which he has taught me. A very humble and considerate he has always remained to me to accommodate me in completion of my thesis. I appreciate his patience and guidance throughout the whole dissertation.

I would like to express my sincere gratitude to Dr. Muhammad Salman Khan, my co-supervisor, whose guidance and expertise played a significant role in shaping my research. I am also deeply grateful to Mr. Aamir Mubashir, who generously granted me access to the Mechanics of Materials Lab, providing me with the resources to conduct my research. Furthermore, I am indebted to the instructors who taught me comprehensively, laying a solid foundation of knowledge that has enabled me to undertake this thesis. Their dedication, expertise, and mentorship have been invaluable in shaping my understanding of the subject matter.

Lastly, I would like to extend my sincere appreciation to all the individuals who have contributed to my research journey, offering valuable guidance, support, and encouragement along the way. Your collective efforts have made a significant impact on my work, and I am truly grateful.

*I am forever grateful to my amazing parents and loving family, whose
unwavering belief in me and unrelenting support have made this
incredible achievement possible*

Abstract

Honeycomb Sandwich structures are critical components in aviation industry owing to its impressive mechanical properties including strength-to-weight ratio, flexural rigidity etc. With the recent advancement in rapid prototyping, traditional manufacturing techniques for honeycomb manufacturing have limited the possibilities for innovative design. The advent of Fused Deposition Modelling (FDM), an AM technique, has expanded the design possibilities and holds the potential to improve the functionality of sandwich panels. In the outlined study, polymer (PLA) based honeycomb sandwich structures manufactured with FDM were subjected to variations in their geometrical features; cell size, wall thickness, and core height. These variations were then evaluated for two major mechanical properties: flatwise compressive strength and flexural stiffness of the structure. The study employed a Design of Experiment based on RSMs Central Composite Design. This research optimized FDM process parameters from existing literature to fabricate sandwich structure specimens. Mechanical properties were evaluated using ASTM C365 and C393 standards, and statistical models were developed to relate input variables to responses. The findings showed that cell size and wall thickness significantly impacted compressive strength, while core height had a greater influence on flexural rigidity. Stress-strain and load-deflection curves consistent with literature were obtained. This study demonstrates the importance of optimizing FDM parameters and geometric variables to minimize weight while maintaining structural integrity, contributing to the development of lightweight sandwich structures.

Key Words: *Sandwich Structures; Regular Hexagon, Homogenous Facing, Fused Deposition Modelling; Flatwise Compressive Strength; Flexural Rigidity; Response Surface Methodology*

TABLE OF CONTENTS

Declaration	i
Plagiarism Certificate (Turnitin Report)	Error! Bookmark not defined.
Copyright Statement	vii
Acknowledgements	viii
Abstract	x
Chapter 1 : INTRODUCTION	1
1.1 Honeycomb Sandwich Structures (HCSS)	3
1.1.1 Evolution and Applications of HCSS	5
1.1.2 Manufacturing Process of Honeycomb Structures.....	6
1.2 Additive Manufacturing	7
1.2.1 Applications and Advantages of AM.....	9
1.2.2 Challenges in AM	10
1.3 Mechanical characterization of HCSS	11
1.4 Research Aim / Objectives & Methodology	13
1.5 Outline of study.....	14
Chapter 2 : LITERATURE REVIEW	16
2.1 Mechanics of Honeycomb	16
2.1.1 Out of Plane Properties of Honeycomb	19
2.1.2 Mechanics of Honeycomb as Sandwich Structure.....	20

2.1.3 Testing Methodology for Honeycomb Structures.....	23
2.2 Background of Additive Manufacturing.....	25
2.2.1 Fused Deposition Modelling.....	26
2.2.2 Process Parameters in FDM.....	28
2.3 Current Research Highlights.....	31
2.3.1 Honeycomb Structures and Geometrical Parameters	31
2.3.2 Selection of optimized printing parameters for FDM.....	32
2.3.3 Polymer based Honeycomb structures manufacturing with FDM.....	34
2.4 Design of Experiment (DOE)	35
2.4.1 Response Surface Method; Overview.....	36
2.4.2 Advantages of RSM over conventional DOE approach	39
2.5 Conclusion	40
Chapter 3 : METHODOLOGY AND RESEARCH DESIGN.....	41
3.1 Selection of Printing Material.....	42
3.2 3D Printing Machine.....	43
3.3 Selection of Printing Parameters.....	44
3.4 Selection of Geometric variables of HCSS.....	45
3.5 Specimen Sizing.....	48

3.6 CAD Modelling	48
3.7 Design of Experiment	49
3.8 Printing of Specimens	51
3.9 Mass Calculations	52
3.10 Experimentation.....	52
Chapter 4 : RESULTS AND DISCUSSIONS	56
4.1 Analysis of the Flatwise Compression Test (ASTM C365)	56
4.1.1 Stress – Strain Curve.....	57
4.1.2 Analytical Results	58
4.1.3 Mean effect and Pareto standardized effect	59
4.1.4 Design Analysis by RSM.....	61
4.2 Analysis of Flexural Testing of Structure (ASTM C393)	69
4.2.1 Load – Deflection Curve.....	69
4.2.2 Analytical Results	70
4.2.3 Mean effect and Pareto standardized effect	71
4.2.4 Analysis of Response Surface Method	73
4.3 Analysis of Performance to weight Ratio	77
4.3.1 Analytical Results	77

4.3.2 Mean effect and Pareto standardized effect	79
4.1.4 Design Analysis by RSM.....	81
4.4 Difference between Experimental and Analytical response	88
Chapter 5 : CONCLUSION.....	89
5.1.1 Way Forward	92
References.....	94

List of Figures

Figure 1-1 : Schematic of Structural Sandwich Structure	3
Figure 1-2 : Expansion Honeycomb Manufacturing Method	6
Figure 1-3 : Corrugation Method of Core manufacturing	7
Figure 1.1-4 (a) 3D Printed Automotive dashboard (c) Aero engine turbine honeycomb seal (c) LEAP Engine fuel nozzle (d) Customized Hip plant.....	10
Figure 1-5 Application of Forces on a sandwich structure	12
Figure 2-1 : Polygons in two dimensional cellular materials: (a) equilateral triangle, (b) isosceles triangle, (c) square, (d) parallelogram, (e) regular hexagon, (f) irregular hexagon..	17
Figure 2-2: Three dimensional polyhedral cells: (a) tetrahedron, (b) triangular prism, (c) rectangular prism, (d) hexagonal prism, (e) octahedron	18
Figure 2-3 : Regular Honeycomb with Hexagon Cells (a) In plane Force direction (b) Out of Plane Force direction	18
Figure 2-4 : Out of Plane Stress Strain Curve of Honeycomb.....	19
Figure 2-5 : Forces and Moments on Sandwich Structure.....	21
Figure 2-6 : Bending Stresses on Sandwich	21
Figure 2-7 : Core Shear Stresses	22
Figure 2-8 : Bending Stiffness of Sandwich Structure	22

Figure 2-9 : Honeycomb Core Structure.....	23
Figure 2-10 : Compressive Testing.....	24
Figure 2-11 : Three Point Bending Test	25
Figure 2-12 : Schematic of Fused Deposition Modelling Process.....	26
Figure 2-13 : Steps involved in Fused Deposition Modelling	28
Figure 2-14 : Build Orientation 0°, 45°, and 90°	30
Figure 2-15 : (a) RSM Plot (b) Contour Plot	37
Figure 3-1: Research Design.....	42
Figure 3-2 : Ender Pro-3 3D Printer	43
Figure 3-3 : Specimen for Compression Testing	49
Figure 3-4 : Specimen for Flexural Testing	49
Figure 3-5 : Central Composite Design	50
Figure 3-6 : Printing of Specimen.....	52
Figure 3-7 : Mass calculation of Specimen.....	52
Figure 3-8 : Flatwise Compression Test	54
Figure 3-9 : Three Point Bending Test	55

Figure 4-1 : Stress – Strain Curve for Flatwise Compression Testing	58
Figure 4-2 : Effect of major influences on (a) Mean value on the Max Comp Strength	60
Figure 4-3 : Pareto Chart of Standardized Effect (a) Compressive Strength (b) Compressive Modulus	60
Figure 4-4 : (a) Residuals vs predicted values for Compressive Strength; (b) Normal Probability plot of the residuals	65
Figure 4-5 : (a) Residuals vs predicted values for Compressive Modulus ; (b) Normal Probability plot of the residuals	65
Figure 4-6 : Effect of Cell Size and wall thickness on the residual stress: (a) response surface and (b) contour plots	66
Figure 4-7 : . Effect of Cell Size and Core Thickness on the Compressive Modulus: (a) response surface and (b) contour plots.....	67
Figure 4-8. Optimal predicted parameters with desirability (Compressive Strength)	68
Figure 4-9 : Optimal predicted parameters with desirability (Compressive Modulus)	68
Figure 4-10 : Load – Deflection Curve (Three Point bend Test).....	70
Figure 4-11 : Effect of major influences on Flexural Rigidity	72
Figure 4-12 : Pareto Chart of Standardized Effect Flexural Rigidity	72

Figure 4-13 : (a) Residuals vs predicted values for Flexural Rigidity ; (b) Normal probability plot of the residuals (Flexural Rigidity).....	75
Figure 4-14 : Effect of Core thickness and Cell Size on the Flexural Rigidity: (a) Response surface plot (b) contour plots	76
Figure 4-15 : Optimal predicted parameters with desirability	77
Figure 4-16 : Optimum desirability for flexural rigidity	77
Figure 4-17 : Effect of major influences on (a) Mean value on Strength / weight ratio (b) Mean value of Flexural Rigidity / Weight Ratio.....	80
Figure 4-18 : Pareto Chart of Standardized Effect (a) Strength / Weight Ratio (b) Stiffness / Weight Ratio	80
Figure 4-19 : (a) Residuals vs predicted values for Strength / Weight (b) Normal probability plot of the residuals	84
Figure 4-20 : (a) Residuals vs predicted values for Stiffness / Weight (b) Normal probability plot of the residuals	84
Figure 4-21 : Effect of Cell Size and wall thickness on Strength / Weight Ratio (a) Response surface and (b) contour plots.....	85
Figure 4-22 : Effect of Cell Size and Core Thickness on the Strength / Weight Ratio (a) response surface and (b) contour plots.....	85

Figure 4-23 Effect of Core Thickness and Wall Thickness on the Stiffness / Weight Ratio (a) response surface and (b) contour plots.....86

Figure 4-24. Optimal predicted parameters with desirability87

Figure 4-25 : Optimal parameters with desirability for stiffness / weight ratio.....87

List of Tables

Table 1-1. Categorization of Additive Manufacturing techniques	8
Table 3-1 : PLA Material Properties.....	43
Table 3-2 : Selected FDM Process parameters	45
Table 3-3 : Selection of Input variables.....	47
Table 3-4 : Constraints for Honeycomb Structure.....	47
Table 3-5. Factors for Geometric Input variables.....	50
Table 3-6 : Experimental Runs as per DOE.....	51
Table 4-1 : Results of Flatwise Compression Test (ASTM C365).....	59
Table 4-2 : Model’s Summary Statistics for Compressive Strength.....	61
Table 4-3 : Model’s Summary Statistics for Compressive Modulus.....	61
Table 4-4 : ANOVA for Quadratic model (Compressive Strength)	63
Table 4-5 : ANOVA for Quadratic model (Compressive Modulus)	63
Table 4-6 : Fit Statistics (Compressive Strength)	64
Table 4-7 : Fit Statistics (Compressive Modulus)	64
Table 4-8. Optimal experimental parameters for Max Strength	68
Table 4-9 : Optimal experimental parameters for Compressive Modulus.....	69
Table 4-10 : Results of Flatwise Compression Test (ASTM C393).....	71
Table 4-11 : Model’s Summary Statistics for Flexural Rigidity.....	73
Table 4-12 : ANOVA for Quadratic model (Flexural Rigidity)	74
Table 4-13 : Fit Statistics (Flexural Rigidity)	75
Table 4-14 : Optimum input variables for Maximum Flexural Rigidity	77
Table 4-15 : Strength / Weight Ratio.....	78
Table 4-16 : Stiffness / Weight Ratio	79

Table 4-17 : Model's Summary Statistics for Strength / Weight Ratio	81
Table 4-18 : Model's Summary Statistics for Stiffness / Weight Ratio	81
Table 4-19 : ANOVA for Quadratic model (Strength / Weight Ratio)	82
Table 4-20 : ANOVA for Quadratic model (Stiffness / Weight Ratio)	83
Table 4-21 : Fit Statistics (Compressive Strength / Weight Ratio)	83
Table 4-22 : Fit Statistics (Stiffness / Weight Ratio)	83
Table 4-23. Optimal experimental parameters for Strength / Weight Ratio	87
Table 4-24 : Optimal experimental parameters for Stiffness / Weight Ratio	87
Table 4-25 : Difference in Analytical and Experimental values.....	88

Abbreviations

AM	Additive Manufacturing
FDM	Fused Deposition Modelling
UTM	Universal Testing Machine
PLA	Poly Lactic Acid
DED	Direct Engery Deposition
ASTM	American Society for Testing and Materials
3D	Three Dimensional
ANOVA	Analysis of Variance
RSM	Response Surface Methodology
DOE	Design of Experiment
E	Young's Modulus
G	Shear Modulus
CAD	Computer Aided Design
TPBT	Three Point Bend Test
UAV	Unmanned Aerial Vehicles

CHAPTER 1 : INTRODUCTION

Honeycomb sandwich structures have long-represented a possible material solution in aerospace, further compounded by the well-touted need for lightweight, high-performance materials. The combination of honeycomb core (which has mechanical properties per weight such as: high strength-to-weight, stiffness to weight ratio, energy absorption and impact resistance) with the robustness and ease-of-use in sandwich construction is nothing short of a cornerstone on which modern aerospace engineering is progressing. With their unique ability to absorb energy, maintain structural integrity under extreme loads; honeycomb sandwich structures have become preferable solution for various aerospace applications, including aircraft panels, satellite components, and rocket payload fairings, enabling the creation of lighter, faster, and more fuel-efficient aerial vehicles that are enhancing the defence capabilities.

The mechanical properties of honeycomb sandwich structures have always remained an area under researcher eye to find the optimal configurations and solutions. Honeycomb structures are profoundly influenced by critical geometrical parameters, including cell size, cell wall thickness, core density, aspect ratio etc. Understanding the intricate relationships between these geometrical parameters and the resulting mechanical properties is fundamental for the design and optimization of honeycomb sandwich structures.

Honeycomb structures are conventionally being manufactures through corrugation and expansion process which are often labour-intensive, time-consuming, and limited in terms of scalability and customization. These traditional methods pose significant challenges, including high tooling costs, material waste, and constraints on cell size and shape. A usual sandwich structures also involves adhesion between the face sheet and core that adds further complexity to the manufacturing process and add problems like delamination, face wrinkling, reduced mechanical strength etc. However, the advent of additive manufacturing (AM) techniques, specifically Fused Deposition Modelling (FDM), offers a capable solution to overcome these limitations. AM enables the manufacturing of complex honeycomb composite structures with customized cells, variable wall thickness, and intricate geometries thus making it a favourable process for manufacturing of small scale UAVs for multiple applications.

The geometric configuration of lightweight polymer sandwich structures manufactured through AM techniques like FDM necessitates further exploration to garner comprehensive design information in particular with weight optimization. While AM offers design flexibility, the intricacies of sandwich structure geometries, such as core thickness, cell size, and face sheet thickness, significantly influence mechanical properties like strength, stiffness, and energy absorption. To fully harness the potential of AM in producing high-performance sandwich structures, a deeper understanding of the interplay between geometric configuration and mechanical behaviour is essential. Therefore, systematic investigations into the response of varying geometric characteristics on the structural response of FDM-manufactured polymer sandwich structures are crucial to develop informed design guidelines and unlock the full potential of AM in this domain.

This thesis endeavours to understand the mechanical properties of polymer-based honeycomb sandwich structures manufactured through additive manufacturing, with a primary focus on optimizing the compressive strength and flexural rigidity to achieve maximum performance-to-weight ratios. By exploiting the design flexibility offered by additive manufacturing, this research seeks to develop novel singular body extruded honeycomb sandwich structures that exhibit enhanced mechanical properties while minimizing material usage. Through a systematic experimental and numerical approach, this study will evaluate the effects of various geometric characteristics of honeycomb such as cell size, wall thickness, and core and face thickness on the structural response of these sandwich structures. The ultimate goal is to establish a comprehensive understanding of the relationships between design parameters, mechanical properties, and weight, enabling the creation of high-performance, lightweight honeycomb sandwich structures with optimal performance-to-weight ratios for various engineering applications with aerospace industry in particular.

The introduction chapter of this thesis offers a thorough explanation of the research project, encompassing its background, context, research problem, research objectives and aims, research questions, significance, and limitations. The background and context section will provide a detailed understanding of the circumstances that motivated the investigation, its relevance, and its importance in the field of honeycomb structures and additive manufacturing. The research problem aims and objectives, research questions, significance, and limitations will be clearly defined, and their significance to the field of study will be highlighted. This

chapter will provide a foundation for the subsequent chapters, where the methodology and results of the research will be presented.

1.1 Honeycomb Sandwich Structures (HCSS)

Honeycomb structures consist of open cells formed by thin sheets of material that are interconnected, creating a network of hollow cells. The ASTM defines:-

“A structural sandwich is a special form of a laminated composite comprising of a combination of different materials that are bonded to each other so as to utilise the properties of each separate component to the structural advantage of the whole assembly”

The core of honeycomb is a cellular design characterized by a network of interconnected cells, typically shaped in a hexagonal pattern. The properties of the cellular solid core depend on the distribution of solid material within the structure's walls, faces and edges. Gibson [1].

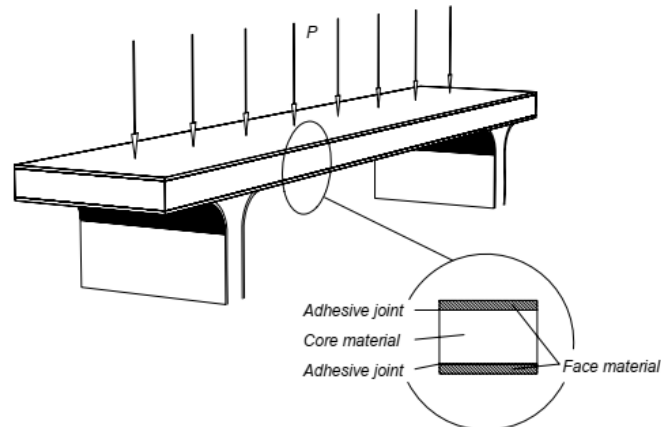


Figure 1-1 : Schematic of Structural Sandwich Structure

Sandwiches function similarly to I-beams, making them efficient structural shapes. In a sandwich, faces replace flanges and cores replace webs. The faces joined with the core at top and bottom resisting external buckling forces. A bond between the faces and core must withstand shear and tensile stresses. Zenkert [2]. The coupled unique properties of sandwich structure exhibit unique properties as follows: -

- (a) ***High Strength to Weight Ratio*** HCSS are characterized by their low density due to the arrangement of the hexagonal cells, allows for significant weight savings while maintaining structural integrity; thus provides excellent strength to weight ratio.
- (b) ***Out-of-Plane Compression and Shear Properties*** Honeycomb structures exhibit relatively high out-of-plane compression and shear properties. The efficient geometric configuration allows for effective load distribution, enhancing the overall mechanical performance under various loading conditions.
- (c) ***Orthotropic Behaviour*** Honeycomb materials display orthotropic mechanical properties, meaning their strength and stiffness vary with the direction of the applied load.
- (d) ***Energy Absorption*** The cellular design of honeycomb structures enables them to absorb significant amounts of energy during impacts. This property is beneficial in applications requiring crashworthiness or protection, as the honeycomb core can deform and dissipate energy effectively.
- (e) ***Efficient Load Distribution*** The interconnected cell walls in honeycomb structures support one another, enhancing compression strength compared to other core materials like foam or corrugated cores. This efficient load distribution contributes to the overall stability and durability of the structure.
- (f) ***Reduced Noise and vibration*** The honeycomb core's cellular structure helps to dissipate noise and vibration, providing a quieter and smoother operation.
- (g) ***Thermal Insulation*** Cellular voids in between the material filled with air provides excellent thermal insulation making sandwich structures suitable for applications where temperature control is essential.

1.1.1 Evolution and Applications of HCSS

Honeycomb is named after the natural honeycomb of bees. Honeycombs are made from any thin material paper or metal. Till now more than 500 different types have been produced. The Chinese invented paper honeycombs around 2000 years ago. The 1905 Budwig Patent in Germany is considered the first to describe a method for manufacturing Kraft paper honeycomb, marking a pioneering milestone in the development of honeycomb technology. The tubular railroad bridge which was built in 1845 in Wales, was one of the first man-made sandwich structures documented. Bitzer [3].

Since inception, the HCSS have undergone significant evolution owing to its remarkable exhibit of properties. Some of noteworthy events pertaining to honeycomb sandwich structures are as follows: -

- (a) In 1845 first known application of sandwich structure was man-made wood egg-crate used as top compression panel.
- (b) In 1915 Hugo Junkers patented the use of honeycomb cores in aircraft, enabling lightweight and strong designs for aviation. Further sandwich panels saw their application in aviation when thin mahogany-faced balsa wood core was used on seaplane pontoons. This innovative design was utilized in the 1930s.
- (c) Norman de Bruyne patented adhesives in 1938 for bonding honeycomb structures, facilitating their use in aircraft radomes and other applications.
- (d) First aluminium sandwich panel produced in 1945 is considered as a major breakthrough. Zenkert [2].
- (e) Since 1980s till present the use of honeycomb structures expanded with advancements in materials and manufacturing techniques, including thermoplastic extruded honeycombs. This led to their widespread application in construction, aerospace, and automotive industries, as well as in modern architectural designs that utilize honeycomb patterns for both aesthetic and structural purposes

(f) Boeing Aviation has used extensively sandwich structures made of Aluminium, Nomex and PEEK thermoplastic in its Aircraft 747, 777 and 787 Dreamliner respectively. Castanie, et al. [4].

1.1.2 Manufacturing Process of Honeycomb Structures

Conventional manufacturing process of Honeycomb structures includes expansion and corrugation as the core technology to produce a large scale structures. Details of these methods are as follows:-

(a) **Expansion Method** The metallic sheet is fabricated to precise dimensions, and adhesive strips are applied in a staggered pattern, with adjacent sheets having a half-pitch offset. Following adhesive solidification and curing, the HOBE block is sliced to the desired core thickness, and then expanded to create the honeycomb structure. Rupani, et al. [5]. Figure 1-2 illustrates the expansion method.

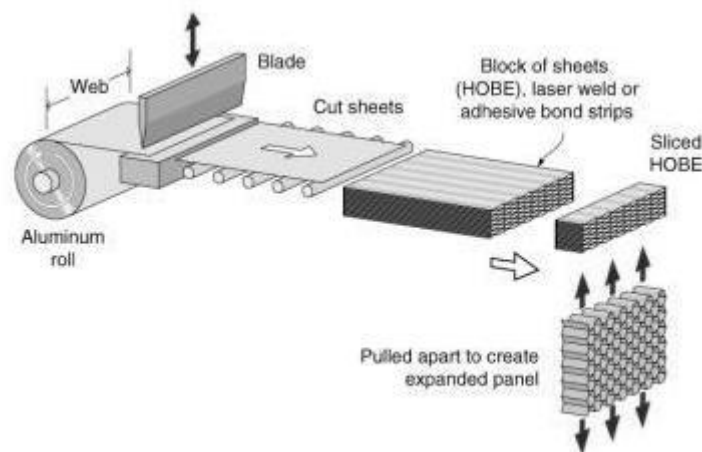


Figure 1-2 : Expansion Honeycomb Manufacturing Method

(b) **Corrugation Method** Figure 1-3 illustrates the corrugation method employed in the manufacturing of honeycomb cores. This process involves passing a metallic sheet through toothed rollers, which impart corrugations onto the material. Subsequently, the corrugated sheets are joined using various techniques such as bonding, brazing, or resistance welding to form the honeycomb core structure. Rupani, et al. [5].

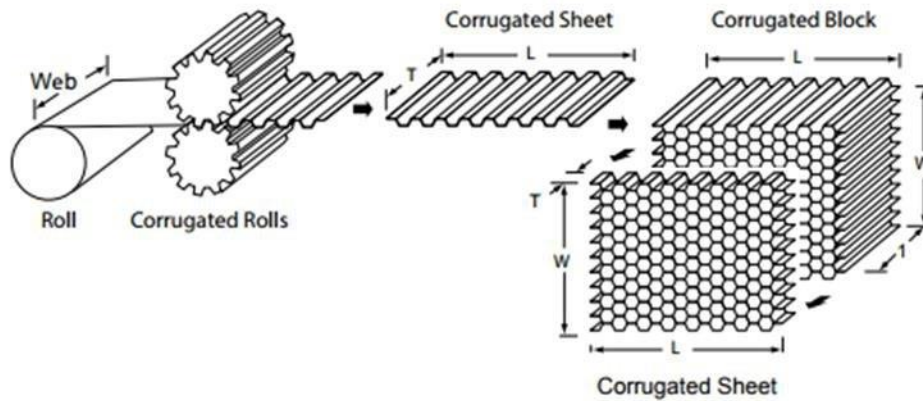


Figure 1-3 : Corrugation Method of Core manufacturing

(c) **Additive Manufacturing** Additive Manufacturing employs construction of three-dimensional objects by combining materials, usually utilizing a layer-by-layer method. This process is suitable for thermoplastic material and can manufacture intricate shapes ISO [6].

1.2 Additive Manufacturing

AM is defined by the ASTM F42 committee: -

“A process that involves the construction of three-dimensional objects by combining materials, usually utilizing a layer-by-layer method, instead of subtractive manufacturing techniques”29211-11e3 [7].

This term encompasses a set of processes that were formerly known as "rapid prototyping" or "rapid tooling". Kruth, et al. [8]. The expression "3D printing," which is widely used to describe AM, is the formal term for what was previously referred to as rapid prototyping. In various industries, the term "Rapid Prototyping" (RP) is used to refer to a technique for rapidly creating a model of a system or component before final release or commercialization. Akhoundi and Behravesh [9]. The integration of state-of-the-art parts made through AM into commercial aircraft, their use in human body implants, and other safety-critical environments, provides substantial proof of the economic viability of this technology. This trend demonstrates the increasing demand and confidence in the capabilities of AM to

produce high-quality, reliable and efficient parts. The versatility of AM in producing complex parts and its ability to reduce time and cost compared to traditional manufacturing processes, make it an attractive option for various industries and applications.

The quintessential aspect of all AM technologies is adding material to create an object rather than subtracting or using moulds. Even though all adherent processing methods incorporate the same basic concept, AM processes can differ in terms of type of material addition, shape or form factor for added material deposition and material delivery technique which subsequently is used to consolidate. The International Organization for Standardization has divided all AM processes into seven categories which have been illustrated in Table 1-1 ISO [6]. Table:

AM is the process of transforming a virtual 3D CAD computer model into a physical object. The amount of AM used to create an item will vary depending on its size and complexity. For simple and small products, AM may be limited to making representations of the appearance only; However, in the case of more complex and larger engineering products manufacturing may take place by employing AM at several stages and iterations within the development process depending on how much iterative testing is required. During the early phase of product development, AM could be used to produce quick-and-dirty parts. In later stages, AM may necessitate post-processing (e.g., cleaning, grinding/sanding or surface treatment/painting), offering greater design freedom with intricate shapes without tooling requirements.

Table 1-1. Categorization of Additive Manufacturing techniques

Category Name	Material	Material Form	Working Mechanism	Cost	Speed	Resolution	Performance
Material Extrusion	Polymer	Wire	Warm extrusion of polymer wire fed through a heated nozzle.	+++	0	-	-
Material Jetting	Polymer	Liquid	Material is deposited in droplet form through heated nozzle	0	-	+	-
Binder Jetting	Sand Metal Ceramic	Powder	Binder in droplet form deposited on powder bed, followed by debinding, sintering and infiltration	-	+	-	-
Powder Bed Fusion	Polymer Metal	Powder	Energy source fully melts powder particles in top layer of powder bed	---	--	+++	++
Directed Energy Deposition	Metal	Powder Wire	Powder or wire is fed into the energy source, mounted on a robotic arm	-	++	0	++
Vat Polymerisation	Polymer	Liquid	UV light polymerizes liquid prepolymer layer by layer	+	0	++(+)	+
Sheet Lamination	Paper Metal	Sheet	Sheet cutouts are stacked and bonded	++	-	---	--

1.2.1 Applications and Advantages of AM

AM is a disruptive technology that is transforming the manufacturing industry even for the manufacturing of Honeycomb structure. AM does not aim to completely replace traditional manufacturing techniques; rather, it offers a complementary approach that allows for the creation of complex geometries and customized parts with a high degree of precision and accuracy. This makes it particularly useful in fields such as aerospace, healthcare, and automotive industries where precision and customization are crucial. AM is also a more sustainable option, as it can minimize the material waste and energy consumption in contrast to traditional manufacturing methods. In order to justify the increased cost of Additive Manufacturing (AM) parts, it is important to leverage the unique advantages that AM offers over other manufacturing technologies. These advantages are derived from the digital nature of the AM process and the ability to create complex geometries. Gibson, et al. [10]. The key advantages of AM includes:

- (a) ***Reduced Material Waste*** AM builds products layer by layer instead of subtracting, thus, reducing material waste and the environmental impact associated with traditional manufacturing methods. This also leads to optimal part design leading to weight saving.
- (b) ***Increased Customization*** AM allows for the creation of customized parts without being limited by conventional production techniques. This allows for the creation of optimal designs that would otherwise be impossible to produce, such as conformal cooling and maximized heat exchanger surfaces.
- (c) ***Rapid production of parts*** 3D files can be printed within days, as opposed to the weeks required during a conventional product design that includes preparing moulds for conventional manufacturing.

Figure 1-4 illustrates the wide range of applications that can potentially benefit from additive manufacturing (AM). Figure 1-4 (a) illustrates the use of full-size polymer models in the automotive industry to efficiently evaluate the aesthetics, feel, and functionality of dashboard designs. Figure 1-4 (b) displays aero engine turbine seal that improved the turbines' efficiency by enhancing the turbine clearance between the rotating and stationary parts of aircraft engines. The additive manufacturing process enables both a production in one step and

weight reduction. Figure 1.1c depicts the fuel nozzle for the LEAP engine produced by General Electric, which is five times more resilient, 25% lighter, and integrates 18 parts into one single component. Lastly, Figure 1.1d portrays a customized hip implant, constructed using CT scans, that allows for the growth of bone into its porous surface for enhanced fixation.

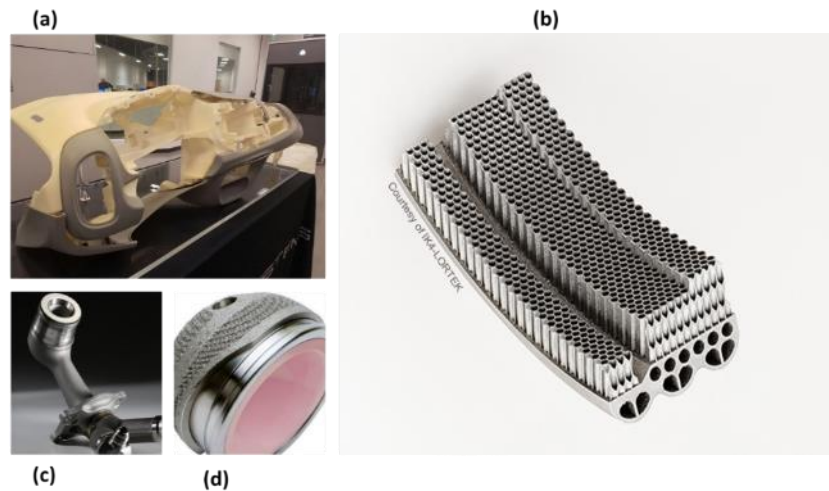


Figure 1.1-4 (a) 3D Printed Automotive dashboard (c) Aero engine turbine honeycomb seal
(c) LEAP Engine fuel nozzle (d) Customized Hip plant

In conclusion, AM offers numerous benefits that can compensate for the additional cost of its parts, and its potential applications are vast and diverse. The technology has the potential to revolutionize the manufacturing industry, offering improved performance, increased efficiency, and the ability to produce customized parts.

1.2.2 Challenges in AM

Over the next few years of AM is poised to cause a much-needed disruption in traditional product development and manufacturing practices. Even though coming a long way in recent years the research on AM technology still have few challenges. Based on the literature review, it is identified that there are a number of research areas in AM, which need to be further improved in order to overcome challenges and lead towards its successful adoption across different industries. These areas include: -

- (a) ***Expansion of the range of materials for AM*** Despite its numerous benefits, the limited number of commercially available material for AM restricts its

applicability. Research is required to expand the range of materials that can be used in the AM process.

(b) Process quality control Additive Manufacturing (AM) promise to provide parts for safety-critical applications however, there is still a special concern about the reliability and consistency of AM components. Enriching the quality during processing control, in AM processes particularly is imperative.

(c) Porosity reduction The use of non-optimal process parameters during additive manufacturing (AM) can cause porosity in the final parts. The impact of this porosity on the mechanical properties of AM parts is still not fully understood. Porosity reduction and a better understanding of its impact on the mechanical properties of AM parts require further research. Gibson, et al. [10].

(d) Improving build rate Despite the common perception of Additive Manufacturing (AM) as a rapid production method, the actual fabrication of parts employing AM can be a slow process, with some jobs taking a week or longer. As an outcome, research aimed at increasing the build rate is critical, as it has the potential to significantly reduce the cost of AM. Kruth, et al. [8].

1.3 Mechanical characterization of HCSS

The mechanical characterization of honeycomb structures is a crucial aspect of understanding their behaviour under various loading conditions. The compressive and flexural properties of these structures are of particular interest, as they are often subjected to such loads in practical applications. The compressive properties, including the compressive strength and modulus, are typically evaluated using universal testing machines, while the flexural properties, including the flexural strength and modulus, are assessed using three-point or four-point bending tests. Additionally, the shear properties and impact resistance of honeycomb structures may also be evaluated using specialized testing apparatus. The mechanical characterization of honeycomb structures is essential for understanding their potential in various engineering applications, such as aerospace, automotive, and energy absorption devices .Hexel-Composites [11].

Typically, two type of forces are being applied on sandwich structure as depicted in Figure 1.5. Face skin takes the compressive load whiles; sandwich core takes the shear loading

component of an applied force.

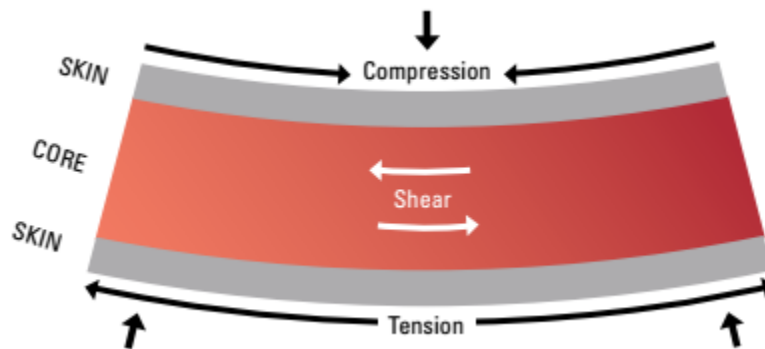


Figure 1-5 Application of Forces on a sandwich structure

Honeycomb structures do exhibit both in-plane and out-of-plane properties, the unique loading conditions encountered by aircraft components in particular, such as transverse shear, normal pressure, and impact, place a greater emphasis on optimizing the out-of-plane performance of honeycomb cores. Key factors requiring due consideration of out of plane properties includes: -

- (a) **Transverse shear and normal loads** Honeycomb cores are effective at resisting out-of-plane shear and normal loads that arise from wing bending, torsion, and cabin pressurization. The cellular structure allows efficient load distribution and high strength-to-weight ratios in the out-of-plane direction. Engelstad, et al. [12].
- (b) **Impact loads** Honeycomb cores excel at absorbing impact energy due to their ability to undergo controlled crushing. This makes them well-suited for protecting against impacts from birds, hail, and other external objects that impart out-of-plane loads.
- (c) **Disband propagation** Face sheet/core adhesion are a critical failure mode for honeycomb sandwich structures under out of plane applied forces. Pressure differentials between the core and environment can drive rapid disband growth, especially during aircraft ascent and descent thus due consideration for this study. Tarlochan [13].

Given the constraints on resources, this study has prioritized the evaluation of out-of-plane properties, specifically focusing on two critical responses that govern the mechanical behaviour of sandwich structures with honeycomb cores: compressive strength and flexural rigidity. These properties are crucial with an optimized core geometry in determining the structural integrity and performance of such structures under numerous loading conditions.

1.4 Research Aim / Objectives & Methodology

As annotated earlier, HCSS exhibits remarkable mechanical properties in terms to weight ratio but applicability of conventional manufacturing process to make small uni body honeycomb core filled aerodynamic structures is a challenge. Idea to explore the implementation of additive manufacturing to make a polymer based Honeycomb structure and study the effects of core geometrical characteristics and their effect on structure. The ultimate aim is to establish a comprehensive understanding of the relationships between design parameters, mechanical properties, and weight, enabling the creation of high-performance, lightweight honeycomb sandwich structures with optimal performance-to-weight ratios for various engineering applications with aerospace industry in particular. In precise terms aim of the study could be defined as:-

“Achieve optimal geometric parameters of homogenous facing polymer based honeycomb sandwich structure to achieve the optimum compressive and flexural properties”

Beside exploring the generic relation, the objective of the work also focuses on: -

- (a) Evaluate the applicability of FDM technique for manufacturing of different geometries of honeycomb sandwich structures.
- (b) Study the effects of cell size, wall thickness, core thickness of mechanical properties of honeycomb structures.
- (c) Testing of specimens in accordance with the ASTM standard for validation.

- (d) Creating a unibody structure to avoid any complexities of adhesion between the face sheet and sandwich core.
- (e) Using Response Surface Method (RSM) for Design of Experiment and process parametric optimization.
- (f) Formation of regression by combining the investigated variables to forecast the
- (g) Optimize the effects, keeping in view the minimum weight as objective function (Study of input variable with strength / weight ratio of specimen)

1.5 Outline of study

Chapter 2 of this study will provide a comprehensive literature review covering the fundamentals of honeycomb cores, hexagonal cells, and their properties. The review will also examine the current state of AM techniques used for honeycomb structures, with a focus on establishing a foundation for the research. The chapter will discuss various types of mechanical properties and their measurement techniques, as well as evaluate the process parameters of FDM to determine the most suitable and optimal settings. Additionally, the review will explore recent research on process parameter optimization, identify gaps in the existing literature, and discuss other relevant areas of research related to honeycomb structures.

Chapter 3 of this study will outline the research methodology employed, encompassing the material properties, geometry, and printing techniques utilized. Furthermore, this chapter will elaborate on the Response Surface Methodology (RSM) based design of experiments (DOE) approach, using Central Composite Design (CCD). The Design of Experiments (DOE) methodology is utilized to systematically investigate the impact of process parameters on the mechanical properties of honeycomb structures, enabling efficient data collection, analysis, and optimization of the manufacturing process.

Chapter 4 will present the results of the statistical analysis using design of experiments (DOE) to investigate the effects of process parameters on the compressive and flexural properties of honeycomb structures. The chapter will discuss the significance of these effects, shedding light on the relationships between the process parameters and the mechanical properties. Furthermore, optimization strategies will be explored to determine the optimal

combination of process parameters that maximize the mechanical performance of the honeycomb structures, providing insights for practical applications.

Chapter 5 will highlight the major outcomes of the study, emphasizing the significance of the results and the impact of statistical techniques on optimizing honeycomb structure performance. The chapter will highlight the benefits of using statistical methods, which enable accurate prediction of optimal parameters while saving time and energy. Additionally, the impediments of the study will be acknowledged, and possible avenues for future research will be identified, providing a foundation for further investigation and improvement in the field.

CHAPTER 2 : LITERATURE REVIEW

This chapter undertakes a comprehensive and systematic review of the extant literature pertaining to honeycomb structures, with a specific focus on their fabrication via additive manufacturing techniques, mechanical properties, and the concomitant effects of geometrical parameters on their structural performance. The primary objective of this review is to establish a robust theoretical foundation for subsequent research by examining the fundamental principles underlying honeycomb structures, the implications of various manufacturing techniques on their mechanical behaviour, and the resultant effects on compressive strength, flexural rigidity, and other pertinent mechanical properties. Furthermore, this review will critically examine the impact of compressive, flexural, and bending stresses on sandwich structures and cores, as well as the diverse applications of honeycomb structures across various fields. Additionally, the evolution and optimization of FDM process parameters will be scrutinized in detail, with a particular emphasis on identifying knowledge gaps and areas requiring further investigation. By synthesizing the existing body of knowledge and highlighting research lacunae, this review aims to contribute meaningfully to the academic discourse on polymer-based honeycomb structures, with a specific focus on the interplay between geometrical parameters and mechanical properties.

2.1 Mechanics of Honeycomb

Honeycombs are a class of two-dimensional cellular materials characterized by a regular, periodic microstructure, drawing inspiration from biological exemplars such as the hexagonal arrays found in bee hive. A critical characteristic of cellular structures is their relative density, denoted by the ratio ρ^*/ρ_s , where ρ^* represents the density of the cellular material and ρ_s signifies the density of the solid material from which the cells are derived. Gibson, et al. [10]. Notably, polymeric foams typically exhibit relative densities within the range of 5% to 20%. In contrast, natural materials such as cork display a relative density of approximately 14%, whereas softwoods generally possess higher relative densities, ranging from 15% to 40%. This variation in relative density significantly influences the mechanical properties and potential applications of these cellular materials. Khan, et al. [14].

The inherently minimal density of cellular structures enables the design of lightweight,

stiff and efficient structures, such as sandwich panels, which offer exceptional mechanical performance while minimizing material usage offering greater weight reduction. Palomba, et al. [15]. The unique combination of low strength and high compressive strains in cellular structures makes them particularly effective in energy absorption applications, where their ability to deform and dissipate energy is highly valued. Moreover, cellular structures are renowned for their excellent thermal insulation properties, attributed to their low thermal conductivity, making them ideal for applications where temperature regulation is crucial. A.Gpoichand [16].

Dimension characteristic of a cell including size, shape are crucial in determining the properties of cellular structures. Li [17]. When cells are equated, the resulting cellular structure exhibits isotropic properties. Figure 2-1 illustrates the various unit cells that can be packed together to form a two-dimensional cellular structure, which can possess either isotropic or anisotropic properties. Gibson [1]. Man-made honeycombs utilize the various unit cells shown in Figure 2-1, with the well-known hexagonal honeycomb featuring six edges surrounding each face, exemplifying a highly ordered and efficient cellular structure. Bitzer [3].

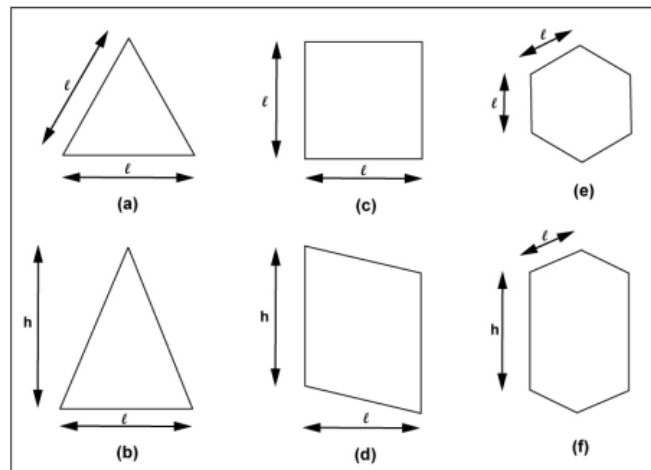


Figure 2-1 : Polygons in two dimensional cellular materials: (a) equilateral triangle, (b) isosceles triangle, (c) square, (d) parallelogram, (e) regular hexagon, (f) irregular hexagon.

Three-dimensional cellular structures exhibit diverse cell shapes illustrated in Figure. 2-2. Idealized unit cell models have proven valuable for understanding mechanical behaviour, particularly effective elastic stiffness and its dependence on relative density.

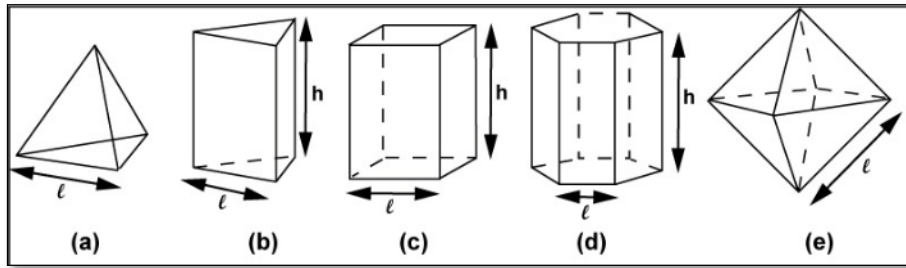


Figure 2-2: Three dimensional polyhedral cells: (a) tetrahedron, (b) triangular prism, (c) rectangular prism, (d) hexagonal prism, (e) octahedron

The three-dimensional honeycomb structure, depicted in Figure 2.3, exhibits varying mechanical properties across different planes. In the X1-X2 plane, which represents the in-plane direction, the honeycomb demonstrates relatively lower strength and stiffness. This reduction is attributable to the bending of the cell walls under stress, which diminishes the structural efficiency in this direction. Conversely, in the X3 plane, which is orthogonal to the cell walls and represents the out-of-plane direction, the honeycomb exhibits superior strength and stiffness. This is because the stresses in the X3 direction involve axial extension or compression of the cell walls, which is a more effective load-carrying mechanism compared to bending, resulting in enhanced structural performance in this plane.

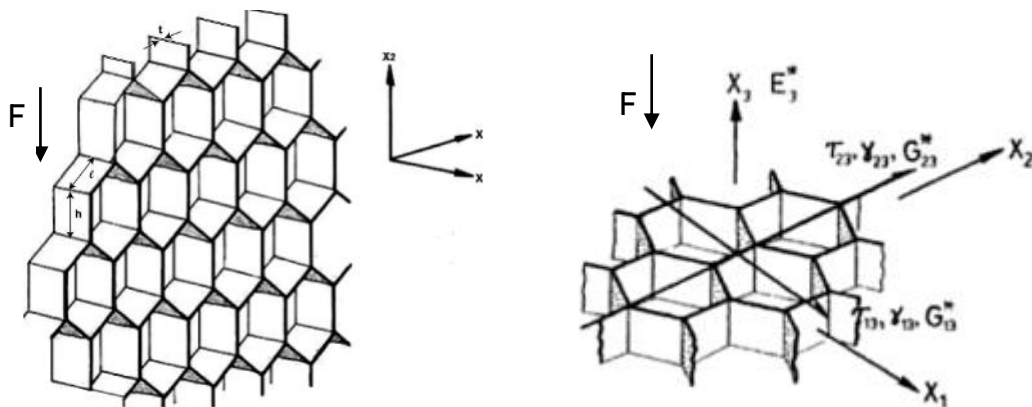


Figure 2-3 : Regular Honeycomb with Hexagon Cells (a) In plane Force direction (b) Out of Plane Force direction

When compressed in the X1-X2 direction, honeycomb cell walls bend, leading to linear elastic deformation. Upon exceeding a critical stress, cells begin to collapse. The deformation

varies with material properties: elastic materials show elastic buckling, plastic materials form plastic hinges, and brittle materials may fracture. At high strains, cell collapse results in densification, where fragments from opposing cells pack together Gibson [1].

In a uniaxial condition, complication begins after linear elastic region. These properties also depend upon the materials; in case of elastomers, cell wall buckles in compression while in tension they stretch and rotate. For a plastic material, cell wall yields in plastic bending. Similarly, for material exhibiting creep, structure creeps but in all cases in plane strength is always much lower than out of plane strength Gibson [1]. For the same reasons, where a structure has to bear higher loads like wings of an Aircraft; structure orientation is kept to take out of plane loads.

2.1.1 Out of Plane Properties of Honeycomb

The out-of-plane properties of honeycomb structures, oriented in the X3 direction, are notably characterized by their high strength and stiffness. In this direction, the cell walls experience axial extension or compression, which is a more efficient load-bearing mechanism compared to bending, thereby enhancing the material's overall performance under applied loads. Gibson [1]. The axial loading facilitates effective stress transfer, contributing to the honeycomb's superior mechanical behaviour in the out-of-plane direction. Hexel-Composites [18] Additionally, at elevated strains, the honeycomb undergoes densification, a process where collapsing cells and their fragments pack together, further temporarily increasing strength and stiffness. This combination of high axial strength and the densification effect makes honeycomb structures particularly effective in applications requiring substantial compressive and tensile properties. A classic stress – strain curve of honeycomb core is depicted in Figure 2-4.

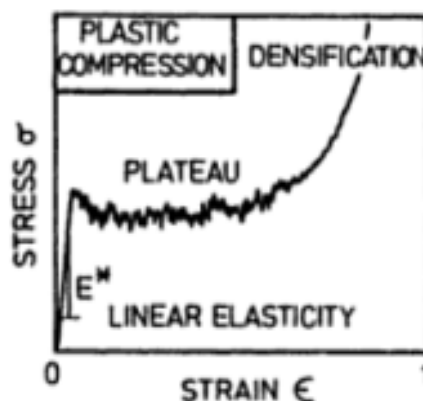


Figure 2-4 : Out of Plane Stress Strain Curve of Honeycomb

The out-of-plane properties of a honeycomb core, oriented in the X3 direction, are distinguished by their linear elastic deformation behaviour under applied loads. In this direction, the cell walls of the honeycomb experience axial compression or extension, which promotes efficient load transfer and results in high strength and stiffness Gibson [1]. When subjected to moderate stresses, the deformation remains within the linear elastic regime, meaning that the material reverts to its original shape once the load is removed, without permanent deformation. Assumption in this regard were taken wall thickness remain very low to node length of cell; $t \gg l$ Gibson [1]. Young's Modulus in the E3 for the normal loading is scaled in comparison to E_s ; Modulus of the solid or material. It barely shrinks down to

$$\frac{E_3^*}{E_s} = \frac{\rho^*}{\rho_s} \approx \frac{t}{l}$$

However, for Poisson ratio, $\nu_{31}^* = \nu_{32}^* = \nu_s$ are equal to solid itself. Calculation of Shear Moduli is not simpler as each cell exhibits a nonlinear deformation due to constraints imposed by it adjacent cell wall and thickness. Considering, regular hexagon, this calculation can be approximated by:-

$$\frac{G_{13}^*}{G_s} = 0.557 \frac{t}{l}$$

For regular hexagon, both shear Moduli are identical as their wall bounds coincide. Normally, out of plane Moduli are larger than in moduli by a factor of 10 to 100. Honeycomb differs in failure mechanism as per application of force direction. Much more complications are exhibited after linear elastic behaviour. However, as they are included in a sandwich structure approximation become much more like an I beam which are being discussed in subsequent chapter.

2.1.2 Mechanics of Honeycomb as Sandwich Structure

The sandwich structure is not a material with inherent mechanical properties, but are combination of material as per design configuration. While designing sandwich structures, several factors must be considered like composite structure, potential anisotropy of materials,

and low core shear modulus, necessitating careful evaluation of shear deformations. The fundamental principle of sandwich construction involves combining thin, dense, and strong facing materials with a thick, lightweight core, leveraging the benefits of each component to achieve optimal performance. Castanie, et al. [4].

In a sandwich structure, individual components (face skin and core) are weak and flexible, but when combined, they create an extraordinarily stiff, strong, and lightweight configuration. Typically, the facings absorb bending loads (one in compression, one in tension) while the core resists shear loads. It's also projected that facing stresses are evenly distributed and the honeycomb core offers minimal bending resistance, enabling efficient load distribution and optimized structural performance.

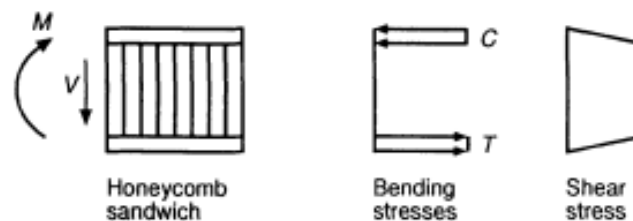


Figure 2-5 : Forces and Moments on Sandwich Structure

The standard method of analysis assumes that the facings bear the entirety of the bending load, which is represented by a pair of equal and opposite forces acting at a distance 'h' apart, where 'h' is the distance between the centroids of the skins as per Figure 2-6. These forces are assumed to induce a uniformly distributed stress across the thickness of the facing, simplifying the analysis and enabling the calculation of stresses and loads in the sandwich structure.

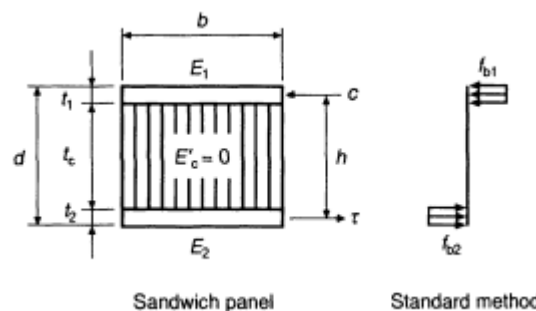


Figure 2-6 : Bending Stresses on Sandwich

The approximate solution for face bending stress

$$f_b = \frac{c}{tb}$$

Here, the moment is $M = c h$, or $c = M / h$, thus eq is as follows:-

$$f_b = \frac{M}{thb}$$

If both facings thickness t is same, then approximation stands for both the facings. As the core, bending stiffness is also to be considered for better accuracy but that usually holds for when facings have different thickness. Moreover, same is also catered in experimental calculations which is main objective of this study. Honeycomb core shear stresses are commonly estimated by assuming a uniform distribution of shear stress across the core, providing an approximate value for design and analysis purposes as per Figure 2-7. This simplifying assumption enables the estimation of shear stresses within the honeycomb core.

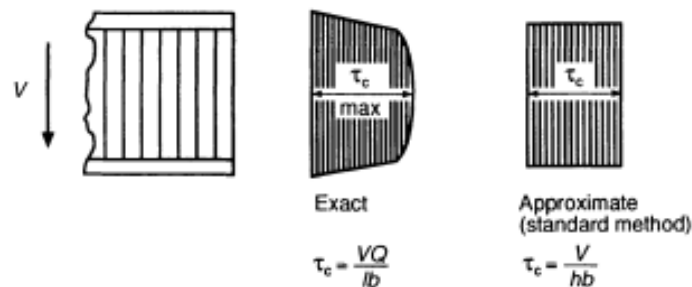


Figure 2-7 : Core Shear Stresses

The approximate solution for Core shear stresses are:-

$$\tau_c = \frac{V}{hb}$$

The total deflection of a sandwich panel or wide-flange beam can be decomposed into two constituent components: bending deflection and shear deflection. The bending deflection arises from the flexural deformation of the structure, whereas the shear deflection results from

the shear deformation of the core or web material. The sum of these two components yields the total deflection of the structure

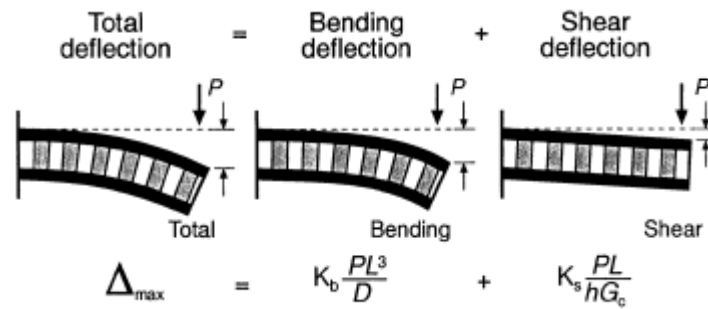


Figure 2-8 : Deflection in Sandwich Beam

Total deflection are further calculated using various assumptions by different Authors as discussed in Literature e.g, Laminate theory, Theory of Plates and Shells, Roark Method or by Experimental method as per ASTM standards Zenkert [2].

2.1.3 Testing Methodology for Honeycomb Structures

The mechanical properties of materials play a paramount role in determining their suitability for specific applications. Notably, sandwich structures featuring honeycomb cores exhibit anisotropic behaviour, characterized by disparate mechanical properties in the longitudinal (L) and width (W) directions as shown in Figure 2-9. Because of the same reasons, mechanical properties are tested in both direction; whereas, this dissertation will mainly focus on out of plane properties.

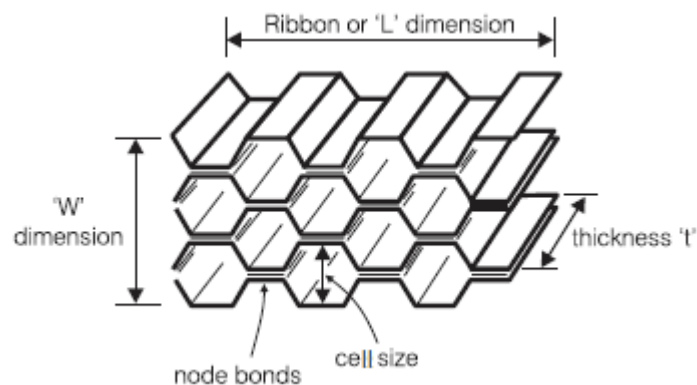


Figure 2-9 : Honeycomb Core Structure

(a) **Compressive Testing** Compressive strength is one the most significant mechanical property and its evaluation is standardized according to ASTM C365. Two distinct testing protocols exist: the bare and the stabilized compression test, specifically designed for sandwich panels. The bare compression test involves specimens with dimensions of 76.2×76.2 mm (non-metallic core), which are subjected to compressive loading at a rate of 0.5 mm/min. In contrast, the stabilized compression test a facing of 0.5-1 mm thickness is bonded to the core, ensuring the core cells maintain their place during compression and enabling more precise determination of compressive strength. This test also allows for the calculation of compressive modulus when appropriate measurement devices, such as extensometers are employed Jędral [19].

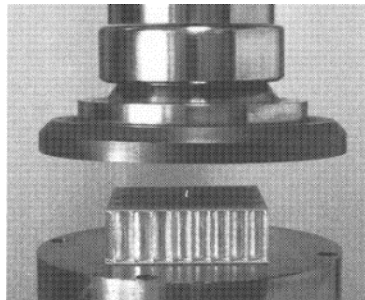


Figure 2-10 : Compressive Testing

(a) **Shear Testing** Shear strength is a critical mechanical property of honeycombs, providing essential information on the maximum shear strength and shear modulus (Kirchhoff modulus). These properties are vital in the design of sandwich material-based elements. The shear strength test can be conducted in accordance with ASTM C273, offering two variants: compression-based shear strength and tension-based shear strength. The former involves compressing the core to determine its shear strength, while the latter involves subjecting the core to tensile forces to achieve the same objective ASTM [20].

Another way of measuring the core shear strength is via three-point bend test. This test basically aims to find the flexural properties of sandwich structure. A typical arrangement of three-point bend test is depicted in Figure 2-11. Details of this methodology is discussed in Chapter 3 of this dissertation.

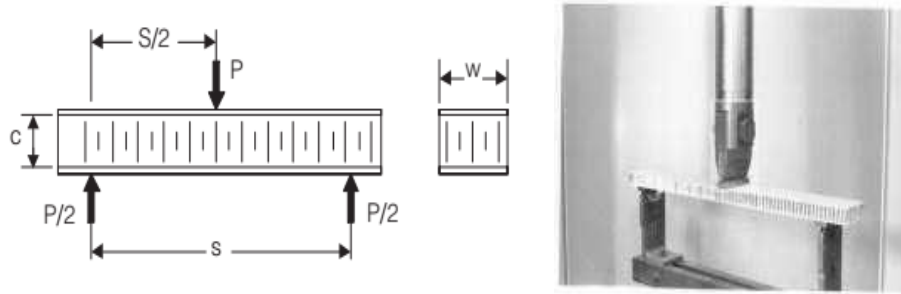


Figure 2-11 : Three Point Bending Test

2.2 Background of Additive Manufacturing

Additive manufacturing constructs objects layer by layer through thermal, chemical, mechanical, or optical binding methods, in contrast to conventional subtractive manufacturing which involves cutting or scraping away material. This method significantly reduces material waste, particularly with costly or rare materials, by efficiently utilizing only the material needed to build the object. Additionally, it facilitates the creation of complex geometries that are challenging to achieve with traditional techniques.

Additive Manufacturing (AM) originated in the 1980s at MIT Kruth, et al. [8] as Rapid Prototyping, primarily for research-based parts and models. The field gained significant academic interest in the 1990s and initially developed in university laboratories and R&D settings, utilizing polymer powders for quick prototyping. Over time, AM expanded to include soluble ceramics and eventually metal production. Kruth, et al. [8].

In recent years, the AM market has experienced exponential growth over decades through integration of automated design and manufacturing solutions, such as Computer-Aided Design (CAD), Computer-Aided Manufacturing (CAM), and Computer Numerical Control (CNC) Singh and Garg [21]. This has facilitated the evolution of AM from Rapid Prototyping to comprehensive 3D Systems Mogan, et al. [22]. Out of the seven different technologies listed in Chapter 1 (ASTM classification), only the FDM has been considered suitable and discussed keeping in view the resource limitations, cost, ease of manufacturing etc. FDM utilizes thermoplastic filaments as its feedstock material. The process involves heating the filaments to their melting point, causing them to liquefy, and then depositing the molten material onto a platform in a layer over layer manner Mogan, et al. [22]. Due to its relevance to the research presented in this thesis, a comprehensive overview of FDM technology will be provided in Section 2.2.1.

2.2.1 Fused Deposition Modelling

FDM is an extrusion-based AM process that fabricates objects from a range of polymeric materials, including Acrylonitrile Butadiene Styrene (ABS), Polycarbonate (PC), Poly lactic Acid (PLA), Polyethylene Terephthalate Glycol (PETG), Polyetheretherketone (PEEK). It was developed by Scott Crump of Stratasys in the late 1980s and commercialized in 1990; FDM has become one of the most widely utilized rapid prototyping technologies Mogan, et al. [22]. This process involves the extrusion of melted polymer filaments through a heated nozzle, depositing them layer by layer to form the desired geometry.

In Fused Deposition Modelling (FDM), the prototyping process commences with the unwinding of the feedstock filament from a reel, which is then fed through the liquefier, situated within the system's working envelope (as illustrated in Figure 2-12). As the filament traverses the liquefier, it is subjected to a gradual temperature increase, facilitated by a series of helically wrapped coils along the axis of the liquefier. This controlled heating process melts the filament, transforming it into a viscous liquid that can be extruded through the heated nozzle.

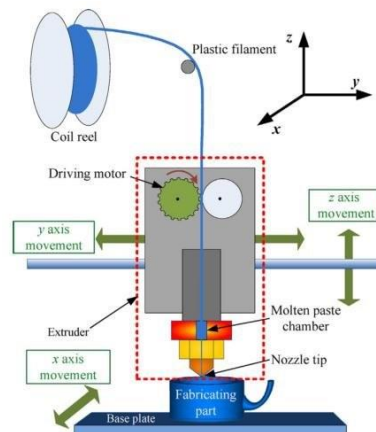


Figure 2-12 : Schematic of Fused Deposition Modelling Process

The process begins with a heated liquefier that melts plastic filament, which is then extruded through a nozzle to control the diameter of the deposited material. Two-step motors at the melted filament entrance maintain a continuous supply of material. The nozzle and liquefier assembly are mounted on a mechanical stage with numerical control in the X-Y plane. According to precise tool paths generated by specialized software coding, the nozzle moves

over a foam substrate; deposits thin layers of thermoplastic material and necessary support structures. Each deposited layer corresponds to a slice modelled in CAD. Once a layer is completed, the substrate is lowered in the Z direction to facilitate the deposition of the subsequent layer. The extruded filaments cool and solidify just below the glass transition temperature of the polymer. The entire build system operates within a temperature-controlled environment including the extruder and bed temperature, maintained just below the polymer's glass transition temperature to ensure bonding between layers. The feedstock material is supplied as filament with diameters of 1.75 ± 0.05 mm. A variety of nozzle tip sizes are used to produce slices ranging from fine to medium resolution, each offering different trade-offs between accuracy and production build time for the final prototype. Akhouni and Behraves [9] Dey and Yodo [23].

Figure 2-13 illustrates the steps involved in the FDM process. The workflow begins with creating a digital model of the part using Computer-Aided Design (CAD) software. Alternatively, 3D scanning and reverse engineering may be employed to develop the digital model. This model is then converted into a Standard Tessellation Language (STL) file, which contains coded details about the surface geometry of the model. The STL file is subsequently imported into slicing software, which generates G-codes that define the conditions for printing. These G-codes, similar to those used in CNC machining, direct the extruder and platform during the printing process. In the FDM process, the nozzle follows the coded instructions to extrude and add layers of melted filament. The G-code controls the extrusion amount, nozzle movement, and extrusion timing. Upon completion of the printing, post-processing is performed to achieve the desired finish of the final product.

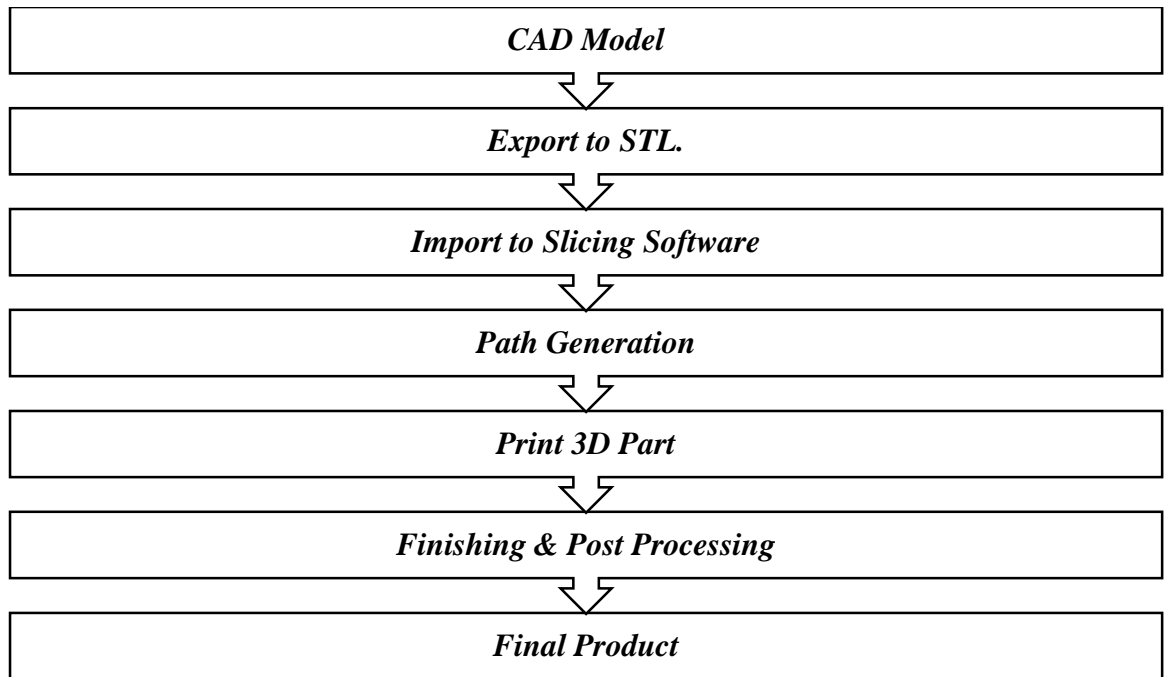


Figure 2-13 : Steps involved in Fused Deposition Modelling

2.2.2 Process Parameters in FDM

Process parameters significantly impact the accuracy, efficiency, and characteristics of the material in FDM. To produce functionally efficient parts using FDM technology, it is essential to conduct a fundamental study of various process factors. Consequently, the FDM printing process involves key parameters which are discussed in subsequent paragraphs.

- (a) **Layer Height** The layer height, also referred as layer thickness, defines the thickness of the material extruded from the nozzle diameter during the printing process. This parameter can be adjusted to match the desired thickness of the printed part, influencing the number of layers formed in a single pass along the vertical axis of the FDM machine. Importantly, the material add up height is always smaller than the nozzle diameter of the extruder head, ensuring precise control over the printing process. In FDM, layer height is determined by the extruder tip diameter and significantly impacts impact and bending properties. A minimum layer thickness enhances bending properties, while thicker layers improve impact properties. Layer thickness contributes approximately 85% to part accuracy, with a direct correlation between layer thickness and part dimension, affecting dimensional variance Pollard, et al. [24]. Moreover, layer

thickness has direct relation with part surface finish as well, lower value of layer thickness exhibits better surface finishes of part Tontowi, et al. [25].

(b) **Nozzle Temperature** Nozzle extrusion temperature is a critical parameter in FDM and is controlled within the heating nozzle before the material is extruded. This temperature affects the viscosity of the printing material, which in turn influences the properties of the final part. The ideal extrusion temperature must be maintained to ensure optimal viscosity and part quality. As the material is extruded, internal tension develops due to temperature variations between the extruder and the chamber, potentially leading to interlayer and intralayer deformation and part failure. If the extrusion temperature is too low, the material's high viscosity can impede extrusion, while excessively high temperatures may cause excessive flow and dripping. Most of the researchers have used Temperature between 200C to 250C as it suits the most variety of polymers like PLA, ABS, PEEK etc for extrusion Mogan, et al. [22], Dey and Yodo [23].

(c) **Bed Temperature** Bed temperature is crucial for achieving high-quality prints. It helps in preventing warping by ensuring more uniform cooling of the printed material, thereby reducing internal stresses that cause distortion. Additionally, an optimal bed temperature improves layer adhesion by increasing the surface energy of the print bed, which enhances the bonding strength of the first layer and minimizes the risk of print failure due to poor adhesion. Maintaining the correct bed temperature also helps retain the heat of the printing platform throughout the process and facilitates easier removal of the finished parts. The highest range adopted by researchers lies within 50C-75C Mogan, et al. [22].

(d) **Printing Speed** Print speed is a crucial parameter that governs the velocity of the printer's motors, including the X- and Y-axis motors and the extruder motor. It determines the rate at which the nozzle deposits filaments onto the build component, directly impacting the print time. Print speed has a significant influence on the fabricated model's quality, with faster speeds potentially compromising accuracy and surface finish Gibson, et al. [10], Dey and Yodo [23]. Optimizing print speed is

essential to balance print time and part quality. The normally used printing speed ranges from 20 mm/s to 40 mm/s, to achieve balance between print time and part quality.

(e) **Infill Ratio** The infill ratio, typically expressed as a percentage, denotes the density of material utilized within a 3D printed object. A higher infill ratio indicates a greater volume of material used internally, which enhances the object's strength and weight Akhoundi and Behravesh [9]. Increased infill ratios generally improve the mechanical properties of the fabricated part, such as tensile strength and impact resistance. However, this also leads to longer print times and greater material consumption. As the infill rate rises, the internal material density of the part increases, leading to enhanced mechanical attributes such as tensile strength and impact resistance. Ayrimis, et al. [26].

(f) **Build Orientation** Build orientation is a critical factor in 3D printing, influencing print quality, layer arrangement, and mechanical properties beyond layer resolution. It defines the angle between the part and the build platform's horizontal axis, determining the alignment with the X, Y, and Z axes. Build orientation significantly affects the final part's strength and mechanical properties, such as strain energy storage capacity and fatigue life Tontowi, et al. [25]. Figure 2-14 shown that varying build orientations (e.g., 0°, 45°, and 90°) can impact performance, with 45-degree angles exhibiting enhanced mechanical properties. This highlights the importance of optimizing build orientation to achieve desired outcomes in 3D printed parts Gonabadi, et al. [27].

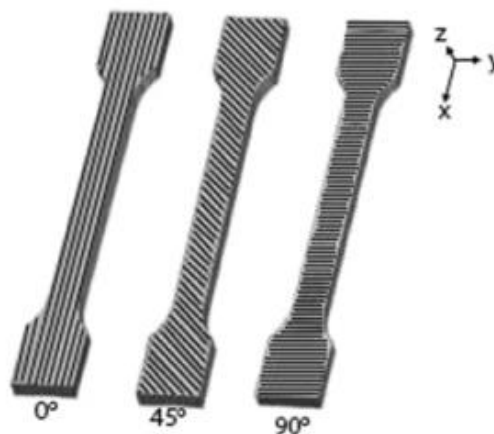


Figure 2-14 : Build Orientation 0°, 45°, and 90°

2.3 Current Research Highlights

2.3.1 Honeycomb Structures and Geometrical Parameters

The mechanical properties and structural efficiency of honeycombs are intricately linked to their cellular geometry, which is characterized by three critical parameters: cell size, wall thickness, and core height. Researchers have extensively explored the relationships between these parameters to formulate a strong understanding of their interdependencies, recognizing that optimizing their combination is crucial to harness the full potential of honeycomb-inspired materials and structures. Highlighted geometrical features also became significant as per analytical equations discussed in Section 1 of this chapter.

Shiping and Lai [28] studies the effect of cell sizes on honeycomb performance. Three difference type of cores including hexagon, triangular and square were studied degree of influence was observed to be significantly dependent on the cell configuration. Kumar, et al. [29] studied the effects of cell size and panel width on the stiffness properties of composite sandwich panels comprising a regular hexagon honeycomb core made of Kevlar and carbon fiber face sheets by variation of cell size from 3.2 mm, 4 mm, and 4.8 mm and panel widths from 40 mm, 45 mm, and 50 mm. The results indicate that cell size has a negligible impact on the stiffness properties of the composite panel. In contrast, increasing panel width significantly enhances the stiffness of the composite panel. In an study conducted by Khan, et al. [14] the effects of relative density (ρ^*/ρ_s) and cell aspect ratio (H/c) of the Nomex and paper hexagonal HC core on the compressive deformation response and out-of-plane compressive and tensile properties of the structure were studied. An exponent rise in compressive strength was observed with increase in relative density. Finite element models in ANSYS were used by Li [17] to investigate the effects of honeycomb cell size on Young's modulus and shear modulus of foam-filled honeycomb cores. Baumgart, et al. [30] demonstrated that high-density steel honeycomb structures with a square shape cells profile exhibit better out-of-plane properties, particularly in terms of specific energy absorption capability, making them suitable for applications requiring high impact resistance and energy dissipation. Thomas [31] highlighted the influence of cell wall thickness, node length, cell size on crushing response of Aluminum based honeycomb core.

Failure modes of sandwich structures are also studied by researches by conducting experimental work. Chahardoli, et al. [32] discussed the crushing characteristics using three-point bending tests. Specimen was made resembling a radiator core. Study found that the crushing parameters were increased with increasing the number of cores. McCormack, et al. [33] studied the failure mode maps are constructed which illustrate the dominant failure mode for practical beam designs of a honeycomb structure. Foam cores with Aluminum facing were used by the Author.

2.3.2 Selection of optimized printing parameters for FDM

The fused deposition modeling (FDM) technology has undergone significant advancements, yielding varying levels of print quality. Nevertheless, the default printing process parameters provided by manufacturers often fail to ensure optimal quality (dimensional accuracy and mechanical strength) of the printed parts. This is because numerous process parameters, which have been extensively investigated by researchers, can significantly influence the printing outcome.

Tontowi, et al. [25] optimized 3D printing parameters for PLA material using Taguchi and Response Surface Methods. RSM approach yielding the optimal setting of layer height 0.05 mm Nozzle Temperature of 199.8°C and Build orientation of 45.1° in comparison to Taguchi and default settings, with layer thickness impacting tensile strength and raster angle affecting dimension error of part printing. Bintara, et al. [34] study investigates the effect of layer height on surface roughness and printing time in FDM 3D printing of PLA material using a Creality Ender 3 printer. Results show that increasing layer height leads to increased surface roughness, while printing time decreases. Optimal layer heights of 0.15 mm and 0.20 mm are identified, achieving a balance between surface roughness (9.11 μm and 10.48 μm) and printing time (158 min and 120 min). Akhoundi and Behravesh [9] research indicate that print speed affects the mechanical properties, including flexural strength, of FDM printed parts. Increasing the print speed generally decreases the tensile and stiffness strength of the structure.

In one of the study Lalegani Dezaki and Mohd Ariffin [35] effects of combined infill patterns on mechanical properties are investigated for 3D printed PLA products. Different patterns including solid, honeycomb, grid etc. were combined and analyzed for tensile strength in different build orientations flat-wise and edge-wise. Finite element analysis revealed that honeycomb and grid patterns exhibited highest strength while being lighter than solid patterns. Bergonzi, et al. [36] research focus on the impact of different infill topologies and densities on the tensile strength of 3D printed parts. Results show that both infill topology and density significantly affect mechanical properties, with different infill patterns exhibiting varying strengths even at the same density. A detailed relation of infill ratio on printed parts is also discussed in a review research by Qamar Tanveer, et al. [37]. FDM internal pattern were also studied by Birosz, et al. [38] with varying infill patterns and percentages through bending tests. The results show that printing time increases with toolpath complexity, while mass differences between patterns are minimal due to overlapping. Honeycomb and Gyroid patterns exhibit superior mechanical resistance compared to Grid pattern.

Ouhsti, et al. [39] quantitatively investigated the mechanical properties of components printed using open source 3D printers with PLA material. A statistical analysis using ANOVA was employed to establish a correlation between 3D printing parameters and the mechanical properties of the printed specimens. The examined printing parameters included deposition angle, extruder temperature, and printing speed. Yang and Yeh [40] experimental results revealed a positive correlation between printing speed and density of Wood-Plastic Composite parts, with slower speeds yielding denser part. Tensile and flexural properties remained largely unaffected by printing speed, whereas compressive strength and modulus exhibited significant decreases of 34.3% and 14.6%, respectively, when printing speed increased from 30 to 70 mm/s. Tran, et al. [41] shows that printing speed of 20mm/sec is the optimum for PLA parts.

Sehhat, et al. [42] presented a study considering 3D printed PLA, PETG, and ABS parts at various temperatures. Results showed that temperature significantly affects tensile strength, with ABS performing best due to its high glass transition temperature. Material type was found to be non-significant, while

temperature was the dominant factor. Similarly, to achieve lower dimensional deviation and improved accuracy, low print speed and high extrusion temperature are recommended. In contrast, maximum tensile strength is obtained at high print speeds. Additionally, build time is minimized at higher print speeds, with no significant impact from extrusion temperature Ansari and Kamil [43].

2.3.3 Polymer based Honeycomb structures manufacturing with FDM

Over the past decade, significant research advancements have been made in the development of polymer-based honeycomb structures fabricated via Fused Deposition Modelling (FDM), a subset of AM techniques, with a growing body of literature exploring their mechanical properties, such as compressive strength, flexural strength, and energy absorption.

In an experimental study by Brischetto and Torre [44], capability analysis has been performed on the geometrical data and the mass of the produced specimens in order to evaluate the production process of PLA based printing of further sandwich specimens. In another study by Naidu, et al. [48], comparative analysis of mechanical properties between 3D printed and injection moulded honeycomb structures using PLA material revealed significant enhancements in the 3D printed structures. 3D printed structures exhibited a 1.74 times compressive strength and impact strength by a factor of 1.20 over injected moulded structure.

Ma, et al. [45] studies the effect of infill ratio on Quasi-static compression tests were performed on 3D printed cubical parts to examine the effects of infill pattern, infill density, and material type on crushing behaviour and energy absorption. Results showed that the honeycomb infill pattern in PLA cubes exhibited the highest energy absorption capacity compared to other infill patterns. Rebelo, et al. [46], studied the nonlinear response of 3D printed PLA honeycomb structures under blast loading, examining their energy absorption capacity. The results show a direct relationship between honeycomb relative density and force peak / plateau stress. In a research conducted by Domínguez-Rodríguez, et al. [47], compressive properties of 3D printed materials with honeycomb and rectangular patterns were investigated. Honeycomb patterns showed higher stiffness and strength, but only when loaded along the orientation direction, exhibiting anisotropic behaviour. Moradi, et al. [48] optimized the FDM printing parameters for honeycomb internal configuration of 3D Printed parts.

Basurto-Vázquez, et al. [49] study showed that infill ratio of 100% exhibits the optimum load distribution when honeycomb core made from PETG is loaded in out of plane direction.

Geometrical configuration like cell size, wall thickness were considered by Gohar, et al. [50] while studying the effect of material type and raster angle on honeycomb cores. Discrepancies pertaining to delamination were exhibited by the specimens due to difference in core and face sheets. Panda, et al. [51] conducted an experimental study on PLA based honeycomb core with cell size and wall thickness as input variable to study the Young's Modulus and Modulus of Elasticity.

Zaharia, et al. [52] studied different typologies of core including diamond, corrugated and hexagon for in plane tensile, compressive and flexural bending as per ASTM C393. Pollard, et al. [24] manufactured the honeycomb cores with FDM. This study investigated the filament bond strength of thin-walled honeycomb cores made from ABS and PLA. Thicker walls showed more plastic deformation and lower yield points, while compressive testing revealed thicker walls exhibited more ductility. Dikshit, et al. [53], studied two novel core structures to perform a compressive testing as per ASTM C365 to evaluate maximum compressive strength.

2.4 Design of Experiment (DOE)

Design of Experiment (DOE) is a statistical methodology employed to elucidate the relationships between variables and their resultant responses. This systematic approach involves manipulating multiple variables and observing the corresponding changes in the response, thereby facilitating the investigation of complex systems and processes. DOE is a versatile tool, widely utilized in diverse fields such as engineering, physics, and life sciences, to analyze and optimize the behavior of intricate systems, enhance process efficiency, and inform data-driven decision-making Uy and Telford [54].

In a DOE study, a subset of factors called independent variables are deliberately selected and their levels are systematically varied to generate a matrix of experimental conditions. The response variable which are desired dependent variables are subsequently measured for each condition, and the resulting data are analyzed to elucidate the relationships

between the factors and the response. This analysis enables the identification of factor interactions, main effects, and optimal factor levels, which can be leveraged to optimize the process or system by selecting the combination of factor levels that yields the desired response Anderson and McLean [55].

Design of Experiment (DOE) studies can be categorized into three primary design types: full factorial designs, fractional factorial designs, and response surface designs. Full factorial designs involve varying all factors at all possible levels, resulting in a comprehensive examination of factor interactions. However, this design is typically feasible only for a small number of factors due to the exponential increase in experimental runs Eriksson, et al. [56]. Fractional factorial designs offer a solution for studies with a large number of factors by selectively varying only a subset of possible factor level combinations, thereby reducing the experimental burden. Response surface designs are employed when the objective is to model and optimize the response surface by identifying the optimal combination of factor levels that yield the desired response. This design is particularly useful for complex systems where the relationships between factors and responses are nonlinear Said, et al. [57].

In conclusion, Design of Experiment (DOE) is a paradigmatic methodology for understanding variable relationships and optimizing processes. Its systematic approach enables researchers to discern interactions, quantify effects, and evaluate significance. As a result, DOE has become an indispensable tool across disciplines, driving innovation and informing evidence-based decision-making in complex systems.

2.4.1 Response Surface Method; Overview

Response Surface Methodology (RSM), introduced by Box and Wilson, offers an empirical approach to understanding the relationship between controllable variables (factors) and a response, particularly when theoretical models are unavailable or overly complex. RSM employs mathematical and statistical techniques to analyse and model complex problems, providing valuable insights into factor-response relationships Anderson and McLean [55].

Consider an experimental response of interest, Y , influenced by k controlled variables (factors) x_1, x_2, \dots, x_k . This setup is typical in response surface methodology, where the goal is to understand the relationship between the output response Y and the input factors x_1, x_2, \dots, x_k ,

and to optimize the response by adjusting the factor levels. The experimental domain is the multidimensional space where the controlled variables x_j are allowed to vary, bounded by practical constraints, limitations, and any other relevant restrictions. This domain defines the feasible region for experimentation, ensuring that the investigation remains within realistic and meaningful limits. The response is some performance measure or quality characteristic Y of the system under observation or control. The relationship between variables and response is governed by an underlying physical mechanism, theoretically described by a functional relation. This relation enables the phenomenon to be sufficiently reproducible, allowing for experimentation and the extraction of meaningful conclusions: -

$$y = f(x_1, x_2, \dots, x_k) + \varepsilon$$

ε represents other sources of variability that were not considered in f like the error in the determination of the response. The function $f(x_1, x_2)$ can be plotted versus the levels of x_1, x_2 as shown in Figure 2-15.

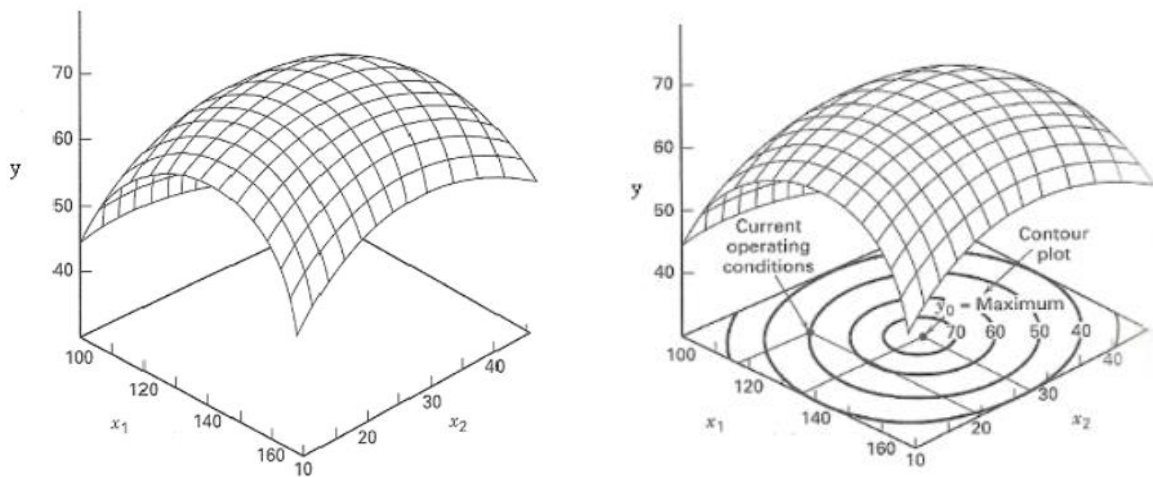


Figure 2-15 : (a) RSM Plot (b) Contour Plot

This three-dimensional graph illustrates the response surface, where each combination of x_1 and x_2 values yields a corresponding y -value. To facilitate easier interpretation, the response surface can be represented in two-dimensional contour plots, which display contour lines connecting x_1 and x_2 pairs that produce identical y -values. These contour plots provide a

simplified yet informative visualization of the response surface, enabling a clearer understanding of the relationships between the variables.

Response Surface Methodology (RSM) employs mathematical models, typically second-degree polynomial equations, to approximate the relationship between input variables and output responses. These models are derived from empirical data, obtained by systematically varying input variable levels and measuring corresponding output responses. The resulting polynomial models are then utilized for predictive purposes, generating output response predictions for novel input variable combinations, which are subsequently validated against experimental data to assess model accuracy and reliability.

With the mathematical model established, the optimization of input variables commences. Response Surface Methodology (RSM) leverages various optimization techniques, including gradient-based methods and heuristic approaches, to identify the optimal input variable settings that yield the desired response. This iterative optimization process involves systematically adjusting input variables and assessing output responses until convergence to the optimal solution is achieved, thereby determining the optimal input variable values that maximize or minimize the response. To approximate the function f , the experimenter typically begins with a low-order polynomial in a localized region. If the response is linearly related to the independent variables, a first-order model is used as the approximating function. A first-order model with 2 independent variables can be expressed as:-

$$y = \beta_0 + \beta_1x_1 + \beta_2x_2 + \varepsilon$$

If there is a curvature in the response surface, then a higher second or third degree polynomial may be used. The approximating function with 2 variables is called a second-order model:

$$y = \beta_0 + \beta_1x_1 + \beta_2x_2 + \beta_{11}x_1^2 + \beta_{22}x_2^2 + \beta_{12}x_1x_2 + \varepsilon$$

RSM integrates Design of Experiments (DOE) techniques to systematically collect experimental data, supplementing the mathematical model. DOE involves designing and executing experiments to elucidate the relationships between input variables and output responses. RSM frequently utilizes structured DOE techniques, such as Central Composite

Design (CCD) or Box-Behnken Design, which enable the estimation of polynomial coefficients and the exploration of nonlinear interactions, thereby facilitating a comprehensive understanding of the underlying system.

2.4.2 Advantages of RSM over conventional DOE approach

RSM, a crucial preliminary step precedes the analysis of the response surface: the identification and screening of significant factors. To ensure an efficient experimental design, it is essential to distinguish between important and unimportant independent variables, thereby eliminating negligible factors and focusing on those that substantially impact the response. Only after identifying the significant factors can the experimenter proceed with confidence to analyse the response surface, ultimately drawing informed conclusions about the presence of an optimum or opportunities for improvement in the system Anderson and McLean [55], Fisher, et al. [58].

The application of RSM in research and industry offers numerous advantages. Firstly, RSM streamlines statistical analysis by integrating techniques such as regression analysis and analysis of variance (ANOVA), facilitating efficient data analysis and interpretation. Additionally, RSM enables the optimization of manufacturing systems, processes, and products by identifying optimal operating conditions, leading to improved process efficiency, reduced costs, and enhanced product quality Cox [59].

RSM also employs systematic experimental design and layout through design of experiments (DOE) techniques, such as central composite design (CCD) and Box-Behnken design, to minimize experimental effort while maximizing information gain. Furthermore, RSM models enable accurate predictions of responses for new, untested conditions, allowing for informed decision-making and reduced experimentation Montgomery and St [60].

The methodology also provides intuitive visualization of variable interactions through response surface plots, contour plots, and other graphical tools. Effective representation of responses and results is achieved through surface plots, graphs, and other visual aids, facilitating understanding and communication of complex relationships between variables.

2.5 Conclusion

In conclusion, the literature review has provided a comprehensive foundation for understanding the fundamental principles of honeycomb cores and sandwich theory, as well as the transformative potential of Additive Manufacturing techniques, particularly Fused Deposition Modelling in optimizing their mechanical properties. Through a critical examination of existing research, this review has highlighted the significance of key properties such as compressive strength, flexural strength, and energy absorption in governing the structural behaviour of honeycomb structures. Furthermore, the optimization strategies employed in AM techniques have been shown to profoundly impact the mechanical properties of these structures, underscoring the need for further investigation into the interplay between AM parameters and structural performance. By synthesizing the findings of recent research in this field, this review has established a robust knowledge base for experimental inquiry into the compressive and flexural properties of sandwich structures, paving the way for the development of innovative, high-performance materials and structures. Ultimately, this research aims to contribute meaningfully to the advancement of knowledge in this field, with far-reaching implications for various industries and applications.

This dissertation presents a study that leverages Response Surface Methodology (RSM) for the design of experiments, with the primary objective of optimizing the compressive strength and stiffness of polymer-based honeycomb structures while minimizing weight and ensuring efficient manufacturing of finished products. The anticipated outcomes of this research are expected to make significant contributions to the field of polymer-based honeycomb structures, providing valuable insights and serving as a foundation for future investigations in this area. By employing RSM, this study aims to identify the optimal combination of design parameters that achieve a balance between structural performance and weight reduction, thereby enhancing the overall efficiency and applicability of these structures in aerospace industry in particular.

CHAPTER 3 : METHODOLOGY AND RESEARCH DESIGN

This chapter presents the research methodology employed to investigate the impact of variation in geometrical characteristics of HCSS manufactured with FDM to employ its effects on its key mechanical properties including compressive strength and flexural rigidity. Initial task was to select the optimal printing parameters for manufacturing of testing specimens further leading to experimental studies to conduct the test and analyse the results. The chapter provides a comprehensive overview of selection of key geometric parameters, highlighting its effects on multi-level on the structure in relation with the literature. The fundamentals of printing parameters along with their impact on manufacturing process are discussed, emphasizing its importance in material properties. Chapter also discusses the utilization of software's used for CAD modelling, writing the G code of the file till manufacturing of finished specimens that could be further used for testing. The testing techniques selected for measuring mechanical properties are described, along with the various techniques employed for this purpose and their respective advantages and disadvantages. The chapter elaborate by outlining the selection of material, geometrical parameters of sandwich structure, process of printing and testing apparatus used in the study. The design of experiments (DOE) is also explained, including how it was utilized to analyse the impact of geometrical parameters on the mechanical response of structure. Overall, this chapter aims to provide a comprehensive and detailed overview of the methodology employed in this study, as well as the tools and techniques utilized to investigate the impact of geometrical parameters of 3D printed HCSS to evaluated its mechanical properties.

Superior mechanical properties of HSCC, especially its high compressive and flexural rigidity and stiffness, make it well-suited for use in critical aerospace applications where high strength and durability are required. Thorough mechanical characterization is essential to ensure the structure meets the stringent requirements for these demanding applications. Beside calculating it numerically with established theories, with the arrival new manufactured techniques, basic output response to be validated for input variables. The relationship established will give a great insight of material and structure performance in multifaceted applications, allowing designers to make informed design decisions and evaluate the impact of variations on structure performance and reliability.

Aforesaid, the following research methodology has been adopted to achieve the objectives:

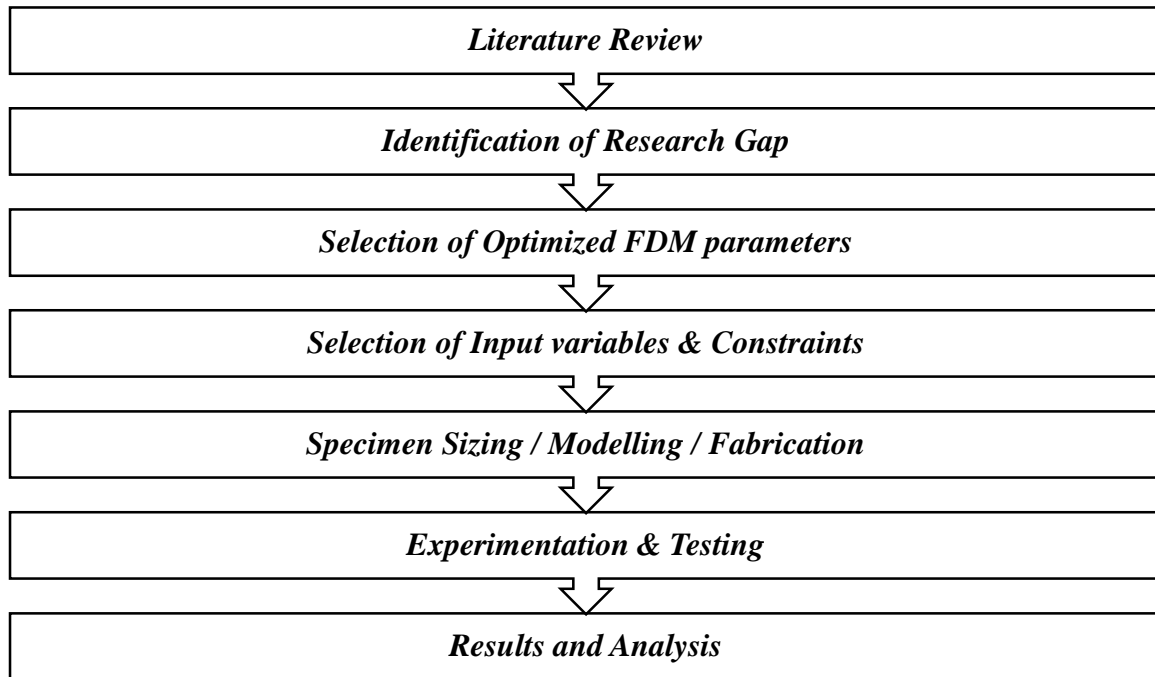


Figure 3-1: Research Design

3.1 Selection of Printing Material

Based upon the defined objective for calculation of mechanical properties, research was design to conduct in a systematic manner following the core principles of theory with conduct to similar experiments. First phase as discussed in literature review was to select the most suitable material for the construction of sandwich structures. 03 Materials including PLA, ABS and PETG were scrutinized to be considered based upon their vast utilization in commercial 3D printers. Although most of the them are polymers but few factors like availability of literature database, better characteristic for stiffness, ease of printing, better finishing, strength and cost makes PLA a preferable choice in the selection of material X and desirable testing also focuses on strength and stiffness related properties. In order to have an approximation of properties of material, PLA from a OEM Polytera was used. Its main properties are given in Table 3.1.

Table 3-1 : PLA Material Properties

<i>Parameters</i>	<i>Values</i>
Density	1.31g/cm ³ at 23°C
Melting Temp	162.6 °C
Young's modulus	1882 ± 141 MPa
Tensile strength	20.9 ± 2.0 MPa
Bending Modulus	2695 ± 541 MPa

3.2 3D Printing Machine

For this research, a commercially available "Ender Pro-3" 3D printer was utilized. This printer features a robust metallic frame and employs belt and rod drive mechanisms to facilitate printing in the X, Y, and Z directions. The machine is capable of processing a variety of materials, including multiple polymers, wood, and copper feedstock. Its extruder can reach temperatures of up to 260°C, while the hot bed can reach temperatures of up to 100°C. The printer is compatible with nozzles ranging from 0.2mm to 0.6mm in diameter and has a build volume of 220mm x 220mm x 250mm.



Figure 3-2 : Ender Pro-3 3D Printer

3.3 Selection of Printing Parameters

Next phase in the research plan was to outline the optimum printing parameters from the literature. Key parameters that were considered to be most affecting the properties were Extruder Temperature, Nozzle Size, Bed Temperature, Layer Height, Infill Ratio and Printing Pattern. Selection of each parameters is discussed in detail: -

(a) **Extruder Temperature** Usually extruder temperature range for PLA is typically 190°C to 220°C. Based upon literature, 210°C was selected that suited the best balance between build rate, layer adhesion, and part integrity Moradi, et al. [48].

(b) **Nozzle Size** Nozzle size from 0.2mm to 0.6mm were evaluated to be used. But as the small dimensions were involved in the manufacturing process i.e minimum wall thickness was to selected as 0.4mm thus process capability could have compromised. Smaller nozzle size allows for extremely high resolution prints, with minimal layer heights of 0.08mm and reduces warping effects and overall improves print quality for small, detailed parts like honeycomb geometry. Moreover, it will also result into better dimensional conformance.

(c) **Bed Temperature** Initially as per optimum values quoted 60°C was selected but warping effect at skin was observed, thus a more careful range of lower degree was selected. PLA generally prints well with a bed temperature around 50-60°C; however, in this case Bed Temperature was lowered to 30°C as overall build time was large thus part was being exposed to high temperature zone for a much larger time overall affecting the part quality.

(d) **Layer Height** Layer height from levels of 0.1 to 0.4mm was scrutinized. Literature indicate that a layer height of 0.2mm is a common and effective choice for 3D printing high-performance sandwich structures, as it allows for excellent mechanical properties and structural integrity without sacrificing too much in terms of print time and complexity. The thin layer height also helps improve the overall structural integrity and load-bearing capacity of the sandwich structures. Thus, for complex hexagonal sandwich structure designs 0.2mm layer height was selected.

(e) **Infill Ratio** Higher infill ratios (more infill material) generally result in stronger and stiffer 3D printed parts. Parts with lower infill ratios (less infill material) tend to be weaker and more flexible. 100% infill results in the strongest and most rigid parts, but also the longest print times and highest material usage. However, keeping in view the porosity challenge of additive manufacturing and further honeycomb lighter weight geometry and singular wall structures of sandwich structure in subject study were present thus, 100% infill ratio was selected.

(f) **Printing Speed** Keeping in view the optimum surface finish, mechanical performance of structure with a trade off with build time, print speed of 20mm/sec was selected for PLA material.

(f) **Build Orientation** Build orientation of 0/45/90 degree were considered from literature. 45/45-degree orientation was selected it gives the optimal strength response for polymer structures.

Table 3-2 : Selected FDM Process parameters

Parameters	Values
Extruder Temperature	210°C
Nozzle Size	0.2mm
Bed Temperature	30°C
Layer Height	0.2mm
Infill Ratio	100%
Printing Speed	20mm/sec
Build Orientation	45 Degree

3.4 Selection of Geometric variables of HCSS

The optimization of honeycomb geometry parameters, namely cell size, wall thickness, and core height, is a critical phase in the design and development of sandwich structures. A thorough review of the existing literature, coupled with considerations of commercial viability and industrial applicability, informed the selection of specific geometry factors for

experimental investigation. These factors were carefully chosen to explore the effects of honeycomb geometry on the structural performance, weight, and cost of sandwich structures, with the ultimate goal of identifying optimal configurations that balance these competing factors.

The average cell size range for commercial-grade honeycomb structures typically falls within a specific interval, as reported in earlier research studies. Hexel-Composites [18]. This range is generally accepted as the standard for industrial applications. Notably, ASTM standard for specimen sizing also dependent on cell size [20, 61]. Consequently, increasing the cell size beyond this range would result in unnecessarily large specimens, leading to increased costs without providing additional benefits. Therefore, this study focuses on exploring the effects of cell size within the established range, ensuring relevance to practical applications and cost-effectiveness.

The cell walls thickness of commercial-grade honeycomb structures, such as those produced by Plascore. Antony, et al. [62], typically falls within a specific range for similar-sized cells. Notably, selecting parameters with cell wall thicknesses below 0.4 mm poses significant challenges in achieving dimensional accuracy using Fused Deposition Modelling (FDM) processes. This limitation is attributed to the restricted nozzle sizes in FDM Dey and Yodo [23], Pollard, et al. [24], which hinder the fabrication of honeycomb structures with precise control over cell wall thicknesses at such small scales. Consequently, this study focuses on exploring the effects of cell wall thickness within the commercially relevant range, ensuring the feasibility of fabrication using established additive manufacturing techniques.

The core thickness of commercial-grade honeycomb panels, widely employed in various industries, typically conforms to a specific range for similar-sized cells. As stipulated by the ASTM standards, the sizing of specimens for testing and evaluation is directly dependent on the cell size. Antony Arul Prakash, et al. [63]. Moreover, the selection of face sheet thickness, a critical parameter in honeycomb panel design, is also contingent upon the cell size. Consequently, any increase in cell size beyond the established range would result in unnecessarily large specimens, leading to increased costs and reduced practicality.

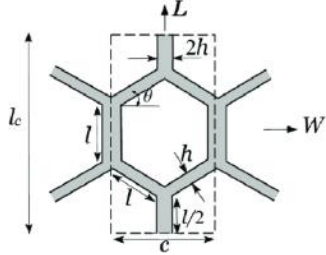
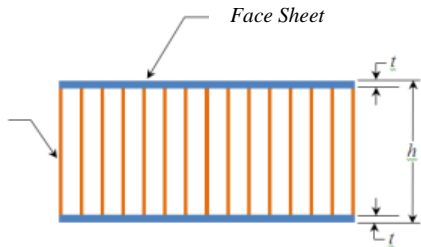
Based upon the discussion annotated above; following characteristic of geometry of core were selected: -

Table 3-3 : Selection of Input variables

<i>Input Variable</i>	<i>Minimum Value</i>	<i>Maximum Value</i>
Cell Size	4mm	12mm
Wall Thickness	0.4mm	1.2mm
Core Thickness	6.35mm	19.05mm

The presence of constraints in experimental design is a crucial aspect of scientific inquiry, as they delineate the boundaries of the problem space and dictate the parameters of investigation. By acknowledging and working within these constraints, a more focused and efficient experimental approach was taken to optimize the resource allocation and minimizing potential errors. In subject study cellular geometry of HCSS, constraints considered to find an optimal solution are tabulated in Table 3-4.

Table 3-4 : Constraints for Honeycomb Structure

<i>Constraints</i>	<i>Selection</i>	<i>Visualization</i>
Core Typology	Regular Hexagon	
Face sheet Thickness	0.6mm ; $t_f / t_c \approx 0.1$ for applicability of Analytical Comparison with Eq [1]	

3.5 Specimen Sizing

Following the selection of the geometry, the next step involved designing the specimens in accordance with ASTM standards. Since two technical properties were targeted as responses, two different specimens were to be manufactured in accordance with ASTM standards, with a deliberate variation in core geometry.

(a) **Specimen for Flat wise Compression Testing (ASTM C365)** Test specimens sizing was carried out with a core or sandwich design, with a square cross-section. The maximum cross-sectional area shall not exceed 400 mm^2 (16 in^2). However, the minimum cross-sectional area shall be dependent on the type of core material used. Specifically, for open-celled cores such as honeycomb as selected in this study with cells 6 mm or greater, the minimum cross-sectional area shall be 5800 mm^2 (9 in^2). However, core thickness has no limitation and can be selected as per user requirement [7]. Keeping in view the requirements; specimens having cross section of 3x3 in were selected. Furthermore, specimen sandwich was selected as per agreed core thickness as input variable.

(b) **Specimen for Flexural Rigidity Testing (ASTM C393)** The test specimen shall have a rectangular cross-section, with a depth equal to the thickness of the sandwich construction and a width that is at least twice the total thickness, three times the dimension of a core cell, and not exceeding half the span length. The specimen length shall be equal to the span length plus 50 mm (2 in.) or half the sandwich thickness, whichever is greater[61]. Sandwich thickness has no limitation and can be selected as per user requirement. Keeping in view the requirements; specimens having rectangular dimension of 150mm x 45mm were selected that fulfils all criteria of ASTM C393 standards.

3.6 CAD Modelling

The specimen geometry was constructed subsequent to sizing. CAD models were generated based on mid-level factors identified through Design of Experiment (DOE)

principles. Specifically, 15 specimens conforming to ASTM C365 and C393 standards were created using SolidWorks 2019 software, adhering to the DOE's simulated run order. This systematic approach ensured the accurate creation of specimens with controlled geometries, facilitating robust experimental investigations. CAD models for each type specimen are depicted in Figure 3.6 & 3.7.

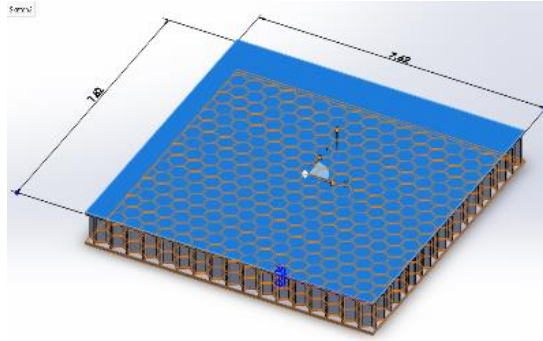


Figure 3-3 : Specimen for Compression Testing

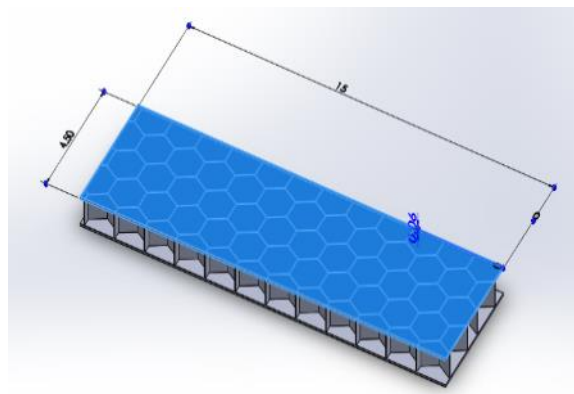


Figure 3-4 : Specimen for Flexural Testing

3.7 Design of Experiment

A Response Surface Methodology (RSM) based Design of Experiment (DOE) was employed to investigate the effects of geometrical variables on the mechanical properties of the sandwich structure. A Central Composite Design (CCD) with a face-centred point was selected for efficient resource management, consisting of 8 cube points, 6 axial points, and 1 centre point in the cube, resulting in 15 factorial runs. These runs were carried out to explore the design space and estimate the main effects and interactions between the three factors. The CCD design provides a robust and efficient approach to understanding the relationships

between the geometrical variables and the mechanical properties of the sandwich structure, enabling the identification of optimal design parameters. An illustration of CCD (Face centered) modelling is depicted in Figure 3.5

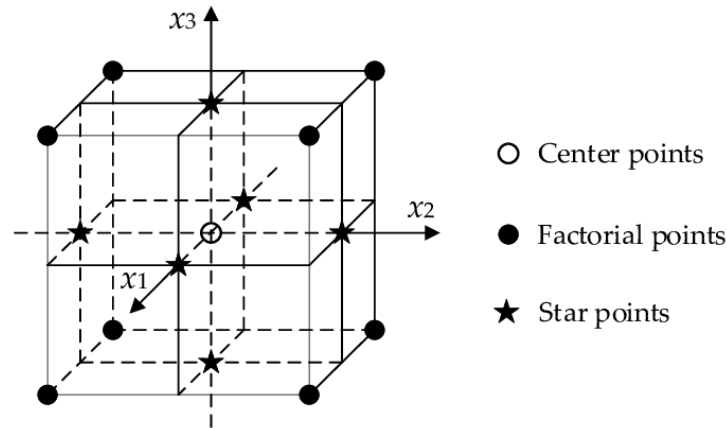


Figure 3-5 : Central Composite Design

Compressive Strength & Compressive Modulus were selected as Response to first experiment. Flexural rigidity was selected as the output response of second experiment. Three level factors which were selected as follows:-

Table 3-5. Factors for Geometric Input variables

<i>Factors</i>	<i>Unit</i>	<i>Levels</i>		
		<i>1</i>	<i>2</i>	<i>3</i>
Cell Size	mm	4	8	12
Wall Thickness	mm	0.4	0.8	1.2
Core Thickness	mm	6.35	12.70	19.05

Response Surface Methodology (RSM) was utilized to optimize the response variable. This approach facilitates the design of experiments (as presented in Table 3.7) and the development of a mathematical model that approximates the relationship between input parameters and output responses. Statistical analysis software, including Design-Expert 13 and Minitab, was employed to design experiments that consider all process parameters and analyse their significance. By integrating these tools, the relationships between input and response variables can be visualized as response surfaces or curves, providing insight into their

interactions and reciprocal influences. This analysis helps us understand how our experimental results relate to the various input parameters. Details discussion pertaining to RSM has already been carried out in Chapter 2. The detailed experimental run designed by Minitab for specimen fabrication with respect to geometrical variations were as follows:-

Table 3-6 : Experimental Runs as per DOE

<i>Experiment Run Order</i>	<i>Cell Size</i> <i>mm</i>	<i>Wall Thickness</i> <i>mm</i>	<i>Core Height</i> <i>mm</i>
1	4	0.4	6.35
2	12	0.4	6.35
3	4	1.2	6.35
4	12	1.2	6.35
5	4	0.4	19.05
6	12	0.4	19.05
7	4	1.2	19.05
8	12	1.2	19.05
9	4	0.8	12.7
10	12	0.8	12.7
11	8	0.4	12.7
12	8	1.2	12.7
13	8	0.8	6.35
14	8	0.8	19.05
15	8	0.8	12.7

3.8 Printing of Specimens

After finalizing the Design of Experiment (DOE) and Computer-Aided Design (CAD) modelling, the next step was to physicalize the specimens using Fused Deposition Modelling (FDM) 3D printing technology. To initiate the printing process, the SolidWorks CAD files were converted into STL format, a standard file type for 3D printing. Next, the printing process parameters were selected as discussed earlier. Initial prototype was printed to verify the finesse of specimen. These parameters were selected based on optimized settings identified in the literature to ensure high-quality prints. The STL file was then sliced into layers and imported into the FDM printer's software, Cura 3D, to generate the G-Code file that controls the printing process. Finally, the specimens were printed layer by layer, following the precise instructions in the G-Code file, to create physical prototypes with complex geometries and precise

dimensions. All the specimens were also subjected to weigh calculation that were later used in performance ratio for weight optimization

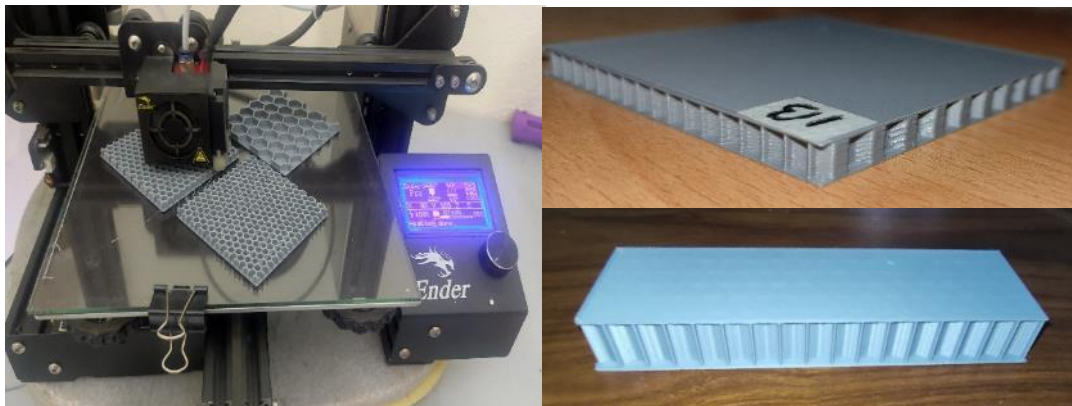


Figure 3-6 : Printing of Specimen

3.9 Mass Calculations

All the specimens printed were subjected to mass calculation in precision measurement Lab facility. These mass calculations were further utilized in performance / weight ratio that are discussed in detail in Chapter 4 Results and Analysis part.



Figure 3-7 : Mass calculation of Specimen

3.10 Experimentation

The selection of the Universal Testing Machine (UTM) was primarily based on availability, but compatibility with ASTM standards for Tensile and Flexural testing was

ensured. In accordance with ASTM standards the UTM was required to have a static and moving head with precise, controlled, and measurable movements. The machine had to be capable of applying load without bending or twisting the sample and measure the load accurately. The serrated gripping clamps were designed to hold the test specimen firmly, preventing slippage during load application without damaging the sample due to the serrated teeth. Additionally, the machine's calibration was verified and certified to be current, ensuring accurate and reliable test results. Both the tests were performed in Mechanics of Materials Lab Qchaida universal testing machine with 10KN load cell. Lab environment was maintained in accordance with ASTM standards of Relative Humidity less than 50% and Temperature of 25C°. Furthermore, each experiment was conducted twice and average value were taken in order ensure effective repeatability of results.

(a) ***Flatwise Compression Test*** The flat wise compression test was performed In accordance with ASTM C365 Figure 3.16., by applying a load to the specimen through a spherical loading block, which ensured uniform distribution of the load across the entire loading surface. The block was suspended and self-aligning, guaranteeing precise alignment and even load distribution. The load was applied at a constant rate, controlled by the cross-head movement of the testing machine, allowing for the determination of the specimen's compressive properties. The test enabled the measurement of key parameters, including compressive strength, modulus of elasticity using following equations:-

$$\sigma = \frac{P}{A}$$

where;

σ = Compressive strength, MPa (psi)

P = Ultimate load, N (lb); and

A = cross-sectional area, mm² (in.²).

Similarly, Compressive Modulus was calculated using Equation

$$E = \frac{St}{A}$$

where;

$E = \text{Compressive Modulus, MPa (psi)}$

$S = \frac{\Delta P}{\Delta u}$ slope of initial linear portion of load – deflection curve

$t = \text{Core thickness, mm}$



Figure 3-8 : Flatwise Compression Test

(b) **Three Point Bend Testing** The three-point bend test (Mid span loading) was performed in accordance with ASTM C393 Figure 3.16. The load was applied at a constant rate at the midpoint of specimen and maximum applied force was recorded at yield point. Following equation are used to calculate responses from load – deflection curve: -

Core Shear Stress is calculated as follows: -

$$\tau = \frac{P}{(d + c)b}$$

where:

τ = core shear stress, MPa (psi);
 P = load, N (lb);
 d = sandwich thickness, mm (in.);
 c = core thickness, mm (in.); and
 b = sandwich width, mm (in.).

Face Bending Stress is calculated as follows: -

$$\sigma = \frac{PL}{2t(d+c)b}$$

where:

- σ = facing bending stress, MPa (psi);
- t = facing thickness, mm (in.); and
- L = span length, mm (in.).

Midspan Deflection is calculated as follows: -

$$\Delta = \frac{PL^3}{48D} + \frac{PL}{4U}$$

total bending shear

where:

- Δ = total beam midspan deflection, mm (in.);
- G = core shear modulus, MPa (psi);
- E = facing modulus, MPa (psi); and
- D = panel bending stiffness, N-mm² (lb-in.²).

$$D = \frac{E(d^3 - c^3)b}{12}$$

same facings

$$D = \frac{E_1t_1E_2t_2(d+c)^2b}{4(E_1t_1 + E_2t_2)}$$

different facings

$$U = \frac{G(d+c)^2b}{4c}$$

U = panel shear rigidity, N (lb)

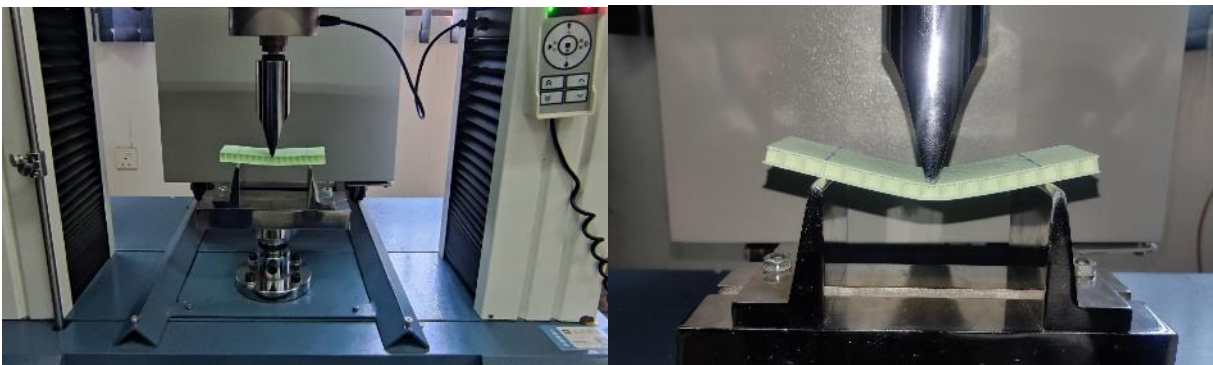


Figure 3-9 : Three Point Bending Test

CHAPTER 4 : RESULTS AND DISCUSSIONS

This chapter presents the results and discussion of the study conducted to analyse the effect of geometrical variations in term on cell size, wall thickness and core height on mechanical characteristics of 3D Printed Honeycomb Sandwich Structure (HCSS). Firstly, the statistical Design of Experiments (DOE) was utilized to analyse the impact of variations in mentioned, and the results obtained from this analysis will be presented and discussed in detail. The chapter will provide insights into the significant effects of each geometrical characteristics and its implications for conducted two experiments; (i) Compressive Strength as per ASTM C365 (ii) Flexural Rigidity as per ASTM C393. Further the performance ratios in terms of strength to weight and flexural rigidity to weight ratios were calculated in order to achieve optimum weight ratio of HCSS. Moreover, the chapter will present the outcomes of response with relation to input variable and its model statistical validation using Design Expert and Minitab software. Statistical validation will be performed using regression analysis, ANOVA and Response Surface Methodology techniques. The optimization strategies aimed at identifying the optimal combination of geometrical features while keeping the maximum compressive strength and minimum deflection in HSCC will be aimed. The chapter will conclude by proposing a regression model that can be used for future predictions of output responses, based on the insights obtained from the experimental results. The proposed model aims to contribute to the advancement of HSCC and in FDM by providing a reliable tool for predicting key mechanical properties, which is a critical factor affecting in designing and selecting the honeycomb structures. Overall, this chapter aims to provide a comprehensive understanding of the impact of geometrical variations of PLA based HSCC manufactured with FDM technology.

4.1 Analysis of the Flatwise Compression Test (ASTM C365)

The data obtained from the Flatwise Compression Test (ASTM C365) was compiled using the data points acquired through built in software of Universal Testing Machine (UTM). Initially, the plots were created on Microsoft Excel and then further analysed on Design Expert and Minitab for a more comprehensive and detailed statistical analysis. Each specimen was

printed and experimented twice to ascertain the confidence on repeatability of values. Mean average of both experimented specimen's data was taken and evaluated.

4.1.1 Stress – Strain Curve

The stress-strain curve as a first step was obtained. It depicted a graphical representation showing the relationship between stress (force applied per unit area) and strain (resulting deformation) of a HSCC. In Figure 4.1 distinct regions such as Linear elastic region, Plateau region, Densification which are main characteristics of Sandwich structure were evident in similar manner as they are classified in literature Gibson [1]. The slope of the curve in the elastic region represents the material's stiffness or Young's modulus, while the area under the curve indicates the material's toughness Gohar, et al. [50]. Understanding the stress-strain curve is crucial in determining the mechanical properties and behaviour of materials under different loading conditions. In the experiment, Samples with larger peak load like 3B did not exhibited the plateau region or densification; probably due to limitation of maximum limit of Ultimate tensile machine (100KN) which was capable of applying load till its 80% peak capability. In case of availability of large load cell, phenomenon of plateau region and densification could have been observed for these specimens too. HSCC structures having core height at mid and high level exhibited more pronounced plateau region in comparison to structures having low level core height.

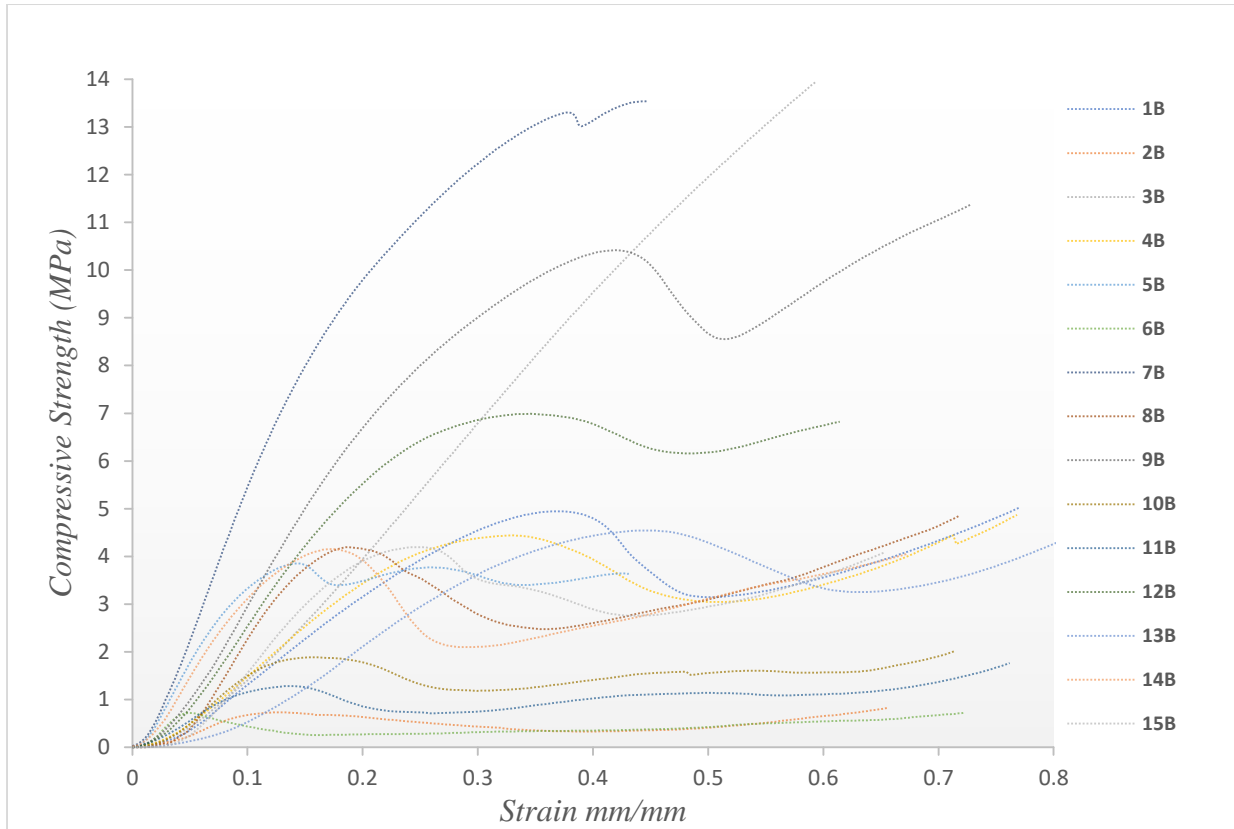


Figure 4-1 : Stress – Strain Curve for Flatwise Compression Testing

4.1.2 Analytical Results

Results obtained from Stress – Strain curve were further used for analytical calculations as per theoretical equations of ASTM standards as discussed in Chapter 3 – Experimentation. Values which were obtained are tabulated below in Table 4.1, where maximum Compressive Strength was exhibited by Specimen 3B which was having minimum cell size, maximum wall thickness and minimum core height. However, Maximum compressive modulus was shown by specimen 7B having maximum core height. Details interaction of these variable with the response are discussed in statistical analysis.

Table 4-1 : Results of Flatwise Compression Test (ASTM C365)

<i>Specimen ID</i>	<i>Cell Size</i> <i>mm</i>	<i>Wall Thickness</i> <i>mm</i>	<i>Core Thickness</i> <i>mm</i>	<i>Ultimate Compressive Strength</i> <i>MPa</i>	<i>Elastic Modulus</i>
1B	4	0.4	6.35	4.94	19.944588
2B	12	0.4	6.35	0.84	10.296947
3B	4	1.2	6.35	13.96	28.159971
4B	12	1.2	6.35	4.44	21.289778
5B	4	0.4	19.05	4.13	45.158251
6B	12	0.4	19.05	0.72	22.602982
7B	4	1.2	19.05	13.54	64.899556
8B	12	1.2	19.05	4.19	39.521013
9B	4	0.8	12.7	10.42	42.423239
10B	12	0.8	12.7	1.89	21.305246
11B	8	0.4	12.7	1.28	15.459923
12B	8	1.2	12.7	6.99	36.019741
13B	8	0.8	6.35	4.54	17.7663
14B	8	0.8	19.05	4.15	40.937391
15B	8	0.8	12.7	4.56	30.098353

4.1.3 Mean effect and Pareto standardized effect

Based upon the compressive testing, main objective function remains to achieve highest value of compressive strength for a HSCC. However, output response of Compressive Modulus was also studied which would also give idea about the deformation and stiffness of structure. Key geometrical features as selected as variables are effecting the compressive strength in comparable manner under specific condition can be determined by plotting them on the chart. A main effects plot was thus plotted to gauge the response at the mean response values at each level of process variables including cell size, wall thickness and core height. Relative strength of the effects these factors can be compared. Figure 4.2 (a) suggest that decreasing the cell size and increasing the wall thickness will increase Compressive Strength and means. However, effect Core height of structure on Compressive strength did not show much contribution. A more strengthen HSCC structure may thus be developed with smaller cell size and increased wall thickness. However, 4.2 (b), Core Thickness play its impact on Compressive Modulus. Effect of first two variable remains the same, but core thickness impact much larger variation on modulus its increase.

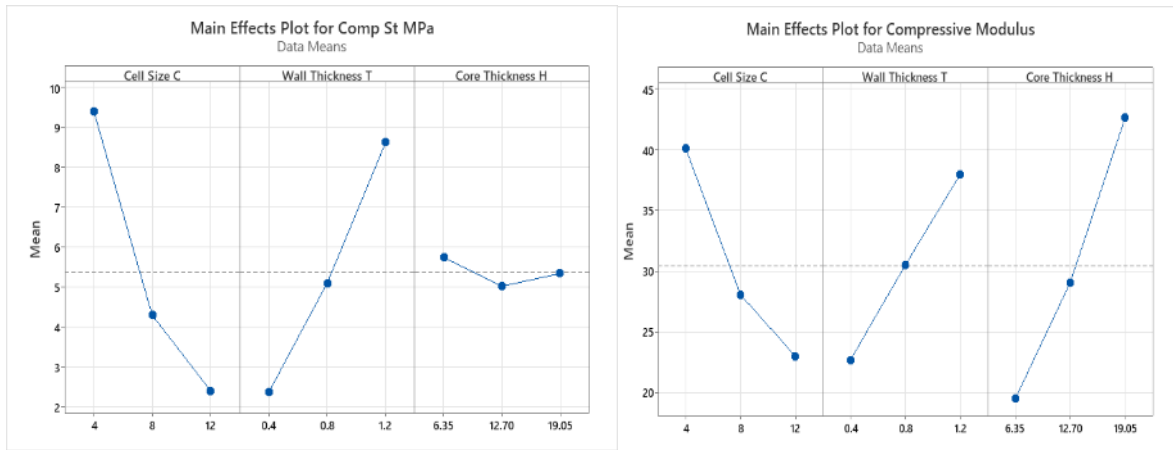


Figure 4-2 : Effect of major influences on (a) Mean value on the Max Comp Strength
(b) Mean value of Compressive Modulus

Similarly, Pareto chart for standardized effect presented at Figure 4.3 (a) Cell Size effects 18.79% to the absolute value of compressive strength in positive manner and Wall thickness effects 16.78%. Meanwhile, Interaction of core height is potentially significant with the compressive strength (below the reference line). For Figure 4.3 (b) Core Height has 13.78% effect on Modulus mean value. Meanwhile effect of cell size and wall thickness remains at 10.1% and 9.09 % respectively.

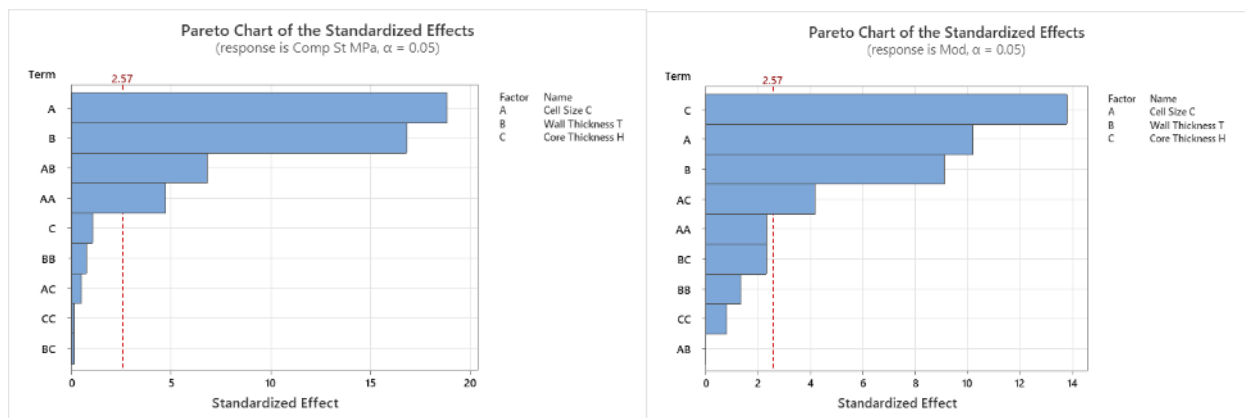


Figure 4-3 : Pareto Chart of Standardized Effect (a) Compressive Strength (b) Compressive Modulus

It proposed that each parameter's significance be listed in descending order on compressive strength is Cell Size > Wall Thickness > Core Thickness. It shows that cell size has the most prominent effect on HSCC compressive strength, and core thickness has the least contributing impact. However, for compressive Modulus order becomes Core Height > Cell

Size > Wall Thickness. It also means that the with the addition of core height structure will be stiffer and tends to low deflection under loads.

4.1.4 Design Analysis by RSM

Response Surface Methodology (RSM) was employed to develop mathematical models that quantify the relationships between variables and Compressive Strength and Modulus. To ensure the accuracy of these models, we conducted Analysis of Variance (ANOVA) tests. Our analysis compared the significance of linear, two-factor interaction (2FI), and quadratic models. The results, presented in Tables 4.2 and 4.3, reveal that the quadratic model best fits the data for Compressive Strength, while the 2FI model is most suitable for Compressive Modulus. Moreover, the high adjusted R-squared values indicate that the regression models effectively explain the underlying processes, providing a reliable foundation for predictions and optimization. In Table 4.2 & 4.3 of this study, the adjusted R² value is 98.04 % & 94.54%, suggesting that the regression model can only explain 1.96% & 5.46% of the changes, indicating that the model's fit is good.

Table 4-2 : Model’s Summary Statistics for Compressive Strength

<i>Source</i>	<i>Std. Dev.</i>	<i>R²</i>	<i>Adjusted R²</i>	<i>Predicted R²</i>	<i>PRESS</i>	
Linear	1.56	0.8915	0.8620	0.7662	57.64	
2FI	1.15	0.9572	0.9252	0.8207	44.21	
Quadratic	0.5879	0.9930	0.9804	0.9359	15.80	Suggested
Cubic	0.1409	0.9999	0.9989	0.7571	59.89	Aliased

Table 4-3 : Model’s Summary Statistics for Compressive Modulus

<i>Source</i>	<i>Std. Dev.</i>	<i>R²</i>	<i>Adjusted R²</i>	<i>Predicted R²</i>	<i>PRESS</i>	
Linear	4.79	0.9132	0.8896	0.8097	553.07	
2FI	3.37	0.9688	0.9454	0.8668	387.18	Suggested
Quadratic	2.66	0.9879	0.9660	0.8786	352.76	
Cubic	1.99	0.9986	0.9809	-3.1193	11971.72	Aliased

The significance of each regression coefficient in our models (Tables 4.4 and 4.5) was examined to determine if they have a substantial impact on the response values. Our tests confirmed that the produced models are statistically significant at a 95% confidence level. Using the backward elimination approach, we analysed the significance of each term in the quadratic equation model for Compressive Strength and removed non-significant terms. We found that terms A, B, C, AB, AC, BC, A², B², and C² are significant, with p-values less than 0.0500. In contrast, terms with p-values greater than 0.1 were deemed non-significant and removed. Similarly, for Compressive Modulus, only terms A, B, C, AB, AC, and BC were significant, and the remaining interactive terms were eliminated.

By integrating the examined variables, the regression model can be leveraged to predict Compressive Strength and Compressive Modulus with enhanced accuracy. Specifically, the optimal predictive equation for Compressive Strength is as follows :-

$$\text{Comp Strength} = 6.06 - 1.958 \times A + 17.51 \times B - 0.035 \times C + 0.1087 \times C^2 - 1.74 \times B^2 - 0.00160 \times C^2 - 0.887 \times A \times B + 0.00425 \times A \times C + 0.0130 \times B \times C$$

MPa

In terms of Compressive Modulus, the regression equation gets formulated as follows:

$$\text{Compressive Modulus} = 11.95 - 4.04 \times A + 30.8 \times B + 1.52 \times C + 0.242 \times A^2 - 14.1 \times B^2 + 0.0336 \times C^2 - 0.004 \times A \times B - 0.1546 \times A \times C + 0.859 \times B \times C$$

To evaluate the significance of the regression models, ANOVA analysis was performed, with results presented in Tables 4.6 and 4.7. The coefficient of variation (CV) for the regression models was found to be 10.94% and 11.08% for Compressive Strength and Compressive Modulus, respectively, indicating a high degree of reliability. The F-statistic values of 28.38 and 24.13, respectively, exceed the desirable threshold of 4, suggesting that the models possess sufficient flexibility for navigation within the design space. The R-squared values of 0.993 and 0.9688, respectively, demonstrate an excellent fit, with minimal discrepancy between predicted and observed values. Furthermore, the high adjusted R-squared

values indicate that the regression models provide an adequate explanation of the underlying processes, supporting their use in predictive applications

Table 4-4 : ANOVA for Quadratic model (Compressive Strength)

<i>Source</i>	<i>Sum of Squares</i>	<i>Degree of freedom</i>	<i>Mean Square</i>	<i>F-value</i>	<i>p-value</i>	<i>Prob>F</i>
Model	244.84	9	27.20	78.71	< 0.0001	Significant
A-Cell Size	122.03	1	122.03	353.08	< 0.0001	
B-Wall Thickness	97.40	1	97.40	281.82	< 0.0001	
C-Core Thickness	0.3954	1	0.3954	1.14	0.3337	
AB	16.10	1	16.10	46.57	0.0010	
AC	0.0934	1	0.0934	0.2704	0.6253	
BC	0.0087	1	0.0087	0.0251	0.8804	
A ²	7.78	1	7.78	22.51	0.0051	
B ²	0.1994	1	0.1994	0.5769	0.4818	
C ²	0.0107	1	0.0107	0.0311	0.8669	
Residual	1.73	5	0.3456			
Cor Total	246.57	14				

Table 4-5 : ANOVA for Quadratic model (Compressive Modulus)

<i>Source</i>	<i>Sum of Squares</i>	<i>Degree of freedom</i>	<i>Mean Square</i>	<i>F-value</i>	<i>p-value</i>	<i>Prob>F</i>
Model	2815.53	6	469.25	41.37	< 0.0001	significant
A-Cell Size	732.22	1	732.22	64.55	< 0.0001	
B-Wall Thickness	584.11	1	584.11	51.50	< 0.0001	
C-Core Thickness	1337.76	1	1337.76	117.94	< 0.0001	
AB	0.0003	1	0.0003	0.0000	0.9963	
AC	123.37	1	123.37	10.88	0.0109	
BC	38.07	1	38.07	3.36	0.1043	
Residual	90.74	8	11.34			
Cor Total	2906.27	14				

Table 4-6 : Fit Statistics (Compressive Strength)

Std. Dev.	0.5879	R ²	0.9930
Mean	5.37	Adjusted R ²	0.9804
C.V. %	10.94	Predicted R ²	0.9359
		Adeq Precision	28.3869

Table 4-7 : Fit Statistics (Compressive Modulus)

Std. Dev.	3.37	R ²	0.9688
Mean	30.39	Adjusted R ²	0.9454
C.V. %	11.08	Predicted R ²	0.8668
		Adeq Precision	24.1368

Residual analysis is a crucial step in statistical modelling, enabling evaluation of model quality, detection of systematic errors, and validation of assumptions. It facilitates outlier identification, model refinement, and ensures reliable insights, thereby enhancing confidence in predictions. The normal probability plot Figure 4-4 (a) exhibits a linear pattern, indicating normality of residuals, while the residual distribution plot Figure 4-4 (b) shows a random and scattered pattern, confirming the absence of systematic errors and supporting the assumption of constant variance. These observations validate the model's assumptions, ensuring its reliability for predictive purposes. These findings confirm the assumption of constant variance, and the study's results collectively substantiate the validity of the model's assumptions, thereby ensuring the reliability and generalizability of the conclusions drawn from the analysis. Similar, same pattern for Compressive Modulus were observed as depicted in Figure 4-5 (a) & 4-5 (b).

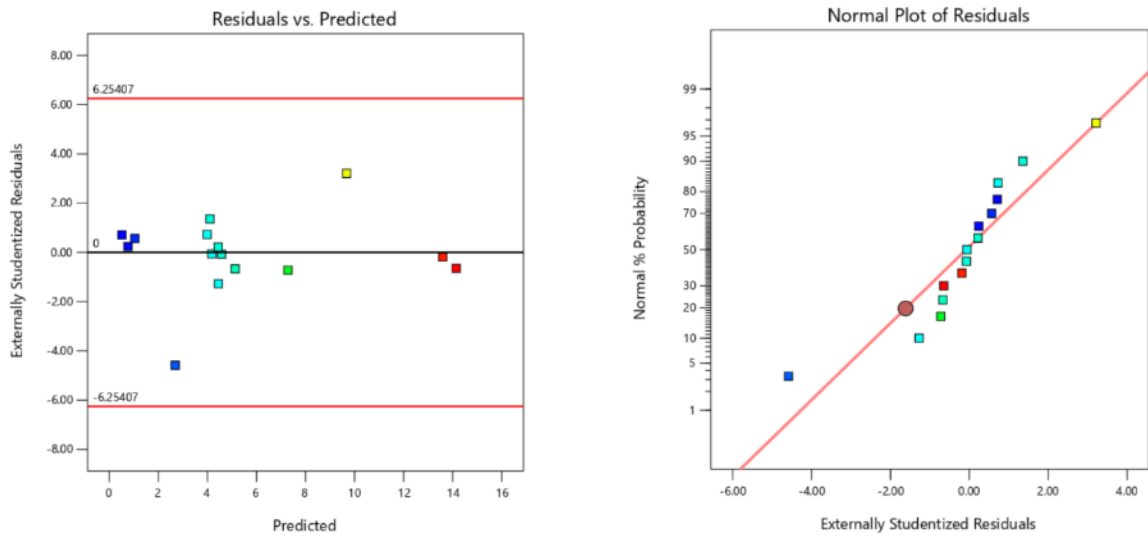


Figure 4-4 : (a) Residuals vs predicted values for Compressive Strength; (b) Normal Probability plot of the residuals

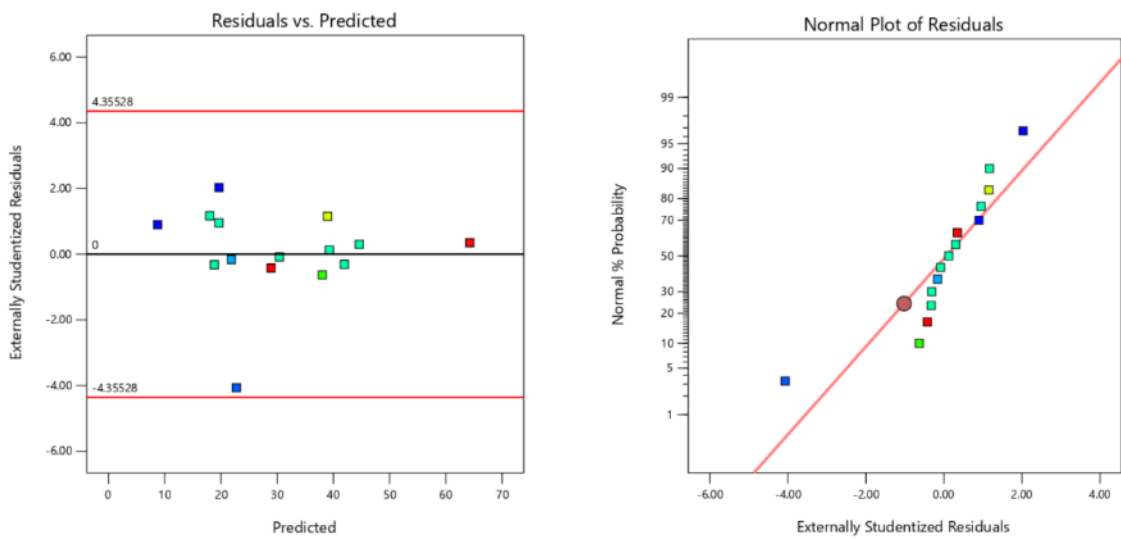


Figure 4-5 : (a) Residuals vs predicted values for Compressive Modulus ; (b) Normal Probability plot of the residuals

To elucidate the effects of cell size, wall thickness, and core height on Compressive Strength and Compressive Modulus, three-dimensional surface graphs and corresponding contour plots were generated using the regression model. The curved sections of these graphs illustrate the relationships between various combinations of factors. Contour plots reveal the impact of interactions between two independent variables as sloping curves, with ellipsoidal contours indicating strong interactions and spherical contours suggesting weaker relationships.

Specifically, Figure 4.4 presents Response surface graphs and contour plots depicting the influence of cell size and wall thickness on Compressive Strength, with core thickness held at its maximum level. These visualizations facilitate a comprehensive understanding of the complex interactions between these variables. As cell size decrease and wall thickness increase, compressive strength increase in stable gradient until it reaches the halfway point, after which it begins to increase steeper gradient until it reaches highest value. Maximum compressive strength is achieved at lowest cell size and highest wall thickness.

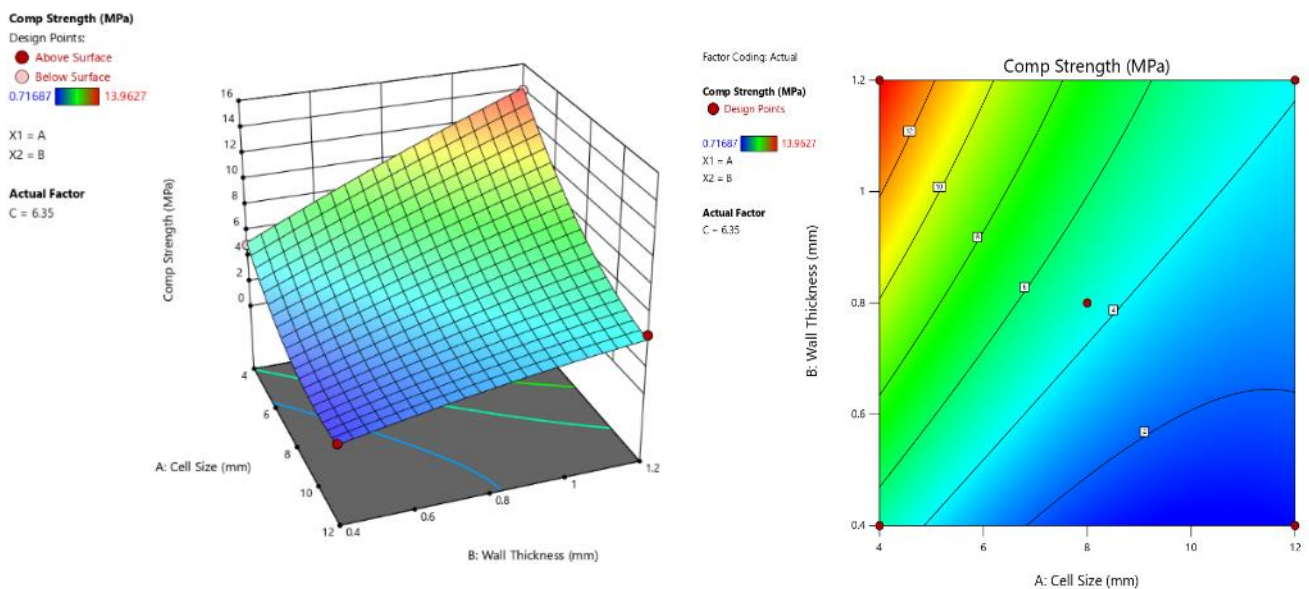


Figure 4-6 : Effect of Cell Size and wall thickness on the residual stress: (a) response surface and (b) contour plots

Figure 4.5. shows the three-dimensional surface and its contours, illustrating the effect on cell size and core thickness on Compressive Modulus while keeping the wall thickness at maximum level.

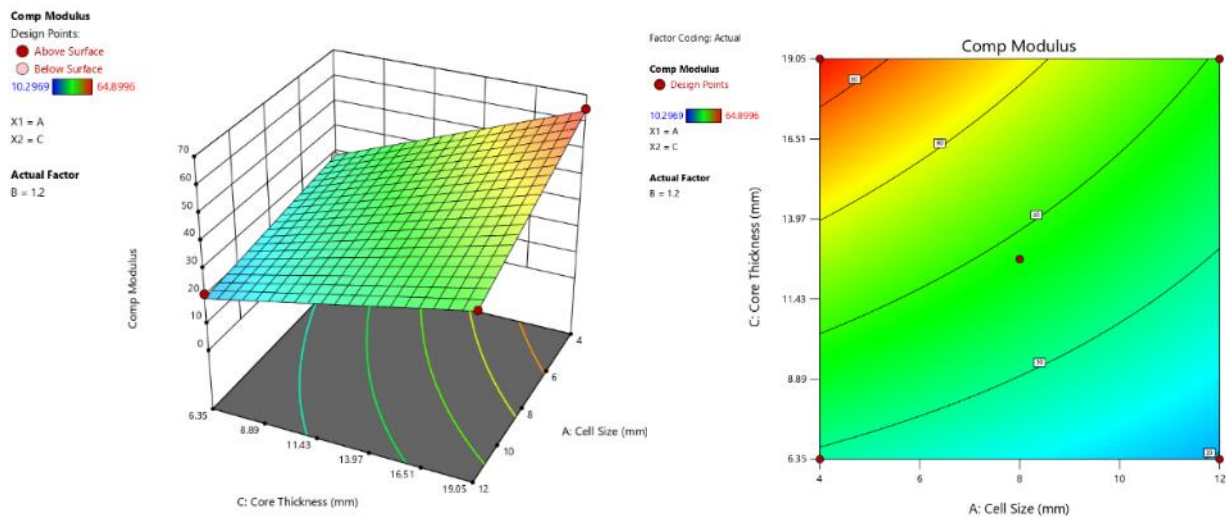


Figure 4-7 : . Effect of Cell Size and Core Thickness on the Compressive Modulus: (a) response surface and (b) contour plots

The surface plots illustrate that increasing core thickness has a profound impact on compressive modulus, consistent with findings from previous model analyses. To optimize the stiffness of the HSCC structure within the experimental design space, a core thickness of 19.05mm is recommended, which concurrently yields maximum compressive strength. Notably, the results indicate a beneficial interaction effect, suggesting that the combined influence of core thickness and other variables enhances the overall performance of the HSCC structure.

This study employs a RSM based optimization approach to identify the optimal parameter set within the design space, aiming to minimize residual stress. Figure 4-8 presents the interaction plot of desirability, where a desirability value of 1 represents the optimal combination of parameters yielding maximum Compressive Strength and Compressive Modulus. As desirability decreases, the response values also decrease, which is not desirable in this context. The optimization results reveal that the optimal parameters for achieving maximum desirability (1) are: Cell size = 4mm, Wall thickness = 0.4mm, and Core thickness = 6.35mm. These parameters constitute the optimal design point within the design space.

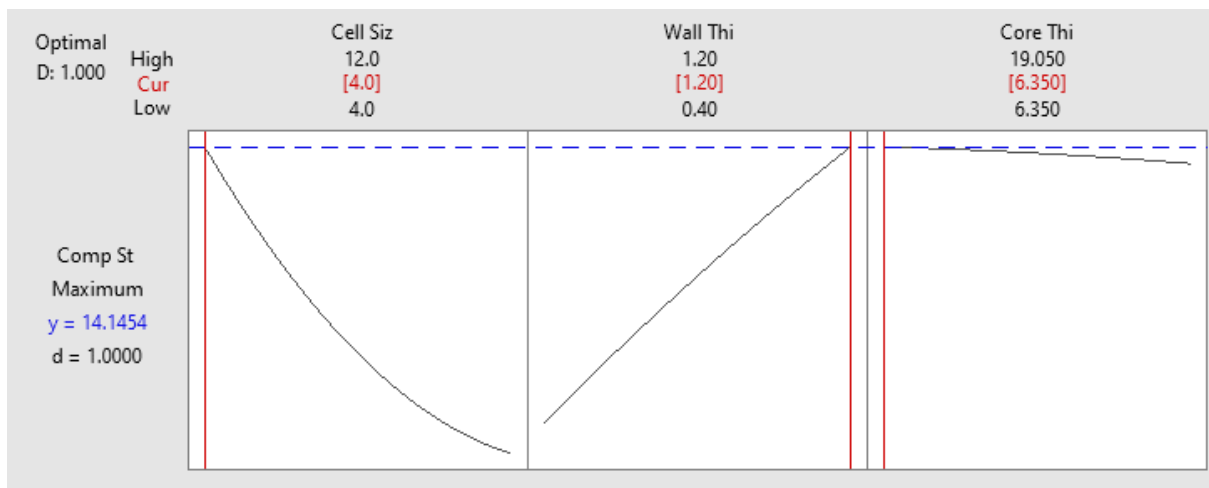


Figure 4-8. Optimal predicted parameters with desirability (Compressive Strength)

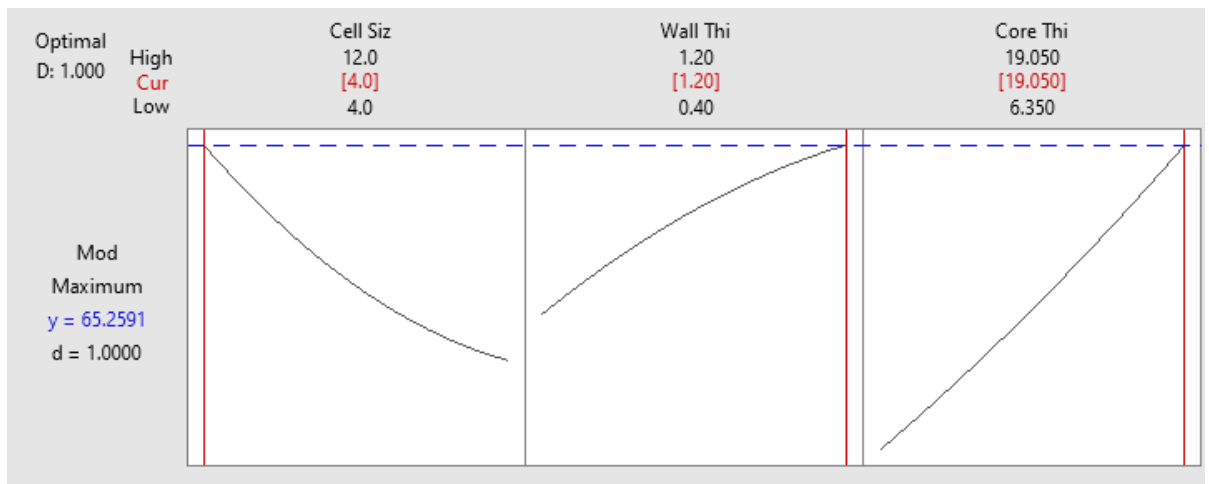


Figure 4-9 : Optimal predicted parameters with desirability (Compressive Modulus)

Table 4-8. Optimal experimental parameters for Max Strength

<i>Optimum Input Variables</i>	<i>Setting</i>
Cell Size mm	4mm
Wall Thickness	1.2mm
Core thickness	6.35mm

Table 4-9 : Optimal experimental parameters for Compressive Modulus

<i>Optimum Input Variables</i>	<i>Setting</i>
Cell Size mm	4mm
Wall Thickness	1.2mm
Core thickness	19.05 mm

4.2 Analysis of Flexural Testing of Structure (ASTM C393)

The data derived from the Flexural testing (ASTM C393) involving a mid-span load (03-point bend test) was gathered using the data points obtained from the Universal Testing Machine (UTM) built-in software. In the beginning, charts were produced in Microsoft Excel and then further examined in Design Expert and Minitab to conduct a more thorough and detailed statistical analysis. Each sample was tested and analysed twice to ensure the reliability of the values. The mean average of the data from both samples was calculated and assessed.

4.2.1 Load – Deflection Curve

First of all, a Load–Deflection curve was obtained; this graphical representation showed the relationship between force and resulting deflection of an HSCC. In Figure 4.8, similar to what is classified in literature (Gibson), peak load was obtained after an elastic region. Beyond the peak load the load applied starts to drop as the structure was not able to sustain applied load. This point represents the highest point on the load-deflection curve defined as peak load was further utilized in provide analytical equations to draw relations among the variables. Almost all specimens showed a common phenomenon of sharp drop in applied force after reaching a peak load depicting a structure breakage. Max peak load of 700N was observed on specimen 5A.

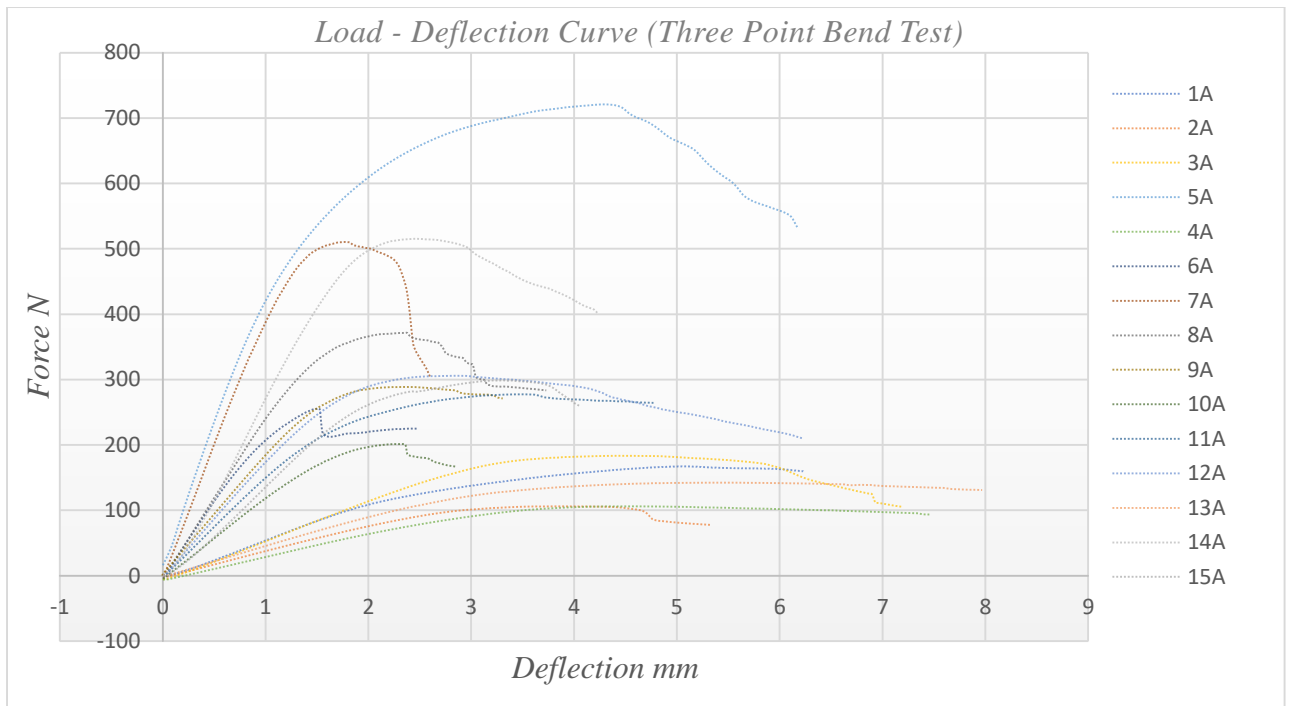


Figure 4-10 : Load – Deflection Curve (Three Point bend Test)

4.2.2 Analytical Results

Results obtained from Load – Deflection curve were further used for analytical calculations as per theoretical equations discussed for ASTM C393. Maximum flexural rigidity as a whole was objection function in this experiment and testing. Values obtained for signification output response are tabulated below in Table 4-10, where maximum flexural rigidity was exhibited by Specimen 7A which was having minimum cell size, maximum wall thickness and maximum core height. Same specimen also depicted minimum deflection in its structure under applied load. Details interaction of these variable with the response are discussed in statistical analysis. A key take from data is the flexural rigidity calculated through experiments and analytical equations showed a significant difference; same will be discussed as observations in the final part of this chapter.

Table 4-10 : Results of Flatwise Compression Test (ASTM C393)

<i>Specimen</i>	<i>Cell Size</i>	<i>Wall Thickness</i>	<i>Core Height</i>	<i>Core Shear Stress</i>	<i>Face Bending Stress</i>	<i>Flexural Rigidity</i>	<i>Exp Deflection</i>
<i>ID</i>	<i>mm</i>	<i>mm</i>	<i>mm</i>	<i>MPa</i>	<i>MPa</i>	<i>N/mm</i>	<i>mm</i>
1A	4	0.4	6.35	0.31	25.60	28.73	6.69
2A	12	0.4	6.35	0.17	14.13	27.61	3.84
3A	4	1.2	6.35	0.29	24.47	40.32	4.56
4A	12	1.2	6.35	0.17	14.17	23.54	4.52
5A	4	0.4	19.05	0.41	34.20	162.86	4.46
6A	12	0.4	19.05	0.13	10.86	123.40	1.87
7A	4	1.2	19.05	0.29	24.25	288.31	1.78
8A	12	1.2	19.05	0.21	17.54	149.56	2.49
9A	4	0.8	12.7	0.24	20.09	124.33	2.32
10A	12	0.8	12.7	0.17	14.01	87.71	2.30
11A	8	0.4	12.7	0.24	20.24	99.68	2.92
12A	8	1.2	12.7	0.26	21.33	106.26	2.88
13A	8	0.8	6.35	0.23	19.19	29.04	4.96
14A	8	0.8	19.05	0.29	24.36	199.58	2.59
15A	8	0.8	12.7	0.28	23.29	115.03	2.91

4.2.3 Mean effect and Pareto standardized effect

Based upon the flexural rigidity, main objective function remains to achieve maximum value to minimize the deflection under an applied load for a HSCC. Key geometric characteristics selected as variables can be assessed for their impact on flexural rigidity by plotting them on a chart. A main effects plot was created to evaluate responses at mean values for each level of process variables such as cell size, wall thickness, and core height. This allows for comparison of the relative influence of these factors. Figure 4-11 suggest that decreasing the cell size and increasing the wall thickness will increase flexural rigidity of the structure and means. Moreover, Core thickness has much more significant impact in its mid to high level values. A more rigid HSCC structure may thus be developed with thicker cores.

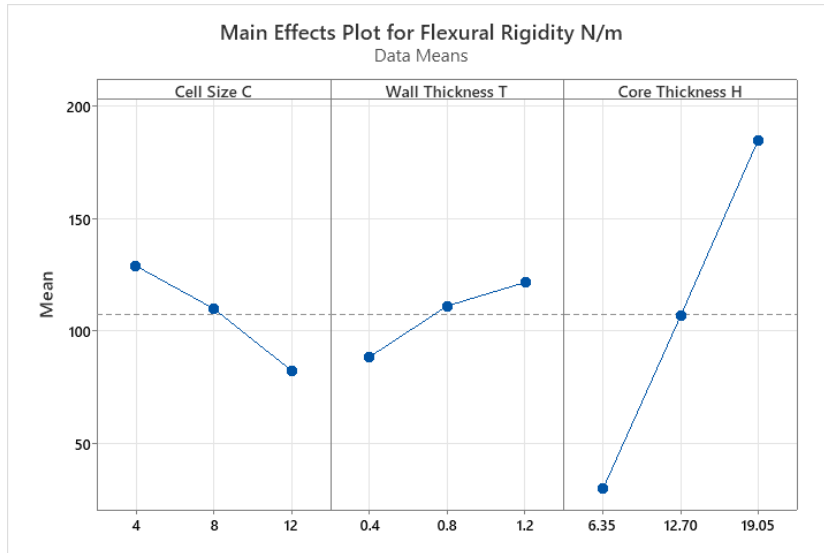


Figure 4-11 : Effect of major influences on Flexural Rigidity

Similarly, Pareto chart for standardized effect presented at Figure 4-12 Core thickness effected 13.87% to the absolute value of flexural rigidity in positive manner, followed by cell size and interaction between core thickness and cell size. Meanwhile, Interaction of wall thickness shows marginal interaction effect on response (Slightly above the reference line).

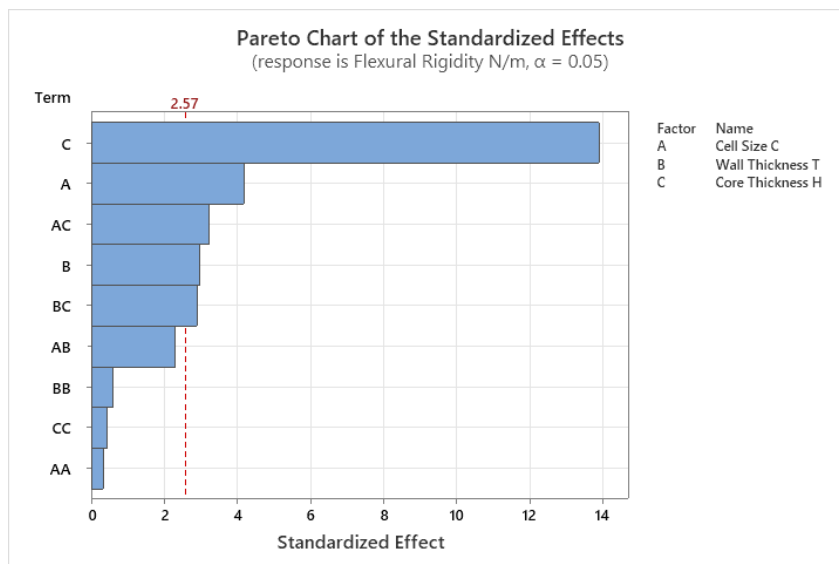


Figure 4-12 : Pareto Chart of Standardized Effect Flexural Rigidity

The results of the optimization study indicate the relative importance of each parameter in descending order Core thickness > Cell size > wall thickness; highlighting their respective

contributions to the optimal design. It shows that core thickness has the most prominent effect on HSCC rigidity, and wall thickness has the least contributing impact.

4.2.4 Analysis of Response Surface Method

RSM was employed to develop quantitative mathematical models for Flexural Rigidity. Analysis of Variance (ANOVA) was conducted to evaluate the significance of various models, including linear, two-factor interaction (2FI), and quadratic models. The statistical results, presented in Table 4.11, indicate that the 2FI model is the most suitable for Flexural Rigidity. The high adjusted R-squared value of 96.04% suggests that the regression model explains a significant proportion of the variation in Flexural Rigidity, with only 3.96% of the changes remaining unexplained. This indicates a good fit of the model, demonstrating its adequacy in explaining the underlying process.

Table 4-11 : Model's Summary Statistics for Flexural Rigidity

<i>Source</i>	<i>Std. Dev.</i>	<i>R²</i>	<i>Adjusted R²</i>	<i>Predicted R²</i>	<i>PRESS</i>	
Linear	28.94	0.8809	0.8484	0.7133	22180.44	
2FI	14.80	0.9773	0.9604	0.7883	16374.09	Suggested
Quadratic	17.65	0.9799	0.9436	0.6484	27195.56	
Cubic	5.19	0.9997	0.9951	-0.0497	81201.60	Aliased

The significance of each regression coefficient in the model, presented in Table 4.12, was evaluated to determine the impact of each term on the response values. The results indicate that the model has a statistically significant level of 95%. Using the backward elimination approach in ANOVA analysis for Flexural Rigidity, the significance of constant, interaction, and square terms was assessed, and non-significant terms were eliminated. P-values less than 0.0500 denote significant model terms. The analysis reveals that terms C, AC, and BC are statistically significant, while the remaining terms can be removed without compromising the model's accuracy.

By combining the investigated variables, the regression model may be exploited to forecast Flexural Rigidity. In terms of Flexural Rigidity, the following equation for optimal exploration in design space is as follows: -

$$\begin{aligned} \text{Flexural Rigidity } N/m &= -118.0 + 14.9 \times A + 89 \times B + 9.85 \times C - 0.221 \times A^2 - 41.2 \times B^2 \\ &+ 0.118 \times C^2 - 8.98 \times A \times B - 0.789 \times A \times C + 7.09 \times B \times C \end{aligned}$$

To evaluate the significance of the regression models, Analysis of Variance (ANOVA) was conducted, with results presented in Table 4-13. The coefficient of variation (CV) for the regression model was found to be 13.82%, indicating a high degree of reliability. The adequacy precision value of 26.32 exceeds the desirable threshold of 4, suggesting that the model possesses sufficient flexibility for navigation within the design space. The R-squared value of 0.9773 demonstrates an excellent fit, with minimal discrepancy between predicted and observed values.

Table 4-12 : ANOVA for Quadratic model (Flexural Rigidity)

<i>Source</i>	<i>Sum of Squares</i>	<i>Degree of freedom</i>	<i>Mean Square</i>	<i>F-value</i>	<i>p-value</i>	<i>Prob>F</i>
Model	75602.01	6	12600.34	57.52	< 0.0001	significant
A-Cell Size	5416.74	1	5416.74	24.73	0.0011	
B-Wall Thickness	2746.55	1	2746.55	12.54	0.0076	
C-Core Thickness	59979.27	1	59979.27	273.79	< 0.0001	
AB	1651.63	1	1651.63	7.54	0.0252	
AC	3212.63	1	3212.63	14.66	0.0050	
BC	2595.19	1	2595.19	11.85	0.0088	
Residual	1752.57	8	219.07			
Cor Total	77354.59	14				

Table 4-13 : Fit Statistics (Flexural Rigidity)

Std. Dev.	14.80	R ²	0.9773
Mean	107.06	Adjusted R ²	0.9604
C.V. %	13.82	Predicted R ²	0.7883
		Adeq Precision	26.3276

The normal probability plot Figure 4-13 (a) displays a linear trend, indicating that the residuals follow a normal distribution, thereby satisfying the normality assumption. Furthermore, the residual distribution plot Figure 4-13 (b) exhibits a random and scattered pattern, confirming the absence of any systematic errors or patterns, and supporting the assumption of constant variance.

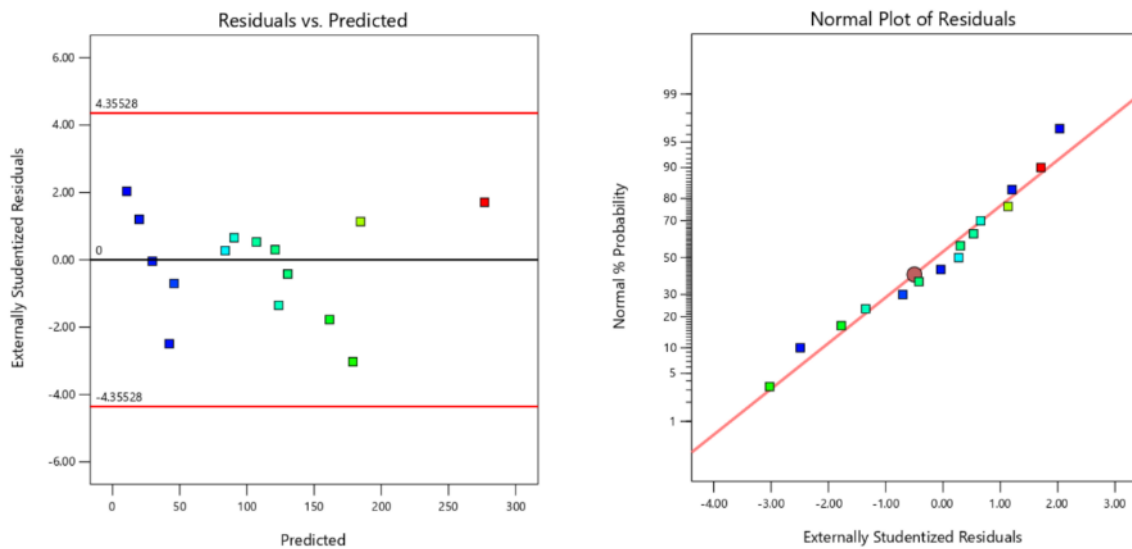


Figure 4-13 : (a) Residuals vs predicted values for Flexural Rigidity ; (b) Normal probability plot of the residuals (Flexural Rigidity)

For Surface plots, significant interaction of Core thickness with cell size is plotted. The influence of cell size and core thickness on Flexural Rigidity is depicted in three-dimensional surface graphs and corresponding contour plots in Figure 4-14. The wall thickness was fixed

at the highest level. As cell size decrease and core thickness increase, flexural Rigidity increases. Higher gradient was achieved with higher values of core thickness making its effect more prominent.

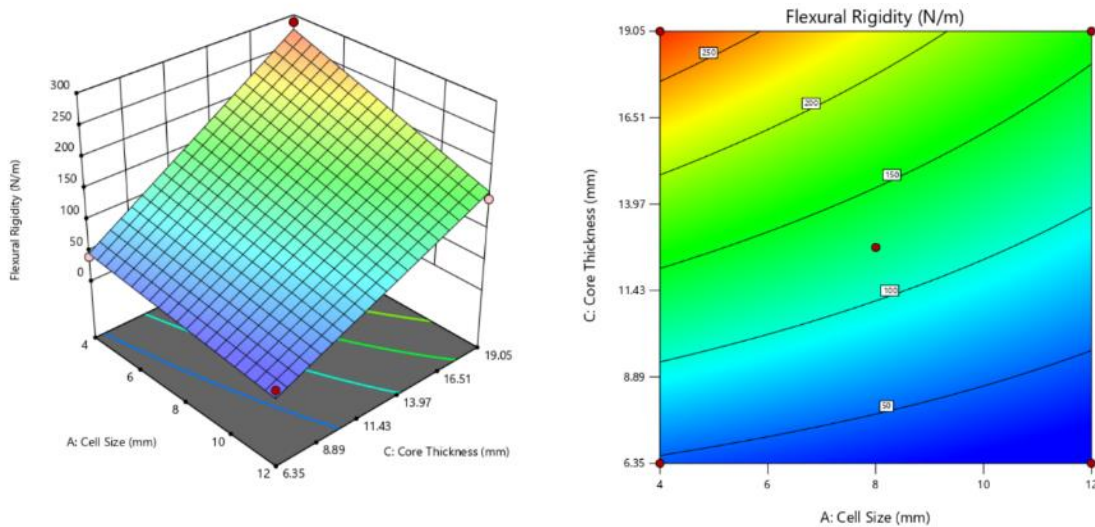


Figure 4-14 : Effect of Core thickness and Cell Size on the Flexural Rigidity: (a) Response surface plot (b) contour plots

Surface plots reveal that as the core thickness increases is significant for flexural rigidity as discussed in other model analysis, in order to make stiffest and rigid HSCC structure in experimental design space, Core thickness of 19.05mm is recommended. The results demonstrate that the interaction effect was beneficial.

As this study aims to find the optimal set of parameters within the design space to minimize the residual stress, an RSM-based optimization approach is used. Figure 4-15. depicts the all factors interaction plot of desirability, Desirability 1 means the maximum possible Flexural Rigidity by an optimal combination of parameters. As desirability decreases, response value decrease, which isn't of interest here. For maximum value as an objective function, the optimum parameters were found to be Cell size at 4mm, Wall thickness at 1.2mm and Core thickness at 19.05mm which gives an desirability of 0.9496.

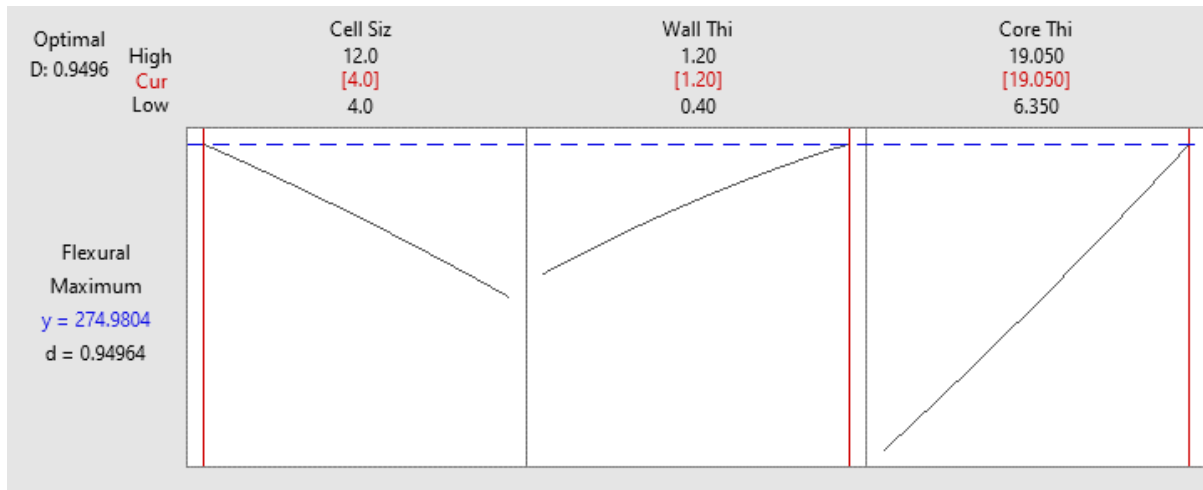


Figure 4-16 : Optimum desirability for flexural rigidity

Table 4-14 : Optimum input variables for Maximum Flexural Rigidity

<i>Optimum Input Variables</i>	<i>Setting</i>
Cell Size mm	4mm
Wall Thickness	1.2mm
Core thickness	19.05mm

4.3 Analysis of Performance to weight Ratio

The performance-to-weight ratio is a critical metric for evaluating the efficiency of sandwich structures. In this context, two key ratios are examined: compressive strength-to-weight ratio which will be titled as strength to weight ratio and flexural rigidity-to-weight ratio which will be titled as stiffness to weight ratio. These ratios provide insights into the structural performance of the sandwich structure relative to its weight, enabling the optimization of materials and design configurations. A higher compressive strength-to-weight ratio indicates improved load-carrying capacity without excessive weight penalty, while a higher flexural rigidity-to-weight ratio signifies enhanced stiffness and resistance to deformation without compromising on weight. By maximizing these ratios, sandwich structures can achieve improved performance, reduced weight, and enhanced overall efficiency.

4.3.1 Analytical Results

To assess the performance-to-weight ratios, the actual measured mass of each specimen was recorded and divided by the respective response values (compressive strength and flexural

rigidity). These ratios were then correlated with the input variables of cell size, wall thickness, and core thickness to investigate their effects on the performance-to-weight ratios. This analysis aimed to establish statistical relationships between the input variables and the performance-to-weight ratios as response.

As per the results in Table 4-15; Max Strength / weight ratio was exhibited by the specimen 3B. This specimen also depicted the maximum compressive strength. Key dimension of this specimen indicates that it holds the smallest cell size, maximum wall thickness and minimum core height.

As per the results in Table 4-16; Maximum Stiffness / weight ratio has been depicted by the specimen 14A. Key dimension of this specimen indicates that it holds the mid-level cell size, and wall thickness and maximum core height. Details interaction of these variable with the response are discussed in statistical analysis.

Table 4-15 : Strength / Weight Ratio

<i>Specimen ID</i>	<i>Cell Size</i> <i>mm</i>	<i>Wall Thickness</i> <i>mm</i>	<i>Core Height</i> <i>mm</i>	<i>Specimen Mass</i> <i>Gm</i>	<i>Compressive Strength</i> <i>MPa</i>	<i>Strength / Weight Ratio</i>
1B	4	0.4	6.35	16.21	4.94	0.305032
2B	12	0.4	6.35	11.255	0.84	0.0743585
3B	4	1.2	6.35	26.18	13.96	0.533334
4B	12	1.2	6.35	15.525	4.44	0.285895
5B	4	0.4	19.05	31.375	4.13	0.131792
6B	12	0.4	19.05	16.36	0.72	0.0438184
7B	4	1.2	19.05	61.58	13.54	0.219909
8B	12	1.2	19.05	31.45	4.19	0.133319
9B	4	0.8	12.7	35.06	10.42	0.297177
10B	12	0.8	12.7	18.715	1.89	0.100738
11B	8	0.4	12.7	16.605	1.28	0.077138
12B	8	1.2	12.7	28.945	6.99	0.241403
13B	8	0.8	6.35	16.295	4.54	0.278875
14B	8	0.8	19.05	31.58	4.15	0.131464
15B	8	0.8	12.7	23.82	4.56	0.191484

Table 4-16 : Stiffness / Weight Ratio

<i>Specimen</i>	<i>Cell Size</i>	<i>Wall Thickness</i>	<i>Core Height</i>	<i>Specimen Mass</i>	<i>Flexural Rigidity</i>	<i>Stiffness / Weight Ratio</i>
<i>ID</i>	<i>mm</i>	<i>mm</i>	<i>mm</i>	<i>Gm</i>	<i>N/mm</i>	<i>Ratio</i>
1A	4	0.4	6.35	27.27	28.73	1.054
2A	12	0.4	6.35	15.20	27.61	1.816
3A	4	1.2	6.35	31.02	40.32	1.300
4A	12	1.2	6.35	18.45	23.54	1.276
5A	4	0.4	19.05	58.52	162.86	2.783
6A	12	0.4	19.05	27.65	123.40	4.464
7A	4	1.2	19.05	70.48	288.31	4.091
8A	12	1.2	19.05	36.14	149.56	4.138
9A	4	0.8	12.7	41.63	124.33	2.987
10A	12	0.8	12.7	22.50	87.71	3.899
11A	8	0.4	12.7	27.55	99.68	3.618
12A	8	1.2	12.7	36.31	106.26	2.926
13A	8	0.8	6.35	22.09	29.04	1.315
14A	8	0.8	19.05	36.92	199.58	5.406
15A	8	0.8	12.7	28.20	115.03	4.079

4.3.2 Mean effect and Pareto standardized effect

Based upon the performance ratio, main objective function remains to achieve highest value of for minimum weight for a HSCC. Main effect plots for these performance ratios are depicted in Figure 4.2. Figure 4.2 (a) suggest that more weight efficient HSCC structure may thus be developed increasing the cell size and the wall thickness. However, effect Core height on this response in inverse. However, 4.2 (b), Cell Size and wall thickness are not much of an effect on the structure. However, Core Thickness play its impact on flexural rigidity / weight ratio.

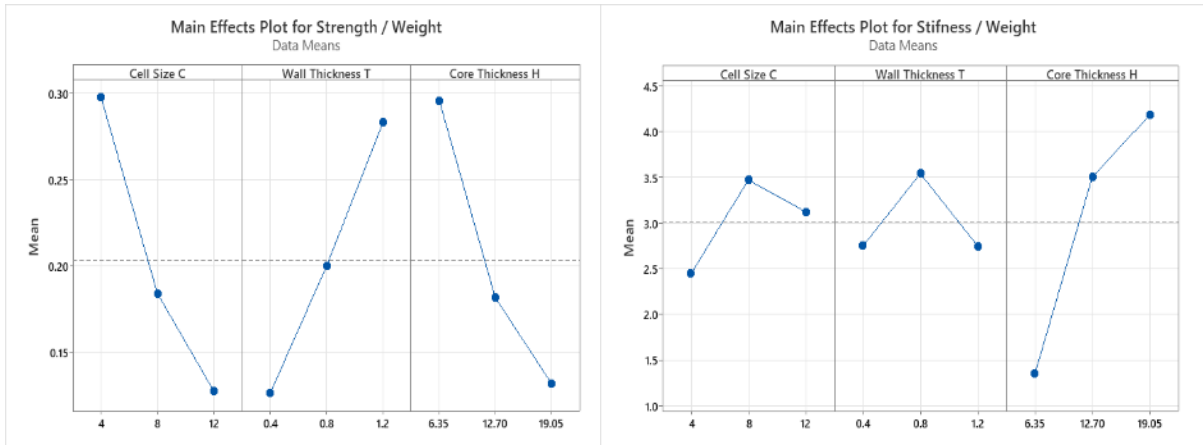


Figure 4-17 : Effect of major influences on (a) Mean value on Strength / weight ratio (b) Mean value of Flexural Rigidity / Weight Ratio

Similarly, Pareto chart for standardized effect presented at Figure 4.3 (a) Cell Size effects 19.92% to the absolute value of strength / weight ratio in positive manner and Wall thickness effects 18.34%. Meanwhile, Interaction of core height is also significant at 19.17%. For Figure 4.3 (b) Core Height has 8.11% effect on Stiffness / weight ratio. Meanwhile effect of cell size and wall thickness remains insignificant.

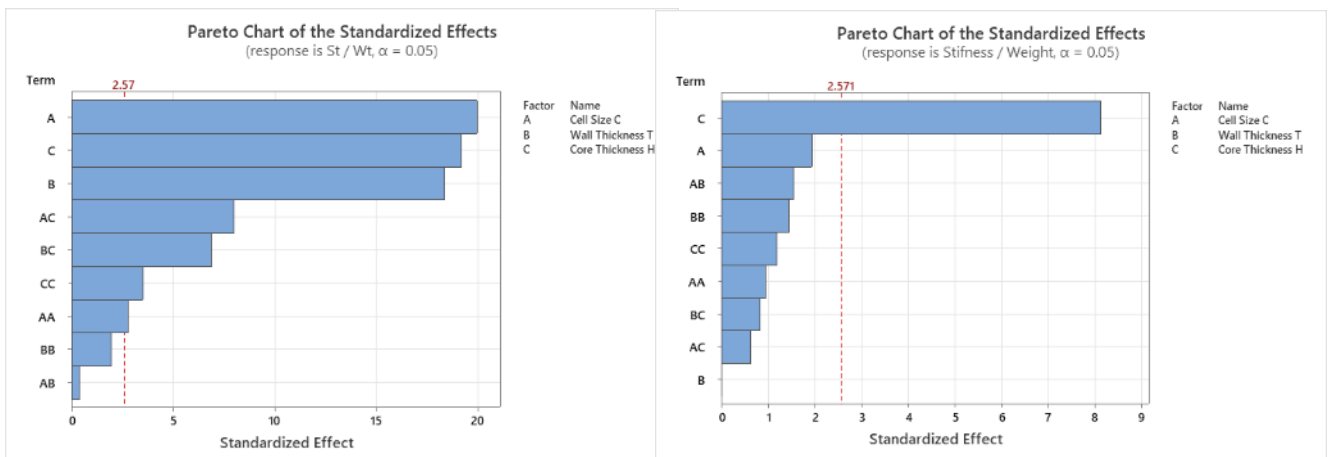


Figure 4-18 : Pareto Chart of Standardized Effect (a) Strength / Weight Ratio (b) Stiffness / Weight Ratio

It proposed that each parameter's significance be listed in descending order on strength to weight ratio is Cell Size > Core Thickness > Wall Thickness. All variable has significant influence on the response in term of strength / weight ratio. However, for Stiffness / weight ratio order becomes Core Height > Wall Thickness > Cell Size. It also means that the with the addition of core height structure will be stiffer and tends to much lower deflection under loads.

4.1.4 Design Analysis by RSM

RSM results, presented in Tables 4.2 and 4.3, reveal that the quadratic model best fits the data for Strength / weight ratio, while the Linear model is most suitable for Stiffness / weight ratio. Moreover, the high adjusted R-squared values indicate that the regression models effectively explain the underlying processes, providing a reliable foundation for predictions and optimization. In Table 4.17 & 4.18 of this study, the adjusted R² value is 98.88 % & 73.17%, suggesting that the regression model can only explain 1.12% & 26.83% of the changes, indicating that the model's fit is good.

Table 4-17 : Model's Summary Statistics for Strength / Weight Ratio

<i>Source</i>	<i>Std. Dev.</i>	<i>R²</i>	<i>Adjusted R²</i>	<i>Predicted R²</i>	<i>PRESS</i>	
Linear	0.0488	0.8843	0.8528	0.7328	0.0604	
2FI	0.0274	0.9734	0.9534	0.8722	0.0289	
Quadratic	0.0135	0.9960	0.9888	0.9670	0.0075	Suggested
Cubic	0.0150	0.9990	0.9861	-1.9886	0.6759	Aliased

Table 4-18 : Model's Summary Statistics for Stiffness / Weight Ratio

<i>Source</i>	<i>Std. Dev.</i>	<i>R²</i>	<i>Adjusted R²</i>	<i>Predicted R²</i>	<i>PRESS</i>	
Linear	0.7156	0.7892	0.7317	0.6039	10.58	Suggested
2FI	0.7562	0.8288	0.7003	-0.0477	27.99	
Quadratic	0.5501	0.9434	0.8414	0.4616	14.38	
Cubic	0.2941	0.9968	0.9547	-8.7679	260.95	Aliased

The significance of each regression coefficient in our models (Tables 4-19 and 4-20) was examined to determine if they have a substantial impact on the response values. Our tests confirmed that the produced models are statistically significant at a 95% confidence level. Using the backward elimination approach, we analysed the significance of each term in the quadratic equation model for Strength / Weight and removed non-significant terms. We found that terms A, B, C, AC, BC, A² are significant, with p-values less than 0.0500. In contrast, terms with p-values greater than 0.1 were deemed non-significant and removed. Similarly, for

Stiffness / Weight Ratio, only terms C is significant, and the remaining interactive terms are in significant.

The optimal predictive regression equation for Strength / weight ratio is as follows: -

$$\begin{aligned} \text{Strength / Weight Ratio} &= 0.5139 - 0.06249 \times A + 0.5333 B - 0.03306 C + 0.001453 A^2 - 0.1027 B^2 \\ &+ 0.000731 C^2 - 0.00120 A \times B + 0.001494 A \times C - 0.01290 B \times C \end{aligned}$$

For Stiffness / Weight, the regression equation gets formulated as follows: -

$$\begin{aligned} \text{Stiffness / Weight Ratio} &= -4.67 + 0.500 \times C + 5.68 \times B + 0.390 \times C - 0.0204 \times A^2 - 3.10 \times B^2 \\ &- 0.01013 \times C^2 - 0.189 \times A \times B + 0.00487 \times A \times C + 0.0628 B \times C \end{aligned}$$

For Fit analysis (Results presented in Tables 4.19 and 4.20) the CV for the regression models was found to be 6.64% and 21.54% for Strength / Weight Ratio and Stiffness / Weight Ratio, respectively, indicating a high degree of reliability for first response in particular. The F-statistic values of 28.38 and 24.13, respectively, exceed the desirable threshold of 4, suggesting that the models have flexibility for navigation. The R-squared values of 0.996 and 0.8584, respectively, demonstrate an excellent fit.

Table 4-19 : ANOVA for Quadratic model (Strength / Weight Ratio)

<i>Source</i>	<i>Sum of Squares</i>	<i>Degree of freedom</i>	<i>Mean Square</i>	<i>F-value</i>	<i>p-value</i>	<i>Prob>F</i>
Model	0.2252	9	0.0250	137.85	< 0.0001	significant
A-Cell Size	0.0721	1	0.0721	397.14	< 0.0001	
B-Wall Thickness	0.0611	1	0.0611	336.60	< 0.0001	
C-Core Thickness	0.0668	1	0.0668	367.84	< 0.0001	
AB	0.0000	1	0.0000	0.1629	0.7032	
AC	0.0115	1	0.0115	63.44	0.0005	
BC	0.0086	1	0.0086	47.34	0.0010	
A ²	0.0014	1	0.0014	7.66	0.0395	
B ²	0.0007	1	0.0007	3.83	0.1079	
C ²	0.0022	1	0.0022	12.30	0.0172	
Residual	0.0009	5	0.0002			
Cor Total	0.2262	14				

Table 4-20 : ANOVA for Quadratic model (Stiffness / Weight Ratio)

<i>Source</i>	<i>Sum of Squares</i>	<i>Degree of freedom</i>	<i>Mean Square</i>	<i>F-value</i>	<i>p-value</i>	<i>Prob>F</i>
Model	22.93	5	4.59	10.91	0.0013	significant
B-Wall Thickness	7.514E-07	1	7.514E-07	1.788E-06	0.9990	
C-Core Thickness	19.94	1	19.94	47.44	< 0.0001	
BC	0.2037	1	0.2037	0.4847	0.5039	
B ²	0.9744	1	0.9744	2.32	0.1622	
C ²	0.7046	1	0.7046	1.68	0.2276	
Residual	3.78	9	0.4203			
Cor Total	26.72	14				

Table 4-21 : Fit Statistics (Compressive Strength / Weight Ratio)

Std. Dev.	0.0135	R ²	0.9960
Mean	0.2030	Adjusted R ²	0.9888
C.V. %	6.64	Predicted R ²	0.9670
		Adeq Precision	44.5036

Table 4-22 : Fit Statistics (Stiffness / Weight Ratio)

Std. Dev.	0.6483	R ²	0.8584
Mean	3.01	Adjusted R ²	0.7797
C.V. %	21.54	Predicted R ²	0.5907
		Adeq Precision	8.7166

The normal probability plot and residual distribution plot Figure 4-19 (a) & (b) displays a linear trend, indicating that the residuals follow a normal distribution and absence of any systematic errors or patterns, and supporting the assumption of constant variance. Same pattern was observed for stiffness / weight ratio in Figure 4-20 (a) & (b).

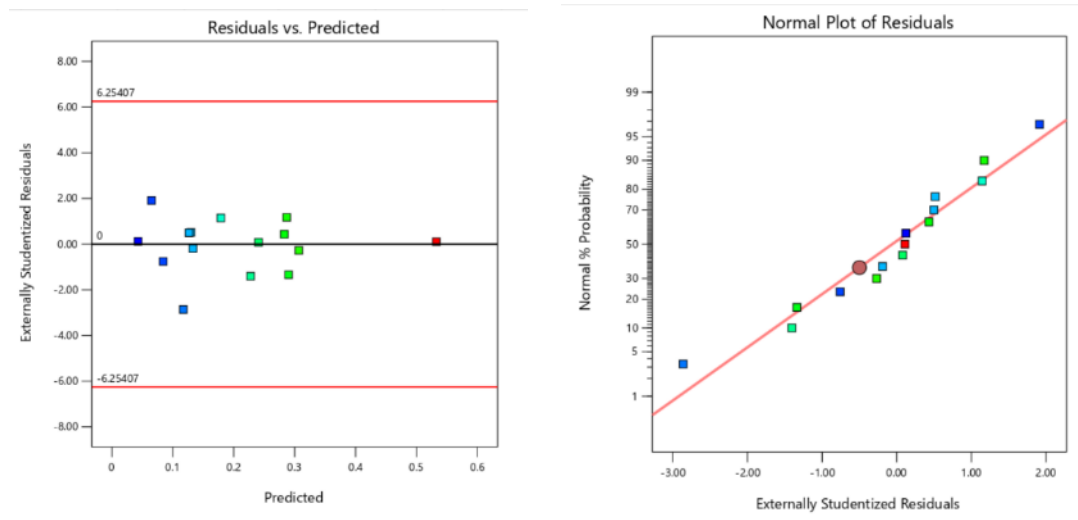


Figure 4-19 : (a) Residuals vs predicted values for Strength / Weight (b) Normal probability plot of the residuals

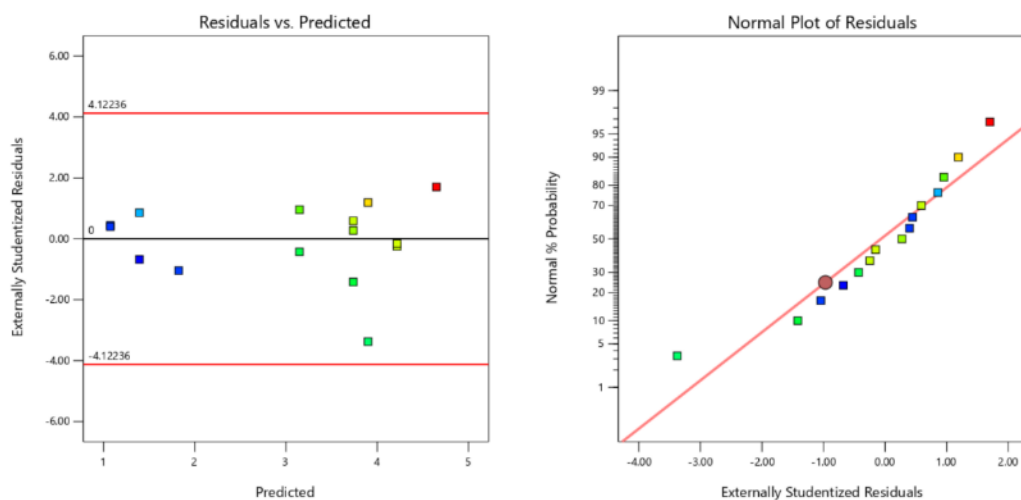


Figure 4-20 : (a) Residuals vs predicted values for Stiffness / Weight (b) Normal probability plot of the residuals

To elucidate the effects of cell size, wall thickness, and core height on Strength / Weight Ratio and Stiffness / Weight Ratio, Surface and contour plots were generated. The curved sections of these graphs illustrate the relationships between various combinations of factors. Contour plots reveal the impact of interactions between two independent variables as sloping curves, with ellipsoidal contours indicating strong interactions and spherical contours suggesting weaker relationships.

Figure 4-21(a) & (b) presents Response surface graphs and contour plots depicting the influence of cell size and wall thickness on Strength / Weight Ratio, with core thickness held at its maximum level. These visualizations facilitate a comprehensive understanding of the quadratic interactions between these variables. As cell size decrease and wall thickness increase, strength / weight ratio increase in stable gradient until it reaches the halfway point, after which it begins to increase steeper gradient until it reaches highest value. Maximum strength / weight ratio is achieved at lowest cell size and highest wall thickness.

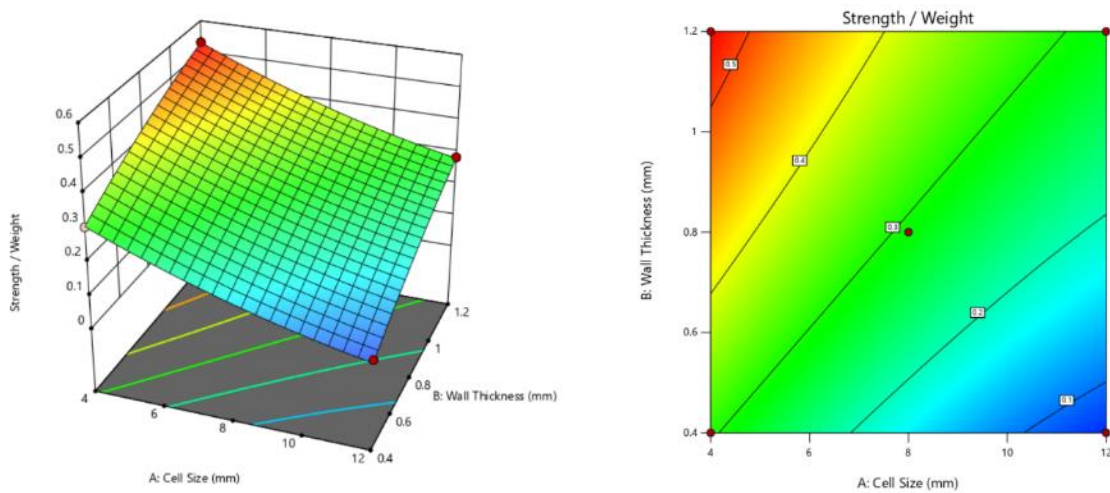


Figure 4-21 : Effect of Cell Size and wall thickness on Strength / Weight Ratio (a) Response surface and (b) contour plots

Figure 4-22 (a) & (b) shows the three-dimensional surface and its contours, illustrating the effect on cell size and core thickness on strength / weight ratio, while keeping the wall thickness at maximum level.

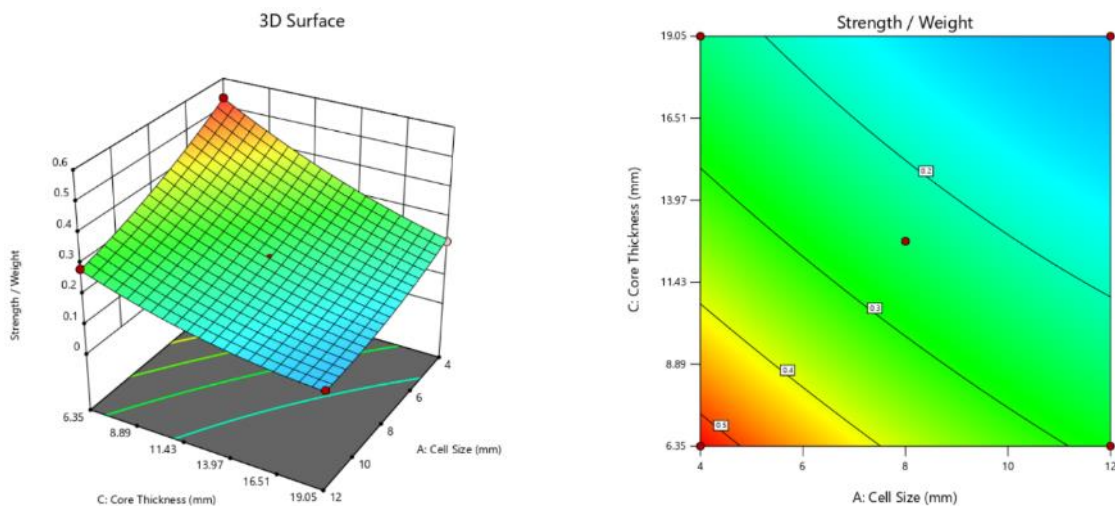


Figure 4-22 : Effect of Cell Size and Core Thickness on the Strength / Weight Ratio (a) response surface and (b) contour plots

The surface plots in Figure 4-23 illustrate that increasing core thickness has a profound impact on stiffness / weight ratio, consistent with findings from previous model analyses. To optimize the stiffness of the HSCC structure within the experimental design space, a core thickness of 19.05mm is recommended. Notably, the results indicate a beneficial interaction effect, suggesting that the combined influence of core thickness and other variables enhances the overall performance of the HSCC structure.

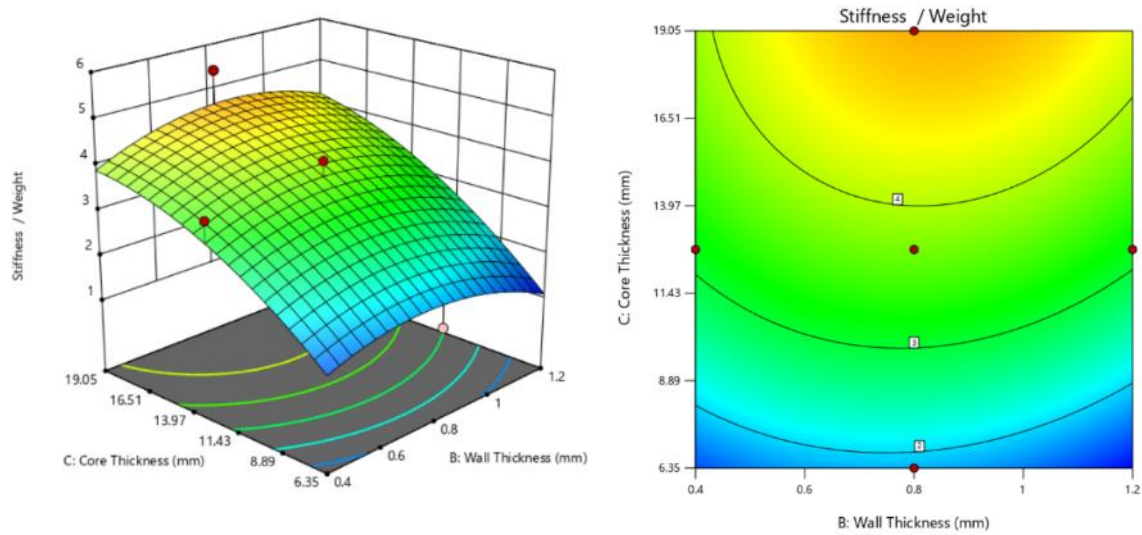


Figure 4-23 Effect of Core Thickness and Wall Thickness on the Stiffness / Weight Ratio (a) response surface and (b) contour plots

This study employs a RSM based optimization approach to identify the optimal parameter set within the design space, aiming to maximize the performance ratios. Response Optimizer feature of Design Expert 13 was used in this regard. Figure 4.24 presents the interaction plot of desirability, where a desirability value of 1 represents the optimal combination of parameters yielding maximum strength / weight ratio. As desirability decreases, the response values also decrease, which is not desirable in this context. The optimization results reveal that the optimal parameters as per Table 4-23. These parameters constitute the optimal design point within the design space. For optimization of Stiffness / weight ratio, maximum desirability along with optimal predicted parameters are annotated in table 4-24 and Figure 4-25 respectively.

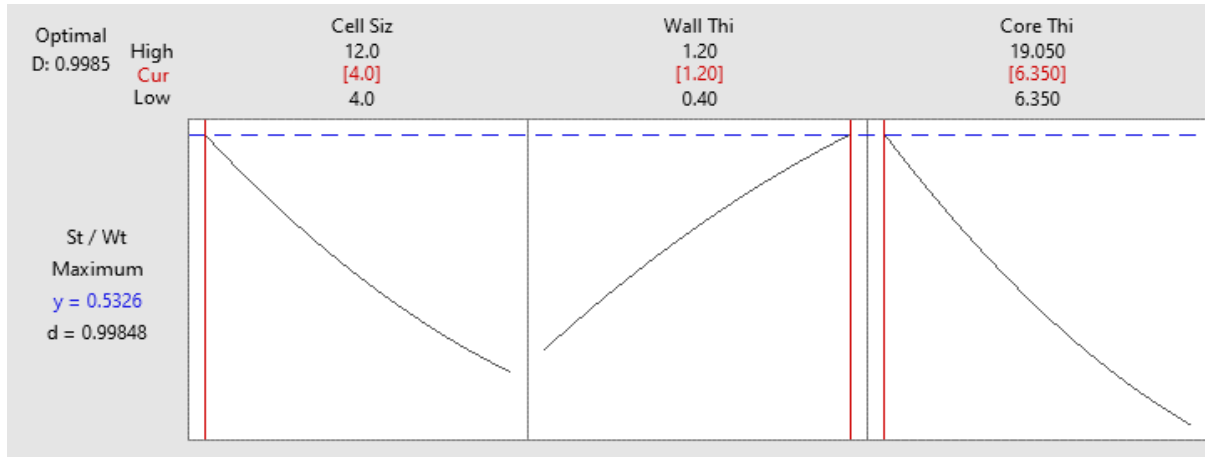


Figure 4-24. Optimal predicted parameters with desirability

Table 4-23. Optimal experimental parameters for Strength / Weight Ratio

<i>Optimum Input Variables</i>	<i>Geometrical Characteristics</i>
Cell Size mm	4mm
Wall Thickness	1.2mm
Core thickness	6.35mm

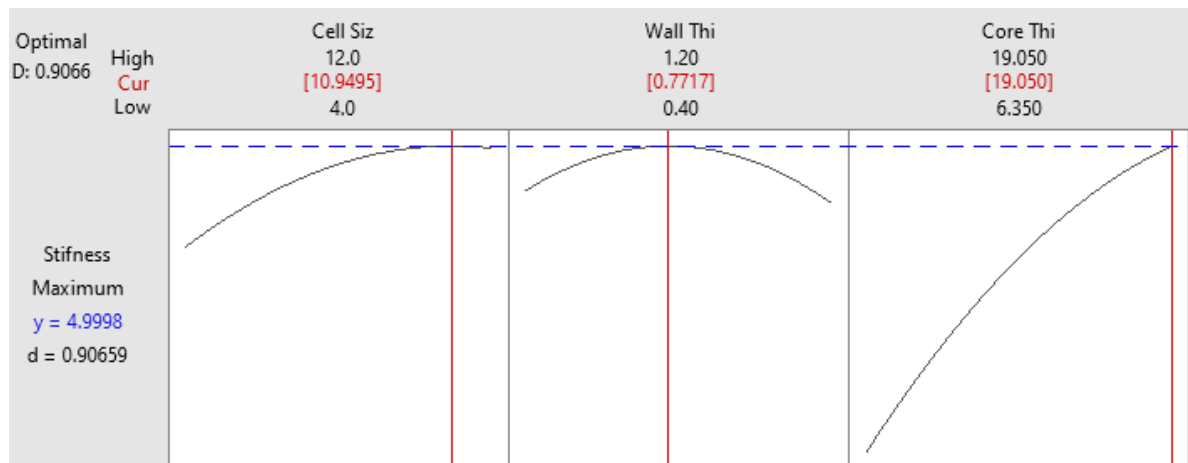


Figure 4-25 : Optimal parameters with desirability for stiffness / weight ratio

Table 4-24 : Optimal experimental parameters for Stiffness / Weight Ratio

<i>Optimum Input Variables</i>	<i>Geometrical Characteristics</i>
Cell Size	10.94mm
Wall Thickness	0.7717mm
Core thickness	19.05mm

4.4 Difference between Experimental and Analytical response

During the analysis process for flexural rigidity and stiffness to weight ratio respectively, a variation in Experimental and Analytical response was observed. Experimentally, values were obtained through maximum deflection and peak force values via ASTM standards. Meanwhile, analytical values were obtained using equations defined in Gibson [1]. A variation in experimental values was observed. For a comparison, these values are annotated in Table 4-25.

Table 4-25 : Difference in Analytical and Experimental values

<i>Specimen</i>	<i>Cell Size</i>	<i>Wall Thickness</i>	<i>Core Height</i>	<i>Flexural Rigidity (Analytical)</i>	<i>Flexural Rigidity (Exp)</i>	<i>Difference</i>
<i>ID</i>	<i>mm</i>	<i>mm</i>	<i>mm</i>	<i>N/mm</i>	<i>N/mm</i>	
1A	4	0.4	6.35	34.31	28.73	16.27%
2A	12	0.4	6.35	27.62	27.61	0.05%
3A	4	1.2	6.35	44.31	40.32	9.00%
4A	12	1.2	6.35	34.10	23.54	30.95%
5A	4	0.4	19.05	334.49	162.86	51.31%
6A	12	0.4	19.05	192.37	123.40	35.85%
7A	4	1.2	19.05	581.98	288.31	50.46%
8A	12	1.2	19.05	331.51	149.56	54.88%
9A	4	0.8	12.7	186.55	124.33	33.35%
10A	12	0.8	12.7	121.16	87.71	27.61%
11A	8	0.4	12.7	109.48	99.68	8.95%
12A	8	1.2	12.7	167.03	106.26	36.38%
13A	8	0.8	6.35	34.44	29.04	15.69%
14A	8	0.8	19.05	334.30	199.58	40.30%
15A	8	0.8	12.7	142.16	115.03	19.08%

Analytical values were found higher from 0.05% to 54.88% (Average 28.68%) at maximum with respect to their experimental value. Difference was observed to be rising for HCSS having higher peak rigidity. This exhibits one the limitation of FDM process or its capability. Another reason could have an inherited porosity in FDM structure due to air gaps in between the layers. Detailed analysis in this regard was beyond research mandate and could be explored as another area of interest in related researches.

CHAPTER 5 : CONCLUSION

Due to its exceptional mechanical efficiency, research into the development and application of sandwich structures has always been intense. As of right now, honeycomb cores have the best stiffness to weight and strength ratios, but adhesion of face sheets has always remained a challenge. The fundamental structure has been created in diverse configurations and tailored for an array of uses, mostly employing a hexagonal configuration for maximum effectiveness. However, with ever growing manufacturing era of rapid prototyping; additive manufacturing process are replacing the conventional processes at a very fast pace. With the advent of AM processes, challenges with older techniques are more in control, however, efficacy of AM manufactured products are yet to be evaluated for mass production and long term performance. Mechanical properties of additively manufactured honeycomb structures made with of Fused Deposition Modelling (FDM) processes requires critical consideration to ensure the production of parts with consistency and high-quality. FDM is a widely utilized additive manufacturing technique that involves heating a thermoplastic polymer above its Glass Transition Temperature and extruding from a nozzle to create a component.

FDM is a promising method to avoid complex conventional method of manufacturing of honeycomb core with corrugation or expansion method and further adhesion of face sheet on core top and bottom layer. A small polymer made UAV having honeycomb core filled in its complete geometry may be manufactured as singular unit while employing FDM avoiding any complexities with adequate mechanical properties.

A honeycomb sandwich structure usually comprises of two high strength rigidity thin-face sheets to take compressive loads and with a low density core possessing high strength and stiffness to take the shear load. The mechanical characteristics exhibited by the face sheet and the core depends upon various aspect involving material, face sheet thickness, core thickness, cell size, core wall thickness which are carefully dimensioned to obtain various properties and desired performance, particularly in high strength-to-weight ratios.

Mechanical properties including compressive strength, tensile strength, energy absorption, flexural rigidity, impact analysis are noteworthy that requires integral insight knowledge to design a structure. Achievement of all these properties up to an optimum value

with minimal weight are usually design problem for any application of sandwich honeycomb structures. Meanwhile, process parameters for FDM process are also under evaluation for their effect on mechanical properties but a number of researchers have elaborated the impact of these parameters and literature has converged to optimal values. A few researchers have also explored the FDM based honeycomb structures but response function in terms performance / weight ratios for singular extruded HCSS with similar face sheet but a with variation of basic hexagon geometry were identified as research gap. Thus, a comprehensive understanding, based on established and published research, was essential to study and establish the relation of geometrical features of HSCC with its mechanical properties while achieving the process finesse with optimized FDM process parameters.

Based upon the ongoing research area, research methodology was deigned to conclude in systematic manner. Availability of resource including 3D Printer, prototyping, procurement of material from reliable OEM, UTM and academia resources were outlined. HSCC characteristic were analyzing in detail with reference to literature; factors that influence mechanical properties, such as cell size, wall thickness, core thickness was selected as input variables. Few constraints were selected to control the process were regular hexagon structures, Mechanical properties including Compressive strength and flexural rigidity were selected based upon the available apparatus.

RSM based Design of Experiment was carefully designed for experimental evaluation. Central Composite Design (Face Cantered) approach was selected owing to its efficient exploration of space for a three level design. 03 input variables selected were given three level upper and lower limits keeping in view multiple comparative factors as well as process limitations. 15 runs for each experiment were marked using Minitab. Each experiment was conducted twice to ensure repeatability of values.

Experimentation was based International acceptable standards (ASTM). 02 Methods were shortlisted for sandwich structures due to limitation of resources. ASTM C365 was referred for conduct of flatwise compression testing that yields maximum compressive strength and evaluates the compressive modulus of structures. ASTM C393 is used for flexural testing of HCSS. Face bending stress, core shear stress, mid span deflection and flexural rigidity of a structure can be evaluated using these standards.

Computer Aided Designing (CAD) modelling was carried out as per level of geometrical factors. As per the process requirement, G Code was written for slicing of product and testing specimens were printed after verification and qualification of prototypes. After printing of each specimen, mass was evaluated carefully in as per standard for utilization of its values while calculating the ratio during the optimization phase.

Experiments were conducted in Mechanics of Materials lab in SMME Dept on UTM in accordance with ASTM conditions of temperature, humidity, load rate etc. Stress – Strain and Load – Displacement curves were obtained for detailed analysis. Max compressive strength, compressive modulus, peak load, maximum deflection and flexural rigidity were the key output responses that were measures after solving the analytical formulae as per ASTM standards.

Initial relation of each response measured was related to in its associated design space with input variable. Statistical modelling was carried out to validate the data and infer valuable conclusions. Lately, the obtained responses were converted to ratio against testing specimen mass in order to study the effect of selected input variables of cell size, core thickness and wall thickness as to achieve maximum strength / weight & flexural rigidity / weight ratio. Statistical tools including ANOVA & RSM were used to verify the optimal parametric findings. As a result of experimental data following conclusions can be drawn: -

- (a) Polymer HSCC specimens with homogenous facing were printed successfully without limitation. No delamination was observed in any of the structure.
- (b) Stress – Strain and Load –Deflection curves shows relatable failures pattern with respect to literature.
- (c) Max Compressive Strength from manufactured structures were observed to be 0.72 MPa to 13.93MPa, Compressive Modules was range in between 10.29 to 64.89 Pascals. Flexural Rigidity was observed to be in between 23.54 to 288.31 N/mm.
- (d) Maximum strength to weight ratio was achieved to be 0.533 for compressive specimen; However, maximum stiffness to weight ratio was achieved to be 5.40.
- (e) The optimal parametric combination as per RSM for predicting the maximum strength / weight ratio is as follows: Cell Size 4mm, wall thickness 1.2mm and Core thickness 6.35mm. Decreasing the cell size and core height and increasing the wall thickness will increase compressive strength, eventually leading to favourable results

of maximum strength / weight ratio. The effect of dimensional characteristics on response in descending order were is Cell Size > Core Thickness > Wall Thickness.

(f) Output response for predicting the maximum stiffness / weight ratio within the design space could be achieved by : Cell Size 10.94 mm, wall thickness 0.774mm and Core thickness 19.05mm. Core thickness has the most prominent effect for stiffness / weight ratio.

(g) An RSM-based quadratic regression models for output responses were developed. The model was statistically significant at 95% based on the ANOVA results. The residuals are all normally distributed. The three-dimensional response surface and contour plots show that all input variables significantly influence the responses in respective testing.

(h) Core thickness remains most influential in increasing the flexural rigidity of HSCC.

(i) Failures modes are per literature were also evident in breakage pattern of HSCC.

(j) A phenomenon for difference in experimental and analytical calculations were observed probably due to porosity effect associated with FDM process. Experimental values were found to be lesser mass in comparison to theoretical calculations.

5.1.1 Way Forward

The geometric features of HSCC plays a critical role in the properties of core further affecting its mechanical properties. The objective of this study was to adjust various geometrical parameters of hexagon honeycomb core including cell size, wall thickness and core thickness to find an optimal balance that mass of the specimen and its capability to withstand compressive and flexural loads in order to produces fully functional components with the adequate performance. The scope of this study allowed for a comprehensive investigation into the combined and individual effects of these parameters on the mechanical properties of Honeycomb Sandwich Structures.

While Fused Deposition Modelling is currently limited to a few specific feedstock such as PLA, ABS, PETG, NYLON etc, this methodology can potentially be applied to new polymers to construct efficient and optimally designed structures. However, evaluating the mechanical properties of new materials can be energy-intensive from both a computational and

production point of view. This research will help to predict the desired optimal results through established regression equations for PLA parts in particular and then manufacture unibody core filled smaller UAVs in particular directly with a 3D printer.

The research scope was limited to analysing the few mechanical properties of HSCC. However, more research developments can be initiated interaction study with other significant HCSS characteristics including Aspect Ratio, t/l Ratio, Relative Density etc. Study of Porosity effect in 3D Printed HCSS is a weak area and required more research for establishing well defined relations. The study was carried out using some constraints with type for core design regular hexagon with fixed face sheet thickness. More core typologies may be explored to find the optimum solution within the design space. A comprehensive study for failure modes in compression and flexural testing may be carried out using modern techniques and equipment.

REFERENCES

- [1] L. J. A. M. F. Gibson, *Cellular solids : structure and properties*. Cambridge: Cambridge Univ. Press (in English), 2010.
- [2] D. Zenkert, *An Introduction to Sandwich Structures* (Student Edition). (in English), 1995.
- [3] T. Bitzer, *Honeycomb Technology-Materials, Design, Manufacturing, Applications And Testing*, First ed. 1997.
- [4] B. Castanie, C. Bouvet, and M. Ginot, "Review of composite sandwich structure in aeronautic applications," *Composites Part C: Open Access*, vol. 1, p. 100004, 2020/08/01/ 2020, doi: <https://doi.org/10.1016/j.jcomc.2020.100004>.
- [5] S. Rupani, S. Jani, and D. Acharya, "Design, Modelling and Manufacturing aspects of Honeycomb Sandwich Structures: A Review," *International Journal of Science & Engineering Development Research*, vol. 2, pp. 526-532, 04/28 2017, doi: 10.1712/ijedr.17013.
- [6] ISO, *Additive Manufacturing: General Principles. Part. 2: Overview of Process Categories and Feedstock*. ISO, 2015.
- [7] A. I. A. 29211-11e3, "Standard Terminology for Additive Manufacturing—Coordinate Systems and Test Methodologies," ed: ASTM International West Conshohocken, PA, 2011.
- [8] J.-P. Kruth, M.-C. Leu, and T. J. C. A. Nakagawa, "Progress in additive manufacturing and rapid prototyping," vol. 47, no. 2, pp. 525-540, 1998.
- [9] B. Akhoundi and A. H. Behraves, "Effect of Filling Pattern on the Tensile and Flexural Mechanical Properties of FDM 3D Printed Products," *Experimental Mechanics*, vol. 59, no. 6, pp. 883-897, 2019/07/01 2019, doi: 10.1007/s11340-018-00467-y.
- [10] I. Gibson *et al.*, *Additive manufacturing technologies*. Springer, 2021.
- [11] Hexel-Composites, "HexWeb™Honeycomb Attributes and Properties," 2022.
- [12] S. P. Engelstad, Z. M. Chen, and V. K. Goyal, "Analysis methodology for the assessment of unvented honeycomb sandwich structures subject to in-plane and pressure loads," *Journal of Sandwich Structures & Materials*, vol. 25, no. 1, pp. 95-111, 2023/01/01 2022, doi: 10.1177/10996362221122701.
- [13] F. Tarlochan, "Sandwich Structures for Energy Absorption Applications: A Review," *Materials*, vol. 14, no. 16, p. 4731, 2021.
- [14] M. S. Khan, S. S. Rahimian Koloor, and M. N. Tamin, "Effects of cell aspect ratio and relative density on deformation response and failure of honeycomb core structure," *Materials Research Express*, vol. 7, no. 1, p. 015332, 2020/01/01 2020, doi: 10.1088/2053-1591/ab6926.
- [15] G. Palomba, G. Epasto, and V. Crupi, "Lightweight sandwich structures for marine applications: a review," *Mechanics of Advanced Materials and Structures*, vol. 29, no. 26, pp. 4839-4864, 2022/10/26 2022, doi: 10.1080/15376494.2021.1941448.
- [16] R. M. A. Gpoichand, N.V.S Sankar, G.Rama Balaji, P.Sandeep Kumar, "Design and Analysis of Copper Honeycomb Sandwich Structure " *International Journal of Engineering and Advanced Technology*, vol. 2, no. 4, 2013.

- [17] Z. Li, "Cell Size Effects on Material Properties of Foam-Filled Honeycomb Sandwich Structures using Finite Element Analysis," *Journal of The Acoustical Society of America - JACOUST SOC AMER*, vol. 129, 04/01 2011, doi: 10.1121/1.3587887.
- [18] Hexel-Composites, "HexWeb™ Honeycomb Sandwich Design Technology," ed, 2000.
- [19] A. Jędral, "Review of Testing Methods Dedicated for Sandwich Structures with Honeycomb Core," *Transactions on Aerospace Research*, vol. 2018, pp. 7-20, 09/01 2018, doi: 10.2478/tar-2019-0006.
- [20] *Standard Test Method for Flexural Properties of Sandwich Constructions*, C. ASTM.
- [21] R. Singh and H. Garg, "Fused Deposition Modeling – A State of Art Review and Future Applications," 2016.
- [22] J. Mogan *et al.*, "Fused Deposition Modelling of Polymer Composite: A Progress," *Polymers*, vol. 15, no. 1, p. 28, 2023.
- [23] A. Dey and N. Yodo, "A Systematic Survey of FDM Process Parameter Optimization and Their Influence on Part Characteristics," *Journal of Manufacturing and Materials Processing*, vol. 3, no. 3, 2019, doi: 10.3390/jmmp3030064.
- [24] D. Pollard, C. Ward, G. Herrmann, and J. Etches, "The manufacture of honeycomb cores using Fused Deposition Modeling," *Advanced Manufacturing: Polymer & Composites Science*, vol. 3, no. 1, pp. 21-31, 2017/01/02 2017, doi: 10.1080/20550340.2017.1306337.
- [25] A. Tontowi, L. Ramdani, R. Erdizon, and D. Baroroh, "Optimization of 3D-Printer Process Parameters for Improving Quality of Polylactic Acid Printed Part," *International Journal of Engineering and Technology*, vol. 9, pp. 589-600, 05/01 2017, doi: 10.21817/ijet/2017/v9i2/170902044.
- [26] N. Ayrimis, M. Kariz, M. Šernek, and M. K. Kuzman, "Effects of sandwich core structure and infill rate on mechanical properties of 3D-printed wood/PLA composites," *The International Journal of Advanced Manufacturing Technology*, vol. 115, no. 9, pp. 3233-3242, 2021/08/01 2021, doi: 10.1007/s00170-021-07382-y.
- [27] H. Gonabadi, Y. Chen, A. Yadav, and S. Bull, "Investigation of the effect of raster angle, build orientation, and infill density on the elastic response of 3D printed parts using finite element microstructural modeling and homogenization techniques," *The International Journal of Advanced Manufacturing Technology*, vol. 118, no. 5, pp. 1485-1510, 2022/01/01 2022, doi: 10.1007/s00170-021-07940-4.
- [28] S. Shiping and Y.-d. Lai, "Effects of Honeycomb Cell Size on Performances of Sandwich Panels," *Journal of Aeronautical Materials*, vol. 31, 04/01 2011, doi: 10.3969/j.issn.1005-5053.2011.2.012.
- [29] A. Kumar, S. Angra, and A. Chanda, "Analysis of effect of variation of Honeycomb core cell size and sandwich panel width on the stiffness of a sandwich structure," *Research on Engineering Structures and Materials*, 01/01 2022, doi: 10.17515/resm2021.308me0606.
- [30] C. Baumgart, T. Halle, C. Weigelt, L. Krüger, and C. G. Aneziris, "Effect of honeycomb cell geometry on compressive properties: Finite element analysis and experimental verification," *Science and Technology of Materials*, vol. 30, no. 1, pp. 35-42, 2018/01/01/ 2018,
- [31] T. Thomas, "Crushing Behaviour of Honeycomb structure: A Review," *International Journal of Crashworthiness*, 06/08 2018.
- [32] S. Chahardoli, T. N. Tran, S. M. Hossaeini Marashi, F. Masoumi, and S. Tatyana Yu, "Experimental investigation of the crushing characteristics in sandwich panels in the

- application of light vehicles using three-point bending tests," *Engineering Failure Analysis*, vol. 129, p. 105725, 2021/11/01/ 2021, doi: <https://doi.org/10.1016/j.engfailanal.2021.105725>.
- [33] T. M. McCormack, R. Miller, O. Kesler, and L. J. Gibson, "Failure of sandwich beams with metallic foam cores," *International Journal of Solids and Structures*, vol. 38, no. 28, pp. 4901-4920, 2001/07/01/ 2001, doi: [https://doi.org/10.1016/S0020-7683\(00\)00327-9](https://doi.org/10.1016/S0020-7683(00)00327-9).
- [34] R. D. Bintara, D. Z. Lubis, and Y. R. Aji Pradana, "The effect of layer height on the surface roughness in 3D Printed Polylactic Acid (PLA) using FDM 3D printing," *IOP Conference Series: Materials Science and Engineering*, vol. 1034, no. 1, p. 012096, 2021/02/01 2021, doi: 10.1088/1757-899X/1034/1/012096.
- [35] M. Lalegani Dezaki and M. K. A. Mohd Ariffin, "The Effects of Combined Infill Patterns on Mechanical Properties in FDM Process," *Polymers*, vol. 12, no. 12, p. 2792, 2020. [Online]. Available: <https://www.mdpi.com/2073-4360/12/12/2792>.
- [36] L. Bergonzi, M. Vettori, L. Stefanini, and L. D'Alcamo, "Different infill geometry influence on mechanical properties of FDM produced PLA," *IOP Conference Series: Materials Science and Engineering*, vol. 1038, no. 1, p. 012071, 2021/02/01 2021, doi: 10.1088/1757-899X/1038/1/012071.
- [37] M. Qamar Tanveer, G. Mishra, S. Mishra, and R. Sharma, "Effect of infill pattern and infill density on mechanical behaviour of FDM 3D printed Parts- a current review," *Materials Today: Proceedings*, vol. 62, pp. 100-108, 2022/01/01/ 2022, doi: <https://doi.org/10.1016/j.matpr.2022.02.310>.
- [38] M. T. Birosz, D. Ledenyák, and M. Andó, "Effect of FDM infill patterns on mechanical properties," *Polymer Testing*, vol. 113, p. 107654, 2022/09/01/ 2022, doi: <https://doi.org/10.1016/j.polymertesting.2022.107654>.
- [39] M. Ouhsti, B. El Haddadi, and S. Belhouideg, "Effect of printing parameters on the mechanical properties of parts fabricated with open-source 3D printers in PLA by fused deposition modeling," *Mechanics and Mechanical Engineering*, vol. 22, no. 4, pp. 895-907, 2018.
- [40] T.-C. Yang and C.-H. Yeh, "Morphology and Mechanical Properties of 3D Printed Wood Fiber/Polylactic Acid Composite Parts Using Fused Deposition Modeling (FDM): The Effects of Printing Speed," *Polymers*, vol. 12, no. 6, p. 1334, 2020. [Online]. Available: <https://www.mdpi.com/2073-4360/12/6/1334>.
- [41] N.-H. Tran, V.-N. Nguyen, A.-V. Ngo, and V.-C. Nguyen, "Study on the effect of fused deposition modeling (FDM) process parameters on the printed part quality," *Int J Eng Res Appl*, vol. 7, no. 12, pp. 71-7, 2017.
- [42] M. H. Sehhat, A. Mahdianikhotbesara, and F. Yadegari, "Impact of temperature and material variation on mechanical properties of parts fabricated with fused deposition modeling (FDM) additive manufacturing," *The International Journal of Advanced Manufacturing Technology*, vol. 120, no. 7, pp. 4791-4801, 2022/06/01 2022, doi: 10.1007/s00170-022-09043-0.
- [43] A. A. Ansari and M. Kamil, "Effect of print speed and extrusion temperature on properties of 3D printed PLA using fused deposition modeling process," *Materials Today: Proceedings*, vol. 45, pp. 5462-5468, 2021/01/01/ 2021, doi: <https://doi.org/10.1016/j.matpr.2021.02.137>.
- [44] S. Brischetto and R. Torre, "Honeycomb Sandwich Specimens Made of PLA and Produced Via 3D FDM Printing Process: An Experimental Study," *Journal of Aircraft*

- and Spacecraft Technology*, vol. 4, pp. 54-69, 01/01 2020, doi: 10.3844/jastsp.2020.54.69.
- [45] Q. Ma, M. R. M. Rejab, A. P. Kumar, H. Fu, N. M. Kumar, and J. Tang, "Effect of infill pattern, density and material type of 3D printed cubic structure under quasi-static loading," *Proceedings of the Institution of Mechanical Engineers, Part C: Journal of Mechanical Engineering Science*, vol. 235, no. 19, pp. 4254-4272, 2021/10/01 2020, doi: 10.1177/0954406220971667.
- [46] H. B. Rebelo, D. Lecompte, C. Cismasiu, A. Jonet, B. Belkassem, and A. Maazoun, "Experimental and numerical investigation on 3D printed PLA sacrificial honeycomb cladding," *International Journal of Impact Engineering*, vol. 131, pp. 162-173, 2019/09/01/ 2019, doi: <https://doi.org/10.1016/j.ijimpeng.2019.05.013>.
- [47] G. Domínguez-Rodríguez, J. J. Ku-Herrera, and A. Hernández-Pérez, "An assessment of the effect of printing orientation, density, and filler pattern on the compressive performance of 3D printed ABS structures by fuse deposition," *The International Journal of Advanced Manufacturing Technology*, vol. 95, no. 5, pp. 1685-1695, 2018/03/01 2018, doi: 10.1007/s00170-017-1314-x.
- [48] M. Moradi, S. Meiabadi, and A. Kaplan, "3D Printed Parts with Honeycomb Internal Pattern by Fused Deposition Modelling; Experimental Characterization and Production Optimization," *Metals and Materials International*, vol. 25, no. 5, pp. 1312-1325, 2019/09/01 2019, doi: 10.1007/s12540-019-00272-9.
- [49] O. Basurto-Vázquez, E. P. Sánchez-Rodríguez, G. J. McShane, and D. I. Medina, "Load Distribution on PET-G 3D Prints of Honeycomb Cellular Structures under Compression Load," *Polymers*, vol. 13, no. 12, 2021, doi: 10.3390/polym13121983.
- [50] S. Gohar, G. Hussain, A. Ali, and H. Ahmad, "Mechanical performance of honeycomb sandwich structures built by FDM printing technique," *Journal of Thermoplastic Composite Materials*, 03/01 2021, doi: 10.1177/0892705721997892.
- [51] B. Panda, M. Leite, B. B. Biswal, X. Niu, and A. Garg, "Experimental and numerical modelling of mechanical properties of 3D printed honeycomb structures," *Measurement*, vol. 116, pp. 495-506, 2018/02/01/ 2018, doi: <https://doi.org/10.1016/j.measurement.2017.11.037>.
- [52] S. M. Zaharia, L. A. Enescu, and M. A. Pop, "Mechanical Performances of Lightweight Sandwich Structures Produced by Material Extrusion-Based Additive Manufacturing," *Polymers*, vol. 12, no. 8, 2020, doi: 10.3390/polym12081740.
- [53] V. Dikshit *et al.*, "Investigation of out of plane compressive strength of 3D printed sandwich composites," *IOP Conference Series: Materials Science and Engineering*, vol. 139, p. 012017, 2016/07 2016, doi: 10.1088/1757-899x/139/1/012017.
- [54] M. Uy and J. K. Telford, "Optimization by Design of Experiment techniques," in *2009 IEEE Aerospace conference*, 7-14 March 2009 2009, pp. 1-10, doi: 10.1109/AERO.2009.4839625.
- [55] V. L. Anderson and R. A. McLean, *Design of experiments: a realistic approach*. CRC Press, 2018.
- [56] L. Eriksson, E. Johansson, N. Kettaneh-Wold, C. Wikström, and S. Wold, "Design of experiments," *Principles and Applications, Learn ways AB, Stockholm*, 2000.
- [57] M. S. M. Said, J. A. Ghani, M. S. Kassim, S. H. Tomadi, and C. Haron, "Comparison between Taguchi method and response surface methodology (RSM) in optimizing machining condition," in *Proceeding of 1st International Conference on Robust Quality Engineering*, 2013, pp. 60-68.
- [58] R. A. Fisher *et al.*, *The design of experiments*. Springer, 1966.

- [59] D. Cox, "Response Surfaces, Mixtures, and Ridge Analyses, 2nd Edition by George E.P. Box, Norman R. Draper," *International Statistical Review*, vol. 75, pp. 265-266, 02/01 2007, doi: 10.1111/j.1751-5823.2007.00015_17.x.
- [60] D. Montgomery and C. St, *Design and Analysis of Experiments, 9th Edition*. 2022.
- [61] *Standard Test Method for Flatwise Compressive Properties of Sandwich Cores*, C. ASTM.
- [62] S. Antony, A. Cherouat, and G. Montay, "Fabrication and Characterization of Hemp Fibre Based 3D Printed Honeycomb Sandwich Structure by FDM Process," *Applied Composite Materials*, vol. 27, no. 6, pp. 935-953, 2020/12/01 2020, doi: 10.1007/s10443-020-09837-z.
- [63] M. D. Antony Arul Prakash, V. L. Jagannatha Guptha, R. S. Sharma, and B. Mohan, "Influence of Cell Size on the Core Shear Properties of FRP Honeycomb Sandwich Panels," *Materials and Manufacturing Processes*, vol. 27, no. 2, pp. 169-176, 2012/02/01 2012, doi: 10.1080/10426914.2011.560227.